PONTIFICIA UNIVERSIDAD CATOLICA DE CHILE
ESCUELA DE INGENIERIA

COUPLING ENERGYPLUS AND TWO IMPROVED AND VALIDATED HEAT AND MASS TRANSFER VEGETATED ROOF MODELS IN MATLAB FOR RETAIL BUILDING ENERGY SIMULATIONS IN SEMIARID CLIMATES

CAMILO IGNACIO PINTO CUEVAS

Thesis submitted to the Office of Research and Graduate Studies
in partial fulfillment of the requirements for the degree of
Master of Science in Engineering

Advisor:
SERGIO VERA ARAYA

Santiago de Chile, June, 2017

PONTIFICIA UNIVERSIDAD CATOLICA DE CHILE
ESCUELA DE INGENIERIA

COUPLING ENERGYPLUS AND TWO IMPROVED AND VALIDATED HEAT AND MASS TRANSFER VEGETATED ROOF MODELS IN MATLAB FOR RETAIL BUILDING ENERGY SIMULATIONS IN SEMIARID CLIMATES

CAMILO IGNACIO PINTO CUEVAS

Members of the Committee:
SERGIO VERA ARAYA
MARCELO GONZALEZ HORMAZÁBAL
PAULO CÉSAR TABARES-VELASCO
WALDO BUSTAMANTE GÓMEZ
IGNACIO CASAS RAPOSO

Thesis submitted to the Office of Research and Graduate Studies
in partial fulfillment of the requirements for the degree of
Master of Science in Engineering

Santiago de Chile, June, 2017

ACKNOWLEDGEMENTS

This work was supported by the National Commission for Science and Technology (CONICYT) under the research grant FONDECYT N° 1150675. The author also gratefully acknowledge the research support provided by the Center for Sustainable Urban Development (CEDEUS) under the research grant CONICYT/FONDAP 15110020.

Apart from the supporting entities, I would like to thank my advisor Dr. Sergio Vera and to Dr. Paulo Tabares, who constantly helped me, guided me, and gave me very important opportunities such as researching abroad.

I would also like to specially thank Nick Kincaid from Colorado School of Mines, who implemented the thermal inertia in the MATLAB model of Dr. Paulo Tabares and stabilized and calibrate the model against the experimental data of Chicago; to Cristian Godoy, who performed constantly the maintenance of the laboratory LIVE, the installation of the sensors, the and the measurement of the experimental data; and to Fabien Rouault, from the civil construction school of the Pontificia Universidad Católica de Chile, who guided me in the use of MLE +. Without their help, this work would have been much harder.

Finally, I would like to dedicate some lines to thank to my family, girlfriend and friends who, although not having anything to do with my research, helped me during my whole MSc by constantly giving me support.

TABLE OF CONTENTS

Pag.

LIST OF TABLES

Pag.

LIST OF FIGURES

Pag.

RESUMEN

Los edificios consumen un 32% de la energía a nivel mundial. Del consumo total correspondiente a edificios, un 17% es atribuible a edificios de retail. Considerando que estos edificios se caracterizan por contar con una gran superficie de techo en comparación a la de sus muros, las cubiertas vegetales se presentan como una opción viable para disminuir su consumo energético.

Para estimar la disminución de ahorro energético con el uso de esta tecnología, diversos modelos de transferencia de calor y masa en cubiertas vegetales se han desarrollado en los últimos 25 años. A pesar de contar con estas herramientas, ni uno de estos modelos ha sido desarrollado para climas semiáridos. Del mismo modo, a pesar de asegurar la disminución del consumo energético en edificios, ni uno de estos modelos ha sido validado mediante consumo de energía ni considerando las condiciones interiores de un edificio real. Dado que se cuenta con muy pocas herramientas de apoyo al diseño de cubiertas vegetales que ayuden a optimizar su desempeño energético en climas semiáridos, el propósito de esta tesis es el desarrollo y validación de una herramienta de simulación que considere el acoplamiento de dos modelos de cubiertas vegetales implementados en Matlab con el software de simulación energética de edificios EnergyPlus. Los modelos fueron validados considerando 3 diferentes cubiertas vegetales ubicadas en el Campus San Joaquín de la Pontificia Universidad Católica de Chile, ubicada en la ciudad de Santiago.

Palabras Claves: Cubiertas vegetales, transferencia de calor y masa, consumo de energía, clima semiárido.

ABSTRACT

The building sector represents 32% of the global energy use. The 17% of the total energy consumption of buildings is attributable to retail buildings. Considering that these buildings are characterized by a greater roof surface compared to the walls surface, the vegetative roofs -so called green roofs- are a viable option to reduce their energy consumption.

In order to estimate the reduction of energy savings with this technology, several models of heat and mass transfer in vegetated roofs have been developed in the last 25 years. Despite having these tools, none of these models has been developed for semiarid climates. In the same way, in spite of ensuring the reduction of energy consumption in buildings, none of these models has been validated by energy consumption, nor considering the interior conditions of a real building.

Due to there are few tools for supporting the design of vegetated roofs in order to optimize its energy performance in semiarid climates, the purpose of this thesis is the development and validation of a simulation tool that considers the coupling of two models of vegetated roofs implemented in Matlab with the building energy simulation software EnergyPlus. The models were validated considering 3 different vegetal covers located in the Campus San Joaquín of the Pontifical Catholic University of Chile, located in the city of Santiago.

Keywords: Vegetative roof, heat and mass transfer, energy consumption, semiarid climate.

1. INTRODUCTION

1.1 Background

To fully understand the importance of vegetative roofs, it is fundamental to understand what benefits can be achieved with this type of technology. For this reason, a brief description of the impact of building energy consumption on greenhouse gas emissions and global warming will be given, and then it is indicated how well-designed green roofs, can be a solution to mitigate these problems.

1.1.1 Impact of energy consumption of buildings on the emission of greenhouse gases (GHG)

In recent years, cities are using more land to accommodate the increasing population and migration from rural areas to the cities (Antrop 2004). This worldwide phenomenon is increasing the demand for new buildings as well as land, water, and energy. The demand may increase even more in the future because of the economic growth of undeveloped and developing regions (Valipour 2014, Valipour 2015).

In particular, the building sector represents 32% of the global energy use in 2010 and causes one-third of the greenhouse gas (GHG) emissions (Lucon et al. 2014, OECD/IEA 2013). In Chile, this sector is responsible for 28.8% of total energy consumption (MinEnergía 2013). Therefore, building energy efficiency plays a key role to limit the global warming and mitigate the impacts of climate change since the majority of these emissions are attributable to electricity consumption for heating, ventilation, air conditioning (HVAC), lighting and equipment operation, which is generated mostly

from fossil fuels such as gas, coal, and oil. This can be achieved by reducing energy consumption during the operation phase of buildings, because this corresponds to more than 80% of the GHG emission during the life cycle of buildings (UNEP 2009).

1.1.2 Energy Consumption of Retail store buildings

In Canada, of the total energy consumed by buildings, 17% is attributable to retail buildings (Oee.nrcan.gc.ca, 2017). This entails both a high GHG emission and a high operational cost. Retailers are implementing strategies to reduce operational cost due to the increased competition. In particular, the profit margin of retail stores is very low, thus operation cost savings can produce important profit increments as energy related costs account for a significant portion of the operational costs (Richman & Simpson 2016). Jamieson (2014) reports energy consumption reduction by 15% increases profit margin of retailers from 4% to 4.75%. Additionally, Jamieson et al. (2016) shows that big-box retail stores in US can reduce energy consumption up to 20-30%. Energy consumption profiles vary significantly between food and non-food retail stores because of the use of refrigeration. In Canada, the average energy intensity use of food and non-food retail stores is around 805 and 388 kWh/m2·year, respectively; while in US, the energy consumption is 549 and 172 kWh/m2·year in food and non-food retail stores, respectively (EPA 2008). Energy consumption associated to HVAC is 20% of the total energy use in food retailers, while it is 40% in non-food retailers (Jamieson 2014).

1.1.3 Relevance of building envelope in the energy consumption of buildings

Several alternatives can be considered in order to reduce the energy consumption of these buildings during the operation phase, such as incorporating the use of renewable energy in their designs (i.e. solar thermal systems and photovoltaic panels); as well as innovating in façade designs that contribute to the reduction of heating and cooling loads (GhaffarianHoseini et al., 2013). Diverse studies evaluate the effectiveness of upgrading the building's envelope on the energy consumption of buildings. For example, Basarir et al. (2012) found that improving the building's envelope in schools in Istanbul (Turkey) can be achieved reduction of 66% on the annual fuel cost. In another study, Osama et al. (2015) found that retrofitting strategies in the envelope of university building in Tripoli (Lebanon) could reduce energy use up to 28%. Also, Aboulnaga et al. (2016) indicate that in university buildings in Cairo (Egypt) that using improved glazing, insulation and vegetated roof can be achieved reductions in the electrical energy consumption of 15%. This energy saving can be achieved by reducing the conductive heat fluxes though the building’s envelope. Among building, big-box retail stores have a large roof surface and only one or two stories (Figure 1). Thus, it matches vegetated roof ideal building geometry to obtain highest benefits.

Figure 1: Examples of big-box retail store buildings

1.1.4 ¿What are the vegetated roofs?

Vegetated roofs, so called green roofs, are a technology that has shown to save energy in buildings, through the use of vegetation on its outermost layer.

The literature shows that several types of green roofs have been used for centuries (Williams et al. 2010, Peri et al. 2012, and Berardi et al. 2014). The first recorded roof gardens are the ancient ziggurats of Mesopotamia between 4.000 and 600 BC (Shimmy 2012). Later, during the fifth century were implemented in Babylon, the hanging gardens, another type of vegetated roof (Williams et al. 2010). Roman culture also considered roof gardens in its architecture. For example, roof garden was found in the Villa of Mysteries, near the northwest gate of Pompeii. The Villa was a U-shaped terraced arcade where vegetation grown directly in the substrate above the roof (Kohler et al. 2002). Vegetated roofs have also been presented in the vernacular architecture in

Northern European countries. For example in Norway, Sod roofs were roofs with a top layer of substrate, with grasses and other plants to stabilize the earth on the roof. Sod roofs provided insulation, mitigated damage to the roof from the rain, and bound and strengthened the roof structure due to the root system (Coutts et al. 2013). During the twentieth century, vegetated roofs were reconsidered in the buildings by the Swiss architect Le Corbusier who included them in the five points of modern architecture (Eisenman 2006). He considered the roof to be an exterior room of the building, being a place to be within and to look without. Considering the aforementioned, several architects acknowledge the vegetated roofs as a method to combine buildings and nature. The vegetative roofs are composed of several layers that play a key role in the performance of the system (Berardi et al 2014). From the inner to the outermost layer vegetated roof are composed by:

- Roof's structural layer: It supports the vegetative roof.
- Thermal insulation layer: It may not be necessary to use it. Usually, it decreases the heat flux through the roof.
- Waterproofing membrane: Film necessary to avoid leakage of water from the substrate to the interior of the building.
- Root barrier: Film necessary to prevent the penetration of the waterproofing layer by roots, which can cause water leaking into the roof structure.
- Drainage layer: Layer necessary to drain the excess of water from the roof. Also it is used as reservoir of water.

- Geotextile filter: Film necessary to prevent the blocking of drainage due to the fine particles of the substrate.
- Substrate: Soil layer necessary to accumulate water and other minerals for vegetation layer.
- Vegetation: Layer of vegetation such as mosses, herbs, grass, shrubs, small trees, etc., that provides shade to the substrate. This layer also provides evaporative cooling to the roof by the evapotranspiration process of the plants.

The vegetated roof composition layers are presented in Figure 2.

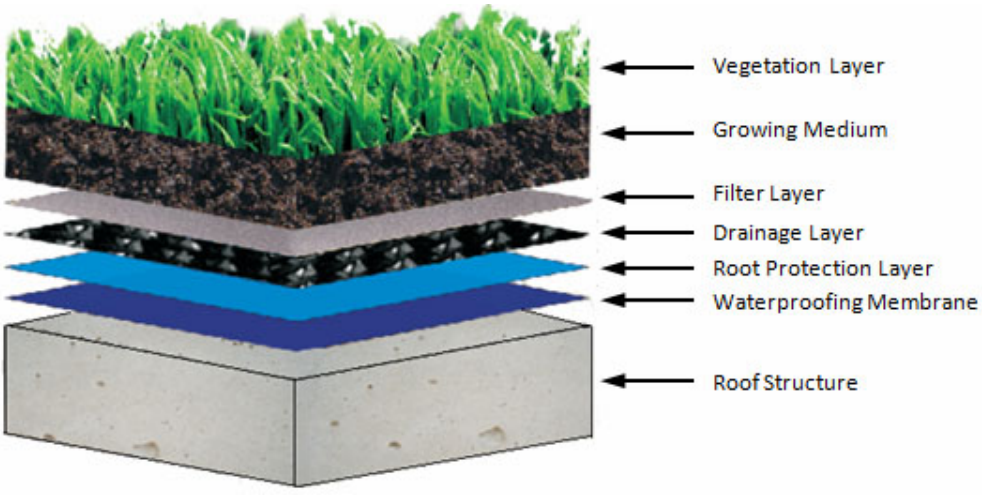

Figure 2: Layers composing a vegetated roof

Vegetated roof substrates are commonly composed of aggregate, sand and organic matter. This last element provides nutrients to the vegetation. Nevertheless, high levels of organic matter are not recommended due to its decomposition, resulting in substrate shrinkage and leaching of nutrients such as nitrogen and phosphorus in the water runoff.

These substrate compositions generally are not natural occurring soils, which are classified by their composition, shape and texture as clay, sandy loam, silt, etc. (Sailor & Hagos 2011).

According to its composition, vegetated roof can be classified as extensive, semi-intensive, and intensive. The extensive vegetated roof considers a thin layer of substrate (< 15 cm depth), which can support lighter plants. The irrigation and maintenance requirement are low. The vegetation considered for these roofs usually includes mosses, succulents, herbaceous plants and grasses. Also these roofs are not designed to be accessible to people. As for intensive roofs, they considers a thicker substrate depth (> 20 cm) allowing a large variety of plants, shrubs and occasional trees. For this reason, irrigation and high maintenance is required. These roofs are usually designed to be accessible to people for recreational purposes. Figure 3 (a) shows an extensive vegetated roof, while Figure 3 (b) presents an intensive vegetated roof. As for the semi-intensive roofs they are a hybrid vegetated roofs with characteristics between the extensive and intensive roofs. Table 1 shows the classification of vegetative roofs based on Berardi et al. (2014).

Table 1: Classification of vegetative roof and its main characteristics

Attribute	Extensive	Semi-intensive	Intensive
Substrate thickness	Under 15 cm	Between 15 - 20 cm	Above 20 cm
Accessibility	Inaccessible (fragile roots)	Accessible	Accessible (can be used as recreational space)
Weight	60-150 kg/m^2	Between 150 – 300 kg/m^2	Above 300 kg/m^2
Diversity of vegetation	Low (mosses, herbs and grass)	Greater plant diversity compared to extensive	High (perennials, shrubs and trees)

Construction	Easy	Technically complex	Technically complex
Irrigation	Low water requirement	Drainage and irrigation systems required	Drainage and irrigation systems required
Maintenance	Simple	Average amount	Complicated
Cost	Low	Moderated	High

Figure 3: Types of vegetated roof. (a) Extensive, and (b) Intensive

1.1.5 Vegetated roofs in Chile

According to a cadaster developed by the Laboratory of Vegetative Infrastructure of Buildings (LIVE, for the acronym in spanish), until 2014 there were 50.000 m^2 of vegetated roofs built in Chile; where the 90% of these are located in the Región Metropolitana. The study also projected for the year 2020, to increase the constructed vegetated roof surface to 240.000 m^2 (Chile Desarrollo Sustentable, 2017).

However, the technology currently implemented comes from more rainy or cold places in the US and Europe, so it is not well designed for optimal performance in the semiarid climate of the central zone of Chile. According to Köppen-Geiger climate classification, the semiarid climates are characterized by high temperatures in summer, a high thermal oscillation, high solar radiation; and scarce rainfalls. For this reason, almost 98% of the vegetation used is foreign, thus about 75% of the vegetated roofs has high water

consumption. Nonetheless, when the vegetated roofs are well designed they offer several benefits for both the building and its surroundings.

1.1.6 Benefits of vegetative roofs

Along with the previous characterization, Berardi et al. (2014) present a list of the main benefits of vegetative roofs. These are summarized in Table 2.

Table 2: Environmental benefits of vegetative roofs

Environmental benefits of vegetative roofs	Remarks for environmental benefits	Source
Reduce Energy Consumption	Decrease cooling and heating loads	Wong et al. 2003; Sailor, 2008; Alexandri & Jones, 2007; Kumar & Kaushik, 2005; Vera et al. 2015; Squier & Davidson, 2016; Erdemir & Ayata, 2017.
	Improve environmental temperature	Kumar & Kaushik, 2005; Erdemir & Ayata, 2017
Urban heat island	Decrease heat island effect	Lehmann, 2014; Kolokotsa et al. 2013; Santamouris, 2014.
	Reducing carbon footprint	Chen, 2014.
Mitigation of environmental pollution	Improve urban air quality	Chen, 2014.
	Mitigating air pollution	Alexandri & Jones, 2007; Oberndorfer, 2007; Getter et al. 2009; Zhang et al. 2012.
Water management	Improve runoff quality	Berndtsson, 2010.
	Improve use of rainwater	Sun et al. 2013.
	Improve urban hydrology	Chen, 2014.

Noise Absorption	Noise insulation	Van Renterghem et al. 2013; Van Renterghem & Botteldooren, 2014
	Noise Absorption	Yang et al. 2013.
Ecological preservation	Increase usable surfaces	Chen, 2014.
	Provide biodiversity	Wolf et al. 2008.

Despite the several benefits offered by the vegetated roofs, this study is mainly focused on its capacity of reduce the energy consumption.

1.1.7 Influence of vegetative roofs on energy consumption of buildings

Despite the large number of studies in the literature about the energy performance of vegetative roofs, it is difficult to predict the energy performance of vegetated roofs due to the several factors affecting its calculation, such as the climate, the architecture, the construction material, and the vegetated roof composition. For this reason there is great variability in the results obtained. For example, Ascione et al. (2013) finds cooling energy savings between 1 and 11% from using a vegetated roof in a 1-story office building in different warm European climates and cooling energy saving up to 7% in cold climates of Europe. Another study compares the thermal performance of a supermarket in Athens, Greece with concrete slab roof and a vegetated roof (Foustalieraki et al. 2016). They find that the supermarket with the vegetated roof showed a reduction of cooling and heating loads up to 18.7% and 11.4%, respectively. In contrast, Julia et al. (2013) find no annual energy savings due to vegetated roof in

mock up buildings in Pennsylvania (USA). In terms of the impact of vegetated roofs on the thermal performance of the roof itself, the canopy and the substrate play a key role in the thermal and energy performance of the system. The most commonly canopy design parameters that have boon studied are: leaf area index (LAI), stomatal resistance, height of plants, leaf reflectivity and leaf emissivity. By LAI refers to the density of leaf of the plant working photosynthetically. In addition substrate parameters are: thermal conductivity, heat capacity, density, and thickness.

Several parametric studies evaluate the impact of some of these design parameters on the building thermal performance showing variability among them. For example, Wong et al. (2003) show that the variation of vegetation type, volumetric water content (VWC) and substrate thickness cause energy savings between 1% and 15% in a 5-story commercial building in Singapore. In a Mediterranean climate, Theodosiou (2003) shows that LAI is the most important parameter that influences the thermal performance of the vegetated roof because LAI increases its cooling capacity by means of evapotranspiration. Another study indicates that LAI is the most important parameter that affects the energy performance of the buildings studied in US cold climates, while higher substrate depth reduces the heating energy consumption. However, most vegetated roof models have not been validated in winter conditions (Sailor et al. 2012). Similarly, Vera et al. (2015) find that cooling loads of a supermarket in a semiarid climate are significantly influenced by LAI, whereas heating loads are mainly influenced by the substrate thermal properties.

The variability among the results gets increased when it is considered the implementation of roof thermal insulation. For example, in a study carried out in a Mediterranean climate, Silva et al. (2016) show cooling energy demand of a room with an insulated vegetated roof is slightly larger than that for a traditional roof. Jaffal et al. (2012) finds energy savings between 10% and 48% for insulated and uninsulated vegetated roofs of a single-family house in the Oceanic climate of La Rochelle (France), respectively, in comparison with conventional roofs. Likewise, Niachou et al. (2001) shows energy savings up to 2%, 7% and 48% for high-insulated, moderate insulated and non-insulated vegetated roofs, respectively, for an office building located in the Mediterranean climate of Athens (Greece). Another study concludes that the modest building energy savings obtained with vegetated roofs were caused by the high level of thermal insulation of the roofing system (Sailor et al. 2012). In an experimental study, Zhao et al. (2014) evaluates the vegetated roof thermal performance for four U.S climate zones and concluded that the insulation layer limited the impact that the vegetated roof have on reducing heat flux through the roof. Finally, an experimental study evaluates the influence of an insulation layer on the cooling energy consumption of houses with vegetated roof in the subtropical climate of Hong Kong (Jim 2014). Depending on the plant species, the cooling energy consumption varies between 5% lower and 18.3% higher for an uninsulated vegetated roof than the insulated scenario.

1.1.8 How can vegetative roofs reduce energy consumption in buildings?

There are several studies that analyze the influence of vegetative roof on energy performance of buildings. These studies also refer to the main mechanisms used by

vegetative roofs to achieve this decrease in energy consumption (Berardi 2014, Castleton 2010, Fioretti 2010, Tabares-Velasco 2009). These may include:

- Thermal inertia of the substrate: The substrate contributes with thermal mass that helps to stabilize the indoor temperatures. For this reason, there is a reduction of the peak loads.
- Shading of vegetation: Vegetation provides a layer that shades the substrate. For this reason, the radiation absorbed by the roof and its surface temperature are lower. This contributes to reduce the heat fluxes through the roof towards the interior of the building, and therefore its cooling loads. Weng (2014) showed that 60% of the radiation that reaches the vegetative roof is absorbed by the vegetation and used for the evapotranspiration process, whereas 20% is reflected, thus transmitting only 20% to the substrate.
- Evapotranspiration: This process considers the evaporation of the water contained in the substrate and the water used by the plants in their transpiration process. This means the water present on the roof turns into water vapor thus absorbing energy. As a result, this process cools the surface of the vegetative roof, decreasing the heat flux towards the interior of the building.
- Thermal insulation of the substrate: The implementation of an extra material layer decreases the U-value of the roofing system. As a result, reductions of the heat fluxes through the roof can be achieved. This phenomenon depends directly on the type of substrate considered and its moisture content.

Due to the biophysics processes of the plant and the volumetric water content (VWC) present in the substrate there are several parameters that affect the previous mechanisms.

1.1.9 Parameters that affect the energy performance of vegetative roofs

Among the vegetation parameters that affect the evapotranspiration and the shading provide by the canopy can be considered the LAI, the stomatal resistance, and the angle of the leaf. The LAI is defined as the one-sided green leaf area per unit ground surface area, so it corresponds to the "density" of leaf of the plant working photosynthetically. Stomatal resistance corresponds to the resistance of plants to transpiration of water vapor during photosynthetic processes. While the angle of the leaf affects directly to the amount of radiation retained by vegetation.

Some studies report that the LAI is the main parameter of the vegetation that influences the performance of the vegetative roof (Jaffal et al., 2012). Theodosiou (2003) demonstrated that LAI is the main parameter of vegetation affecting surface temperatures and heat fluxes through the roof. At the same time the study showed that the height of the plant does not show a considerable impact in the results in comparison to the LAI.

As for the parameters of the substrate that affect the inertia and thermal insulation of the substrate can be mentioned the thermal conductivity of the substrate, its density and its specific heat. These three parameters depend directly of the VWC present in the substrate.

Studies have demonstrated the direct relationship between the thermal properties of the substrate and the substrate's VWC (Sailor 2011). For example Figure 4 presents the relationship between the substrate thermal conductivity and the moisture in the substrate.

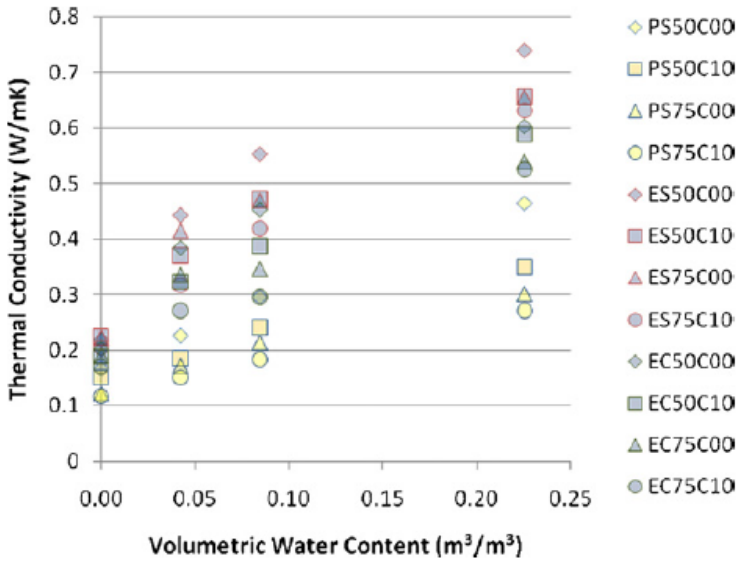

Figure 4: Thermal conductivity as a function of the moisture content on the substrate (Sailor, 2011).

Considering the previous parameters and mechanisms several heat and mass transfer vegetated roof models have been developed in the last three decades.

1.1.10 Heat and mass transfer vegetated roof models

Between the years 1982 and 2017, 18 vegetated roof models have been developed in order estimate the thermal performance of vegetative roofs. Figure 5 shows that most of simulation models have been developed since 2010s.

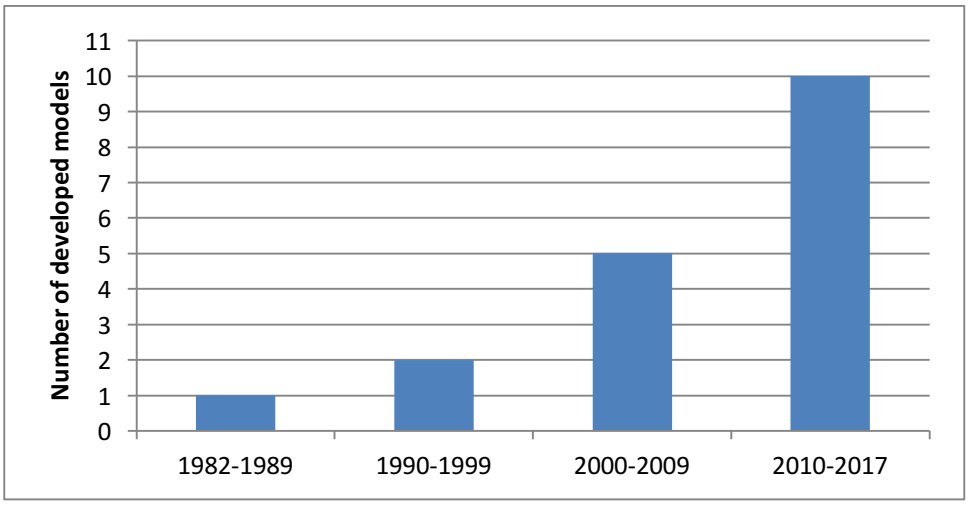

Figure 5: Number of vegetated roof models developed in the last decades.

Developing an analysis of the climatic data considered for the development and validation of the models, it was observed that the 33.3% of the models were made for humid subtropical climates; while the 22.2% have been developed for oceanic climates. However, no models have been developed for semiarid climates. Figure 6 presents the number of models developed for different climates according to Köppen-Geiger classification.

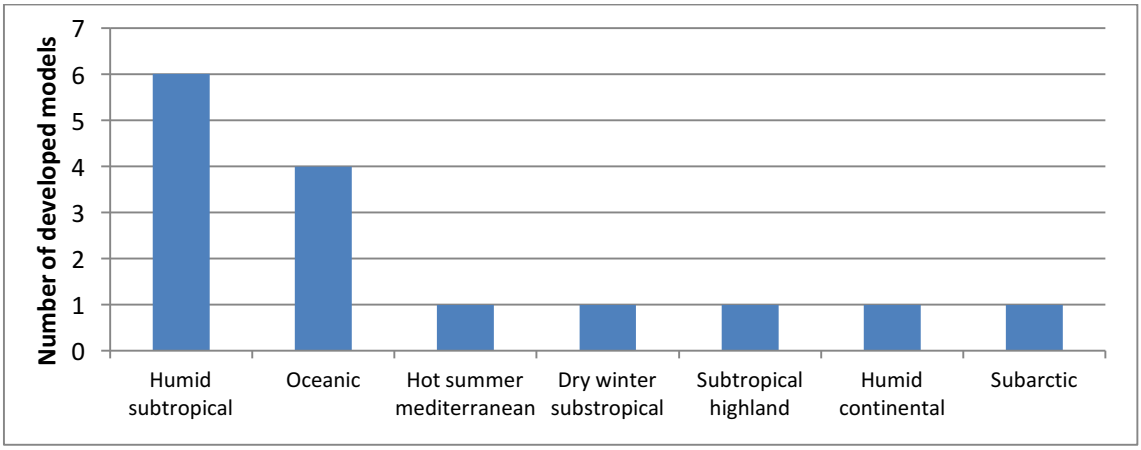

Figure 6: Number of model developed according to Köppen-Geiger climate classification.

Table 5 presents the outputs considered in these vegetated roof models. Despite the literature review dictates that vegetative roof improves the energy performance of buildings, these models have only been validated by surface temperatures, heat flows through the roof, evapotranspiration rates, net radiation above the roof, and by the VWC of the substrate. Also there are a few models that have not been validated against experimental data.

Table 5: Output considered for validation of vegetative roof models.

Surface temperature	**ET**	**Heat flux**	**Net radiation**	**VWC**	**Not validated**
Nayak 1982 Alexandri 2007 Sailor 2008 Tabares 2011 Ouldboukhitine 2011 Tabares 2012 Wang 2013 Chen 2015 Heidarinejad 2015 Quezada 2017	Lazzarin 2005	Jim & He 2010 Tabares 2011 Tabares 2012 Chen 2015	Jim & He 2010 Tabares 2011 Tabares 2012 Wang 2013	Alexandri 2007 Wang 2013	Nayak 1982 Del Barrio 1998 Takebayashi 2006 Tiana 2015

However none of these models have been validated by energy consumption, or considering the interior conditions of the building coupled to the vegetated roof model. For this reason, there is no certainty that vegetative roof models are good buildings energy performance estimators.

These models represent the heat and mass transfers in the vegetative roof, which are complex processes that consider diverse variables, such as the short-wave and long-wave radiation, convection, conduction and evapotranspiration.

Refahi et al. (2015) emphasized that for a correct analysis of the impact of vegetated roof on the energy consumption it is necessary to consider the following phenomena:

- Short and long wave radiative exchange within the plant canopy
- Conductive heat transfer (and storage) in the substrate
- Convective heat transfer between the substrate-foliage system and the air
- Latent heat transfer by evapotranspiration in the foliage and soil

Although there are common aspects in the developed models, there are still many differences among them. For example, evapotranspiration can be modeled by vapor pressure difference (VPD), Bowen's ratio or by the FAO-Penman Montheit equation. The modeling of stomatal resistance, depending on the moisture content of the substrate, the wind velocity, the ambient temperature and the type of plant (among other factors) can also be modeled in several ways (Tabares-Velasco 2012). Despite many of the models consider the relation of the substrates properties with VWC, most of them do not consider the increase or decrease of the moisture content due to irrigation, rainfall, drainage and evapotranspiration (Tabares- Velasco 2012).

Notwithstanding many vegetated roof models have been developed, only the model of Sailor (2008) was implemented in the building energy simulation tool called EnergyPlus. This software is a free energy simulation tool developed by the U.S. Department of Energy (DOE). Due to EnergyPlus does not have a user-friendly graphical interface, the projects should be entered by command lines. For this reason, users require specific knowledge in order to use this software. This implies that the studies on the influence of vegetative roofs on building energy consumption can not be properly used by vegetative roof designers (i.e. architects, engineers). Furthermore, if they are really interested in consider all the benefits of this technology, beyond the

aesthetic benefits, they should explore the literature. The previous process requires time they do not have product of the shorts constructions periods. Despite that this software allows the users to select different values for the vegetated roof parameters, it only offers very limited ranges for design.

1.2 The problem

From the previous sections it is possible to observe a large number of heat and mass transfer vegetated roof models developed in the last three decades. However, none of these models have been developed for semi-arid climates.

Despite these models and a large number of studies claim that it is possible to achieved energy savings by the implementation of vegetative roofs, there are no validated models through building energy consumption neither through substrate surface temperature considering the coupling of the green roof to a building.

Also, only one of these models has been currently implemented in building energy simulation tool EnergyPlus. Nevertheless, (1) the users required specific knowledge in order to use this software, and (2) this tool offers limited design options to users.

For this reason is difficult for designers of vegetative roofs (i.e. architects, engineers) to fully take advantage of the energy performance benefits of this technology.

Thus, flexible validated simulation tools that allow evaluating the design parameters of vegetative roofs that affect the energy performance of retail store buildings in semi-arid climates are required.

1.3 Hypothesis

Coupling vegetated roof models with EnergyPlus provide an accurate estimation of the energy performance of retail store buildings in semiarid climates.

1.4 Objectives

The general objective of this research:

- Is to couple two heat and mass vegetated roof models with EnergyPlus to evaluate the influence of vegetated roof on the energy performance of retail store buildings in semi-arid climates.

The specific objectives are as follows:

1. Evaluate the current vegetated roof model implemented in EnergyPlus.
2. Implement Tabares and Sailor vegetative roof models in MATLAB.
3. Add thermal inertia to the vegetated roof models of Tabares and Sailor.
4. Validate Tabares and Sailor vegetative roof models in semiarid climate against experimental data.
5. Couple Tabares and Sailor vegetative roof models to EnergyPlus through MLE+.
6. Validate the coupled models to EnergyPlus in semiarid climate against experimental data.
7. Determine the main parameters of the vegetative roofs that influence the energy performance of retail store buildings in semi-arid climates.

1.5 Scope

The scope of research considers the following topics:

- Extensive vegetative roofs: A substrate layer with a thickness lower than 15 cm with low height vegetation will be considered.
- Climate: The semi-arid climate will be considered for the study.
- Vegetative roof models: Modelling in MATLAB heat and mass transfer vegetated roof models.
- Co-simulation: Vegetative roof models coupled with EnergyPlus through the MLE+ toolbox.
- Validation: Through experimental data recorded in LIVE laboratory located in San Joaquín campus of the Pontificia Universidad Católica de Chile; and in commercial building located in Chicago, Illinois. This last field data correspond to the original data considered by Professor Tabares in the validation of his vegetated roof model.

1.6 Methodology

The methodology used in this research is composed of several methods, where the literature review is constant and extensive throughout the research process.

In order to demonstrate the hypothesis presented in the previous section, the following methodology is proposed:

a) Literature review: It corresponds to both the revision of the theory and of the heat and mass transfer models developed for vegetative roofs. This focuses on phenomena of transport, climatology and environmental biophysics. In the literature review of heat and mass transfer models, are considered the 18 models developed since 1982.

b) Qualitative evaluation of vegetative roof models: Once all models have been reviewed, a qualitative comparison is made between them in order to select 2 models to be implemented in MATLAB. Here the following points will be considered:

    i. **Transport phenomena considered:** models that consider mass and energy balances simultaneously will be prioritized for the implementation. These models represents more accurately, compared to models that only consider energy balance, the behavior of vegetated roofs. However if a model with only energy balance is selected, it should be possible to add mass balance in later stages.

ii. **Assumptions considered:** Several models consider assumptions that are not completely valid to simplify analyzes. One of the most common is to consider that the substrate thermal conductivity does not vary with the moisture content, which in itself is not true because it does it linearly. At the same time, simplifications can be found in the way of measuring the evapotranspiration of the substrate, so it would be prioritized models that consider the variation of moisture content, LAI, stomatal resistance, radiation and vapor pressure differential.

iii. **Implementation in building energy simulation tools:** models that have been currently added to building energy simulation tools will be prioritized for the implementation.

c) Evaluation of the vegetated roof model currently implemented in EnergyPlus: The model available in EnergyPlus will be evaluated for different cities with semiarid climate, different vegetated roof compositions, and different construction materials for the roof structure. The results of this stage will give an idea of how the vegetated roof models to be later implemented in Matlab should work, and what results must be expected.

d) Implementation of vegetative roof models: Once the qualitative evaluation is completed, a quantitative evaluation of the 2 selected models is carried out. This will be done through the implementation of these models in MATLAB, considering as input the environmental data recorded in the LIVE laboratory

during the year 2017; as well as data recorded in a commercial building in Chicago during July 2007. The purpose of this stage is to know how these models behave among themselves. In order to implement correctly these models is necessary to fully understand the phenomena behinds the equations. This is not an easy task considering that not all the equations or assumptions considered are always available in the published studies. Since not all the developed models have implemented the substrate thermal inertia, it will be incorporated through the use of finite differences. This method allows considering several material layers in the vegetated roof composition and to vary the volumetric water content in the substrate. To analyze the results, substrate surface temperature was recorded in the laboratory LIVE, in order to compare these temperatures against the calculated by the mathematical models.

e) Validation of vegetative roof models: Once the 2 models have been implemented in MATLAB, they are validated with experimental data recorded in LIVE laboratory located in San Joaquín campus of the Pontificia Universidad Católica de Chile; and in a commercial building located in Chicago, Illinois.

f) Coupling of vegetated roof models with EnergyPlus: In order to check the hypothesis presented, the two implemented and validated vegetated roof models are coupled with EnergyPlus through MLE+.

g) Validation of coupled vegetative roof models: Once the 2 models have been coupled with EnergyPlus, they are validated with experimental data recorded in

LIVE laboratory located in San Joaquín campus of the Pontificia Universidad Católica de Chile.

h) Data analysis: Once the validated and coupled heat and mass transfer vegetative roof model is available, it is possible to evaluate the influence of the vegetation and substrate parameters on energy consumption. Thus, the variables to be considered in this phase are:

- Independent variables
    - Height of the vegetation (from 0.1 to 0.3 m increasing by 0.1 m)
    - LAI (from 1.0 to 5.0 increasing by 2.0)
    - Minimum stomatal resistance (from 100 to 500 s/m increasing by 200 s/m)
    - Thermal conductivity of the substrate (from 0.5 to 1.5 W/mK increasing by 0.5 W/mK)
    - Specific heat of the substrate (from 1000 to 3000 kJ/kg increasing by 1000 kJ/kg)
    - Density of the substrate (from 500 to 1500 kg/m3 increasing by 500 kg/m3)
- Dependent variables
    - Substrate temperature
    - Thermal loads

1.7 LIVE laboratory description

The laboratory building consists of 4 modules with high level of thermal insulation in their walls and floors. For this reason, the facade can be assumed as adiabatic (except by the roof). This implies that all variations of temperature and consumption inside the laboratory are due to the heat transfer through the roof, which corresponds to a vegetative roof.

In the following figure, module D corresponds to a lightweight steel roof deck composed by two metal sheets of 2 mm with 5 cm of insulation, while modules A, B and C correspond to concrete slabs of 15 cm. Modules B, C and D have a floor surface of 5x5 m^2, whereas module A has an area of 7x5 m^2.

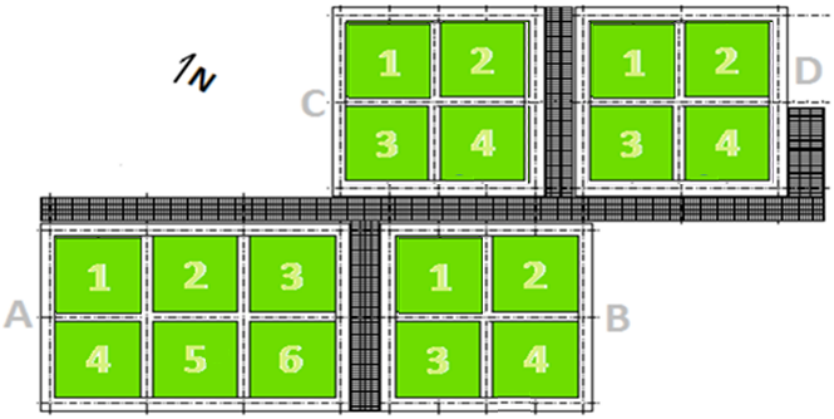

Figure 7: Laboratory layout. Floorplan.

A more detailed description of the laboratory and the measuring instruments is given in Chapter 4.

1.8 Thesis Structure

Besides this introduction, the thesis is composed by other four chapters, each one of them being an auto-contained journal article. Those chapters correspond to (2) Literature review of the heat and mass transfer models, (3) Influence of Vegetation, Substrate, and Thermal Insulation of an Extensive Vegetated Roof on the Thermal Performance of Retail Stores in Semiarid and Marine Climates, (4) Implementation and evaluation of two transient heat and mass transfer vegetated roof models for semiarid climate and humid continental climate, and (5) Coupling of the vegetated roof models implemented in MATLAB to EnergyPlus in order to identify the most important parameters that affect the energy performance of the vegetative roof. Chapter 3 corresponds to an already journal paper published in Energy & Building; while chapters 2, 4 and 5 are potential journal papers. It should be noted that chapters 4 and 5 are those that validate the hypotheses, and accomplish the general objective and the specific objectives of this thesis. Chapter 3 will evaluate the main vegetative roof parameters that influence the retail building energy performance with Sailor's vegetated roof model available in EnergyPlus (accomplishing partially the specific objectives); providing information on the operation of the vegetated roof models, and the results to be obtained in the Matlab simulations. Finally, chapter 2 will provide fundamental information to select the models considered in chapters 4 and 5.

1.9 Conclusions

The literature review developed in the chapter 2 of this thesis evaluates the 18 vegetative roof models that have been developed between 1982 and 2017. The main conclusions obtained show that the 33.3% of these models have been developed for humid subtropical climate and 22.2% for oceanic climate. However, no model has been validated for semiarid climates. Since the validation of vegetative roof models has been developed for other climates, there is no way to assert its correct performance for semiarid climates. Also, the 55.5% of the developed vegetative roof models has been validated with the substrate surface temperature, while the 22.2% has not been validated. Although the literature ensured that vegetative roofs improve the energy performance of buildings, no model has been validated by experimental measurements of neither energy consumption nor substrate surface temperature with the vegetative roof model coupled to building simulation software.

The conclusions of chapter 3 present that vegetation is more effective than insulation on reducing cooling loads due to the evapotranspiration of the vegetation-substrate system and canopy's shading effect. Actually, uninsulated vegetated roofs not only reduce roof's solar heat gains but also allow internal heat gains dissipate through the roof. In addition, thermal insulation can decrease the vegetated roof's ability to reduce cooling loads. Also, the results indicate that LAI is the most influential parameter of the vegetated roof in reducing the retail building cooling loads.

The conclusions of chapter 4 indicate that the substrate temperatures obtained in the implementation of the vegetated roof models in Matlab represent accurately the

experimental data collected in the vegetated roofs of Santiago and Chicago, thus the vegetated roof models of Tabares (2011) and Sailor (2008) are capable of represent accurately vegetated roofs in semiarid climates.

Finally, chapter 5 concludes that the coupled models with EnergyPlus are capable of simulate accurately vegetated roofs in semiarid climates. The simulations performed show that, similarly to chapter 3, LAI is the most influential parameter of the vegetated roof in reducing the cooling loads. Also, the results indicate that the presence of thermal insulation reduce the influence of the vegetated roof on the building thermal loads. However, this chapter shows that despite having 2 validated vegetated roof models against experimental data, these models will not necessarily behave in the same way in other scenarios because the models do not consider the same vegetated roof parameters ranges.

1.10 Perspective and future works

Considering the scope and results of the present study the following future work is proposed:

a) Add a full mass balance to the implemented vegetated roof models.

b) Evaluate different substrates with their hydraulic and thermal properties in order to add them to the implemented models. These studies are fundamental to develop an accurate balance mass transfer model.

c) Modify the implemented vegetated roof models in order to simulate green walls – so called living walls.

d) Evaluate the implemented vegetated roof models with other climates than the semi-arid and humid subtropical of Chicago.

e) Add to the current models a user-friendly interface in order to facilitate the use of the implemented models.

f) Translate the MATLAB code to Python due to the free available version of the latest.

2. LITERATURE REVIEW: A REVIEW OF SIMULATION MODELS OF HEAT AND MASS BALANCE IN VEGETATIVE ROOFS FOR THE EVALUATION OF ITS THERMAL AND ENERGETIC PERFORMANCE

2.1 Abstract

The vegetated roofs are an envelope building technology whose use has become more widespread in the last decade. However, to fully obtain the benefits of this technology is important to count with accurate numerical models that assist developers to design vegetative roofs. For this reason, several heat and mass transfer vegetated roof models have been developed in order to simulate the thermal performance of this roofing system.

This paper provides an overview of 18 vegetative roof models developed for the energy and thermal performance of buildings between 1982 and 2017. The purpose of this study is to understand how these models work and to obtain information that indicates if these models can be considered to design properly vegetative roofs for the semiarid climates.

The results of this research present that the 33.3% of the vegetative roofs models have been developed for humid subtropical climate, while the 22.2% for oceanic climates. No model has been validated for semiarid climates. Also, the 55.5% of these models has been validated with experimental data for the substrate surface temperature, while 22.2% of the models have not been validated. Despite the literature evidences that vegetative roofs improve the energy performance of buildings, no model has been validated by

experimental measurements of energy consumption. Thus, it can not be asserted that the developed models so far are good predictors of the thermal and energy performance of vegetative roofs in semi-arid climate, such as Santiago's climate.

2.2 Introduction

In recent years, cities are using more land to accommodate the increasing population and migration from rural areas to the cities (Antrop 2004). This worldwide phenomenon is increasing the demand for new buildings as well as land, water, and energy. The demand may increase even more in the future because of the economic growth of undeveloped and developing regions (Valipour 2014, Valipour 2015). In particular, the building sector represents 32% of the global energy use in 2010 and causes one-third of the greenhouse gas emissions (Lucon et al. 2014, OECD/IEA 2013). In Chile, this sector is responsible for 28.8% of total energy consumption between 2000 and 2016 (MinEnergía 2013). Therefore, building energy efficiency plays a key role to limit the global warming and mitigate the impacts of climate change because the majority of these emissions are attributable to electricity consumption for heating, ventilation, air conditioning, lighting and equipment operation. This electricity consumption is generated mostly from fossil fuels such as gas, coal, and oil.

This can be achieved by reducing energy consumption during the operation phase of buildings, because this corresponds to more than 80% of the GHG emission during the life cycle of buildings (UNEP 2009).

There are several alternatives to reduce the energy consumption of the buildings during their operation phase. For example, innovating in façade designs in order to reduce the heating and cooling loads (GhaffarianHoseini et al., 2013).

Within the advances existing in the last time in this topic has appeared as an option the use of vegetal roof façades. This kind of façades, so called green roofs, is a technology that, through the use of vegetation on its outermost layer, aims to improve the energy performance of roofs.

There are several studies that analyze the influence of vegetative roofs on energy performance of buildings. These studies also refer to the main mechanisms used by vegetative roofs to achieve this decrease in energy consumption of buildings (Berardi 2014, Castleton 2010, Fioretti 2010, Tabares-Velasco 2009). These may include:

- Thermal inertia of the substrate: The substrate contributes with thermal mass that helps to stabilize the indoor temperatures. For this reason, there is a reduction of the peak loads.
- Shading of vegetation: Vegetation provides a layer that shades the substrate. For this reason, the radiation absorbed by the roof and its surface temperature are lower. This contributes to reduce the heat fluxes through the roof towards the interior of the building, and therefore its cooling loads. Weng (2014) showed that 60% of the radiation that reaches the vegetative roof is absorbed by the vegetation and used for the evapotranspiration process, whereas 20% is reflected, thus transmitting only 20% to the substrate.

- Evapotranspiration: This process considers the evaporation of the water contained in the substrate and the water used by the plants in their transpiration process. This means the water present on the roof turns into water vapor thus absorbing energy. As a result, this process cools the surface of the vegetative roof, decreasing the heat flux towards the interior of the building.
- Thermal insulation of the substrate: The implementation of an extra material layer decreases the U-value of the roofing system. As a result, reductions of the heat fluxes through the roof can be achieved. This phenomenon depends directly on the type of substrate considered and its moisture content.

Due to the aforementioned, vegetative roofs are complex envelope systems, which have great potential to influence the energy performance of buildings. As result of all the parameters of the vegetated roof that impact on the building energy consumption it is not trivial to design vegetated roofs. Therefore, it is important to study the parameters of the substrate and vegetation involved on heat and mass transfer through the vegetative roof and the impact on the building energy performance.

2.2.1 Importance of vegetative roofs

Although most of studies indicate that vegetated roof cause building energy savings, it is difficult to evaluate the accuracy of these results, because there are other parameters that must be considered, such as internal heat gains (i.e. loads generated by people, lighting and equipment) and the heat gains and losses through the other envelopes, which are building parameters. Furthermore, these variables have a direct impact on the energy consumption for Heating, Ventilating and Air Conditioning (HVAC). For this reason,

despite the large number of studies in the literature about the energy performance of vegetative roofs, there is great variability among the results obtained.

For example, Ascione et al. (2013) finds cooling energy savings between 1 and 11% from using a vegetated roof in a 1-story office building in different warm European climates and cooling energy saving up to 7% in cold climates of Europe. Another study compares the thermal performance of a supermarket in Athens, Greece with concrete slab roof and a vegetated roof (Foustalieraki et al. 2016). They find that the supermarket with the vegetated roof showed a reduction of cooling and heating loads up to 18.7% and 11.4%, respectively. In contrast, Julia et al. (2013) find no annual energy savings due to vegetated roof in mock up buildings in Pennsylvania (USA). In terms of the impact of vegetated roofs on the thermal performance of the roof itself, the canopy and the substrate play a key role in the thermal and energy performance of the system. The most commonly canopy design parameters that have boon studied are: leaf area index (LAI), stomatal resistance, height of plants, leaf reflectivity and leaf emissivity. In addition substrate parameters are: thermal conductivity, heat capacity, density, and thickness.

Several parametric studies evaluate the impact of some of these design parameters on the building thermal performance showing variability among them. For example, Wong et al. (2003) show that the variation of vegetation type, volumetric water content (VWC) and substrate thickness cause energy savings between 1% and 15% in a 5-story commercial building in Singapore. In a Mediterranean climate, Theodosiou (2003) shows that LAI is the most important parameter that influences the thermal performance

of the vegetated roof because LAI increases its cooling capacity by means of evapotranspiration. Another study indicates that LAI is the most important parameter that affects the energy performance of the buildings studied in US cold climates, while higher substrate depth reduces the heating energy consumption. However, most vegetated roof models have not been validated in winter conditions (Sailor et al. 2012). Similarly, Vera et al. (2015) find that cooling loads of a supermarket in a semiarid climate are significantly influenced by LAI, whereas heating loads are mainly influenced by the substrate thermal properties.

Most of new buildings have insulated facades and rooftops. Nevertheless, there is a lack of studies on how this layer affects the thermal and energy benefits of vegetated roofs on buildings. For example, a study in the Mediterranean climate, Theodosiou (2003) concludes that the lack of insulation increases the cooling capabilities of vegetated roofs in summer. Also in a Mediterranean climate, Silva et al. (2016) show cooling energy demand of a room with an insulated vegetated roof is slightly larger than that for a traditional roof. Jaffal et al. (2012) find energy savings between 10% and 48% for insulated and uninsulated vegetated roofs of a single-family house in the Oceanic climate of La Rochelle (France), respectively, in comparison with conventional roofs. Likewise, Niachou et al. (2001) shows energy savings up to 2%, 7% and 48% for high-insulated, moderate insulated and non-insulated vegetated roofs, respectively, for an office building located in the Mediterranean climate of Athens (Greece). Another study concludes that the modest building energy savings obtained with vegetated roofs were caused by the high level of thermal insulation of the roofing system (Sailor et al. 2012).

In an experimental study, Zhao et al. (2014) evaluates the vegetated roof thermal performance for four U.S climate zones and concluded that the insulation layer limited the impact of the vegetated roof have on reducing heat flux through the roof. Finally, a unique experimental study of Jim (2014) evaluates the influence of an insulation layer on the cooling energy consumption of houses with vegetated roofs in the subtropical climate of Hong Kong (China). Depending on the plant species, the cooling energy consumption varies between 5% lower and 18.3% higher for an uninsulated vegetated roof than the insulated scenario.

At the same time it is possible to detect gaps in the assertion that vegetative roofs decrease the energy consumption of buildings. This is because several of the existing models have been validated by measurements of either surface temperatures or heat flux through the rooftops but not by measurements of heating and cooling loads (Sailor et al., 2012).

The only model that has been incorporated to EnergyPlus is Sailor's vegetated roof models (Sailor, 2008). This model has been validated by evaluating surface temperatures. Even though the green roof model developed by Tabares (2012) that is currently being incorporated into EnergyPlus was also validated against experimental surface temperatures.

2.2.2 Aim of the study

This study makes acritical review about the developments of the vegetative roof models. Between the years 1982 and 2017, different studies have been done in order estimate the

thermal performance of vegetative roofs. Figure 8 shows that most of simulation models have been developed since 2010s. Moreover, some of these models have been used in several studies to evaluate the impact of vegetated roof on building energy performance and the effect of specific vegetated roof parameters. The focus of this study is to evaluate qualitatively the advantages and disadvantages of the developed vegetated roof models in order select to two of them to be implemented in later stages of this study. These models will allow designing properly vegetative roofs for the semiarid climate. In order to achieve this, an analyze of the models has been done to understand how they work, which phenomena they consider, what are they inputs and outputs, what assumptions they consider and how and where they were validated.

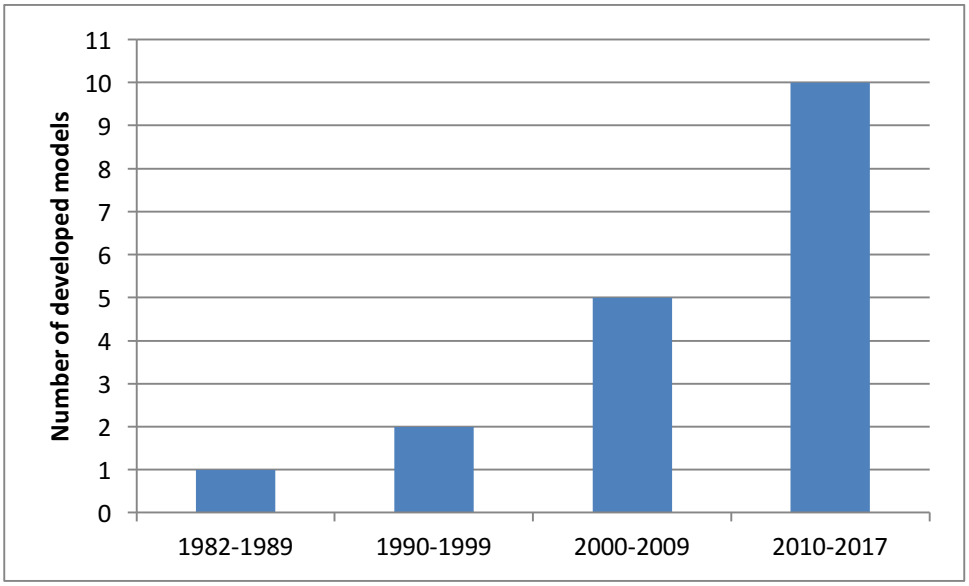

Figure 8: Number of vegetated roof models developed in the last decades.

2.2.3 Reviews of developed vegetative roof models

Up to the best of my knowledge, there are no studies focused on reviewing vegetative roof models that have been developed the last three decades. However three studies carried out to develop vegetative roof models include a brief review about some previous models (Djedjig et al. 2012, Tabares et al. 2012, and Chen et al. 2015).

Djedjig et al. (2012) considers the studies developed by Del Barrio (1998), Alexandri & Jones (2207), Sailor (2008), Jim & He (2010), Ouldboukhitine et al. (2011) and Tabares & Srebric (2011). This review briefly mentions the assumptions implemented in the studies and a short description of the models.

Tabares et al. (2012) consider the vegetative roof models developed by Nayak et al. (1982), Del Barrio (1998), Lazzarin et al. (2005), Gaffin et al. (2005), Takebayashi & Moriyama (2007), Alexandri & Jones (2207), Sailor (2008), and Tabares & Srebric (2011). Tabares et al. (2012) indicate that all the studied models consider heat balance, however not all of them consider simultaneously mass balance. This review also indicates the inputs considered for the evapotranspiration equations, the assumptions implemented in the models, the roof discretization used and the outputs considered for the validation of the models. Tabares et al. (2012) also indicate the assumptions mentioned in the studies are:

1. Plants and substrate of the vegetation roof are horizontally homogeneous.
2. Horizontal heat and mass transfer are negligible.
3. Air beneath stomata is saturated.
4. Photosynthesis of the plant result in negligible heat fluxes.

5. Conductive heat transfer in the plants is negligible.
6. Plants are well irrigated, healthy and in the fully growth.
7. Volumetric water content within the substrate is homogeneous.
8. Vegetation-substrate layer is free from mulch.
9. Green roof substrate is completely covered by plants.

On the other hand, Chen et al. (2015) review the models developed by Takebayashi & Moriyama (2007), Alexandri & Jones (2207), Sailor (2008), Ouldboukhitine et al. (2011), Djedjig et al. (2012), and Tabares et al. (2012). This study only considers the outputs used by the validation of the model, the substrate thermal properties behavior against the volumetric water content on it, and the lower boundary conditions considered in the energy balance.

Table 3 summarizes the relevant information of the heat and mass transfer vegetated roof models developed since 1982.

Table 3: Vegetative roof models for energy performance of buildings developed between 1982 and 2017.

Study	Authors - Year	Balance	ET	Stomatal resistance	Shading effect	Substrate thermal properties	VWC range	Thermal Inertia	Inputs	Outputs	Validation	City - Climate of validation
The relative performance of different approaches to the passive cooling of roofs	Nayak et al. 1982	Energy	VPD	Not considered	Percentage affecting incoming radiation	Constant	Not considered	Not considered	Weather data and substrates parameters	Substrate and Foliage temperature	Not validated	Not considered
A heat balance model for partially vegetated surfaces	Zhang et al. 1997	Energy	Estimated using a wind profile above and within the vegetation	Solar irradiance, air temperature and VPD	Percentage affecting incoming radiation	Constant	Wilting point and capacity field	Not considered	Weather data and surface temperatures	Substrate and Foliage temperature	Not validated	Not considered
Analysis of the green roofs cooling potential in buildings	Del Barrio 1998	Energy and Mass	VPD and stomatal resistance	Solar irradiance, air temperature and VPD	Extinction coefficient	Constant	Wilting point and capacity field	Considered	Weather data, substrate and plants parameters	Temperature profile and VWC	Not validated	Athens – Hot Summer Mediterranean
Energy balance modeling applied to a comparison of white and green roof cooling efficiency	Gaffin et al. 2005	Energy	Bowen Ratio	Not considered	Extinction coefficient	Constant	Not considered	Not considered	Weather data	Surface temperatures	Surface temperatures	State College - Subarctic
Experimental measurements and numerical modelling of a green roof	Lazzarin et al. 2005	Energy and Mass	Penman Monteith	Not considered	Extinction coefficient	Varies with VWC	Capacity field	Considered	Weather data and substrates parameters	Heat fluxes	Not validated	Vicenza - Humid subtropical
Developing a one-dimensional heat and mass transfer algorithm for describing the effect of green roofs on the built environment: Comparison with experimental results	Alexandri & Jones 2007	Energy and Mass	VPD, stomatal resistance and wind speed	Solar irradiance, air temperature and VPD	Percentage affecting incoming radiation	Varies with VWC	Wilting point and capacity field	Considered	Weather data, substrate and plants parameters	Temperature profile and VWC	Surface temperatures and VWC	Cardiff - Oceanic
Surface heat budget on green roof and high reflection roof for mitigation of urban heat island	Takebayashi & Moriyama 2007	Energy and Mass	Bowen Ratio	Not considered	Not considered	Varies with VWC	Capacity field	Considered through coefficients	Weather data and surface temperatures	Heat fluxes and ET	Heat fluxes and ET	Kobe - Humid subtropical

*ET = Evapotranspiration, VPD = Vapor pressure differential, VWC = Volumetric water content

Table 3: Vegetative roof models for energy performance of buildings developed between 1982 and 2017 (continued).

Study	Authors - Year	Balance	ET	Stomatal resistance	Shading effect	Substrate thermal properties	VWC range	Thermal Inertia	Inputs	Outputs	Validation	City - Climate of validation
A green roof model for building energy simulation programs	Sailor 2008	Energy	VPD, minimum stomatal resistance, Radiation, VWC, LAI and wind speed	Solar irradiance, air temperature, VPD and VWC	Percentage affecting incoming radiation	Constant	Wilting point and capacity field	Not considered	Weather data, substrate and plants parameters	Substrate and Foliage temperature	Surface temperatures	Orlando - Humid subtropical
Simulation of thermodynamic transmission in green roof ecosystem	Jim & He 2010	Energy	Bowen Ratio	Not considered	Shading efficiency model (SEM)	Constant	Not considered	Not considered	Incoming radiation	Heat Fluxes and Net radiation	Heat fluxes	Hong Kong – Dry winter subtropical
Assessment of a green roof thermal behavior: A coupled heat and mass transfer model	Ouldboukhitine et al. 2011	Energy and Mass	Penman Monteith	Solar irradiance, air temperature, VPD and VWC	Percentage affecting incoming radiation	Varies with VWC	Wilting point and capacity field	Not considered	Weather data, VWC, substrate and plants parameters	Substrate and Foliage temperature and VWC	Surface temperatures	La Rochelle - Oceanic
A heat transfer model for assessment of plant based roofing systems in summer conditions	Tabares & Srebric 2011	Energy	VPD, minimum stomatal resistance, Radiation, VWC, LAI and wind speed	Solar irradiance, air temperature, VPD and VWC	Extinction coefficient	Varies with VWC	Wilting point and capacity field	Not considered	Weather data, VWC, substrate and plants parameters	Substrate and Foliage temperature, Heat Flux and Net radiation	Surface temperature, Heat Fluxes, Net radiation and ET.	Not considered – Steady State – Laboratory setup data
Development and validation of a coupled heat and mass transfer model for green roofs	Djedjig et al. 2012	Energy and Mass	VPD, minimum stomatal resistance, Radiation, VWC, LAI and wind speed	Solar irradiance, air temperature, VPD and VWC	Percentage affecting incoming radiation	Varies with VWC	Capacity field	Considered	Weather data, substrate and plants parameters	Substrate and Foliage temperature and VWC	Surface temperatures	La Rochelle - Oceanic
Validation of predictive heat and mass transfer green roof model with extensive green roof field data	Tabares et al. 2012	Energy	VPD, minimum stomatal resistance, Radiation, VWC, LAI and wind speed	Solar irradiance, air temperature, VPD and VWC	Extinction coefficient	Constant due to CTF	Wilting point and capacity field	Considered with CTF	Weather data, VWC, substrate and plants parameters	Substrate and Foliage temperature, Heat Flux and Net radiation	Surface temperature, Heat Fluxes, Net radiation and ET.	Chicago - Humid continental

*ET = Evapotranspiration, VPD = Vapor pressure differential, VWC = Volumetric water content

Table 3: Vegetative roof models for energy performance of buildings developed between 1982 and 2017 (continued).

Study	Authors - Year	Balance	ET	Stomatal resistance	Shading effect	Substrate thermal properties	VWC range	Thermal Inertia	Inputs	Outputs	Validation	City - Climate of validation
A coupled energy transport and hydrological model for urban canopies evaluated using a wireless sensor network	Wang et al. 2013	Energy and Mass	VPD and stomatal resistance	Solar irradiance, air temperature and VPD	Percentage affecting incoming radiation	Constant	Capacity field	Not considered	Weather data, substrate and plants parameters	Substrate and Foliage temperature	Surface temperatures	Princeton - Humid subtropical
Toward the practicability of a heat transfer model for green roofs	Chen et al. 2015	Energy	Penman Monteith modified with cover factor	Solar irradiance, air temperature and VPD	Extinction coefficient	Constant	Not considered	Not considered	Weather data, substrate and plants parameters	Surface temperatures and Heat flux	Surface temperatures and Heat flux	Taipei City – Humid subtropical
Numerical simulation of the dual effect of green roof thermal performance	Heidarinejad & Esmaili 2015	Energy and Mass	Not specified	Solar irradiance, air temperature and VPD	Extinction coefficient	Varies with VWC	Not considered	Considered	Weather data, VWC, substrate and plants parameters	Substrate temperature	Substrate temperature	Cardiff - Oceanic
Dynamic simulation of the Green Roofs Impact on Building Energy Performance, Case Study of Antananarivo, Madagascar	Tiana et al. 2015	Energy and Mass	Weather data and LAI, stomatal resistance constant	Constant	Percentage affecting incoming radiation	Constant	Not considered	Considered	Weather data, substrate, plant and structure parameters	Surface temperature	Not validated	Antananarivo – Subtropical highland
Heterogeneous model for heat transfer in Green Roof Systems	Quezada – García et al. 2017	Energy	Not specified	Not considered	Not considered	Varies with VWC	Not considered	Considered	Weather data, substrate, plant and structure parameters	Surface and interior air temperature	Substrate temperature	Guangzhou – Humid tropical

*ET = Evapotranspiration, VPD = Vapor pressure differential, VWC = Volumetric water content

2.3 Mechanism used by vegetation roofs to decrease building energy consumption

The main mechanisms used by vegetative roofs to decrease Building energy consumption are (1) the thermal inertia, (2) the thermal insulation of the substrate, (3) the shading of the vegetation, and (4) the evapotranspiration of substrate-vegetation biophysical system (Berardi 2014, Castleton 2010, Fioretti 2010, Tabares-Velasco 2009). Despite the aforementioned, not all the developed vegetative roof models consider the thermal inertia.

The mathematical models aim to represent the complex processes that occur in reality, thus simplification are needed which involves considering assumptions.

2.3.1 Thermal inertia of the substrate

The substrate contributes with thermal mass that helps to stabilize the indoor temperatures. This depends of the absorptivity, specific heat, thermal conductivity, thickness, and VWC of the substrate. To calculate the thermal inertia it is fundamental to discretize the substrate in several nodes. By the specific heat of the substrate, the thermal inertia dampens the temperature of the substrate as the depth increases. The discretization of the substrate is a specific feature of transient models.

Due to it is much easier to control steady state variables, the number of models that consider steady-state is much greater than those in the transient state. 9 of the analyzed models implement the thermal inertia of the substrate (Del Barrio 1998, Lazzarin et al. 2005, Alexandri & Jones 2007, Takebayashi & Moriyama 2007, Djedjig et al. 2012,

Tabares et al. 2012, Heidarinejad & Esmaili 2015, Tiana et al. 2015, and Quezada-García et al. 2017).

2.3.2 Thermal insulation of the substrate

All the evaluated models consider in the vegetated roof heat energy balance the shortwave and longwave radiation; and the conductive, latent, and sensible heat fluxes. The conductive heat flux is affected by the thermal insulation of the substrate according to Fourier's law (Eq. 1).

$$\nabla(k\nabla T) = \dot{q_v} \quad \text{(Eq. 1)}$$

The element of the left side corresponds to the conductive heat flux through the substrate; where k is the substrate thermal conductivity ($W \cdot m^{-1} \cdot K^{-1}$); T is gradient of temperature between the top and the bottom of the substrate ($K \cdot m^{-1}$); and $\dot{q_v}$ is the conductive heat flux through the substrate ($W \cdot m^{-2}$).

Since the thermal conductivity can be considered as a constant value or as a function of the VWC, the conductive heat flux displays greater variation among the vegetative roof models.

Vegetative roof model considers assumptions to reduce the complexity of the equations used and the number of inputs required. One of the most common assumptions used in several of the models is to consider the thermal conductivity of the substrate constant (Nayak 1982, Zhang 1997, Del Barrio 1998, Sailor 2008, Jim & He 2010, Moura et al. 2012 and Wang et al. 2013). However, this assumption reduces the accuracy of the results due to the thermal properties of the substrate depends directly of the moisture

content on this layer. According to Sailor and Hagos (2011), depending of the substrate's composition and increment of the VWC from 0 m^3/m^3 to 0.25 m^3/m^3 can increase the substrate's thermal conductivity between 0.15 W/mK and 0.55 W/mK.

The rest of the vegetated roof models consider the thermal conductivity of the substrate as a linear function of the VWC, they can be divided into two groups. The first group corresponds to the models that consider the VWC as inputs to the models (Tabares & Srebric 2011). While, in the second group are the models that calculate VWC (Lazzarin et al. 2005, Alexandri & Jones 2007, Takebayashi et al. 2007, Ouldboukhitine et al. 2011 and Djedjig et al. 2011). This last classification points out the models that develop a more complete mass balance on their equations.

2.3.3 Shading by the vegetation

The use of a vegetation layer above the roof provides shades to the substrate below the plants. For this reason the surface temperature of the substrate and the radiation absorbed by the roof are lower compared to conventional roofs. This contributes to reduce the heat fluxes through the roof towards the interior of the building, and therefore its cooling loads might be reduced.

However, not all of the vegetative roof models consider this effect (Takebayashi 2007, Quezada-García 2017), which could lead to very inaccurate results.

The vegetated roof models that implement the shading effect consider it by two methods. The first way is using a directly a fractional coverage factor in the energy balance, which diminish the amount of incoming shortwave radiation to the substrate

layer (Alexandri & Jones 2007, Sailor 2008, Jim & He 2010, Djedjig 2012, Tiana et al 2015). The second method is to implement the shortwave extinction coefficient. This indicates the percentage of radiation absorbed by the foliage layer, and therefore the remaining radiation reaching the substrate layer (Gaffin 2005, Lazzarin 2005, Tabares & Srebric 2011, Tabares et al. 2012, and Heidarinejad 2015). Due to the two methods act in the same way, it is not a fundamental factor which of the two methods is employed.

2.3.4 Evapotranspiration

Evapotranspiration (ET) is the combined effect of the substrate evaporation and plant transpiration. ET is an important factor that affects the thermal performance of the vegetative roofs, which can be modeled by numerous different equations. ET is primarily generated by solar radiation, but it is also influenced by vegetation properties (e.g. stomatal resistance, albedo, health and LAI), other environmental conditions (e.g. air temperature, wind speed and relative humidity) and available substrate moisture (Marasco et al. 2015).

There are two ET that can be calculated: the potential evapotranspiration (PET) and the actual evapotranspiration (EAT). The PET calculate the maximum possible ET according to the environmental conditions, while AET considers factors neglected by the PET, such as the variation of the substrate moisture availability, surface conditions, plant physiology and plant vitality. Despite of this, the variation between PET and AET mainly depends of the VWC available in the substrate to the plant. This factor is based

on a combination of the actual substrate moisture, the field capacity of the substrate and the wilting point.

There are several ways to represent the ET, which varies the inputs considered and the complexity of the equations implemented. Depending if the model develops just energy balance or energy and mass balances varies the way that ET is considered. Overall, the models that only have energy balance calculate the ET through the latent heat fluxes of the substrate and the foliage. On the other hand, the models that include mass balance consider VWC variation in the substrates due to ET. For this reason, in these models the ET is not only considered as a heat flux.

One of the simplest methods to calculate the ET is by the Bowen ratio, which was implemented by Jim & He (2010). This coefficient represents the ratio between the sensible heat flux and the latent heat flux. The way to implemented in the vegetative roof models is to consider the latent heat flux as a fraction of the sensible heat flux. Since this method does not directly consider the environmental conditions nor the characteristics of the vegetation is the less accurate method to represent the ET. In a similar way, Takebayashi et al. (2007) consider an efficiency factor and the latent heat of vaporization of the water to calculate the ET.

In terms of the vegetative roof models that are based on PET methods, several models can be considered. Morau et al. (2012) calculates the ET considering the stomatal resistance, the vapor pressure differential (VPD) and the LAI, but the VWC of the substrate is not considered. Lazzarin et al. (2005) consider the equation of Penman-Monteith (FAO, 1998) to calculate the ET. This formula only calculates the PET, and

for this reason in the study a factor is considered to simulate the effect of the plant. However, this method is inaccurate because the factor does not vary through the time nor consider the water available for the ET. Also, there are other models that consider mainly the VPD and the stomatal resistance for the ET calculations (Nayak 1982, Zhang 1997, Del Barrio 1998, Kumar 2005, Wang et al. 20013); however none of these models contemplate the VWC.

For vegetated roof models based on AET, there are five vegetative roof models that considered it. Alexandri & Jones (2007) considers the VPD, the minimum stomatal resistance, the aerodynamic resistance and the weather conditions to calculate the latent heat flux in order to calculate the ET. The VWC is not directly considered in the transpiration of the plant but it is contemplated in the evaporation of the substrate. In a similar way, Sailor (2008) and Tabares & Srebric (2011) also consider the VPD, the minimum stomatal resistance, the aerodynamic resistance and the weather conditions to calculate the latent heat flux. However, in these two models the VWC is considered to calculate the stomatal resistance of the plant. Both models only develop an energy balance, thus the ET is just considered as a latent heat flux.

Based on these two previous models, Ouldboukhitine et al. (2011) and Djedjig et al. (2012) incorporated the mass transfer. For this reason, these two studies not only consider the ET as a latent heat flux but also as a factor that affects the VWC.

2.4 Stomatal Resistance

The stomatal resistance is a characteristic of the vegetation. This parameter is an indicator of the metabolic relation between the plant and the environment. The value of the stomatal resistance depends directly of the amount and size of the plants stomas, and the metabolism of the plant (Klein and Coffman, 2015). The stoma is a microscopic opening that controls the water vapor and carbon dioxide exchange rate. The guard cells surrounding the stoma are the responsible of the stomatal resistance value (Heidarinejad and Esmaili, 2015). These cells can open or close the stoma according to the environmental conditions (e.g. solar radiation, air temperature, water content in the air, wind speed and VWC). For this reason, the stomatal resistance is not a constant value. Despite the relevance of this biophysical parameter of the canopy, Tiana et al. (2015) consider the stomatal resistance as a constant value.

Among the models that consider this parameter, there are two different groups: the models that calculate it considering the VWC, and the ones that not. This is a very important difference, since the stomatal resistance of a plant is directly associated with the amount of water available for the vegetation. If the substrate is dry, the plant does not have water for evapotranspiration, and it will recess the water inside closing its stomas. This increases the value of stomatal resistance. Therefore, there is an inverse proportionality between the VWC and the stomatal resistance that only a few models take into consideration (Sailor 2008, Tabares & Srebric 2011, Ouldboukhitine et al. 2011, Tabares et al. 2012, and Djedjig et al. 2012).

Notwithstanding, other models assume the constant availability of water for evapotranspiration and calculate it only with the environmental conditions (Alexandri & Jones 2007, Wang 2013, Chen 2015, Heidarinejad 2015).

Also, there are several models that not consider this parameter as an input and they assume it implicitly through the evapotranspiration values considered (Gaffin 2005, Lazzarin 2005, Takebayashi 2007, Jim & He 2010, and Quezada-García et al. 2017).

2.5 Heat and mass transfers in vegetated roof models

In order to calculate the energy performance of vegetative roofs, models can perform two balances through their equations. These correspond to energy balance and mass balance. The energy balance corresponds to the energy budget of the vegetated roof considering the shortwave and longwave radiations; and the conductive, latent and convective heat fluxes. The mass balance corresponds to the transport of vapor water and liquid water in the substrate layer. Of these two balances, only the first is performed by all the models evaluated in the review.

At the same time, two energy balances are performed in the vegetative roof, one in the vegetation layer and another in the substrate layer. The next equations indicate the elements considered in the balance of the substrate (Eq. 2) and the foliage (Eq.3) in the study performed by Sailor (2008). These equations allow calculating the canopy (T_f) and substrate surfaces (T_g) temperatures that are used to calculate the heat flux through the whole roofing system.

$$F_f = \sigma_f \left[I_s\left(1-\alpha_f\right) + \varepsilon_f I_{ir} - \varepsilon_f \sigma T_f^4\right] + \frac{\sigma_f \varepsilon_g \varepsilon_f \sigma}{\varepsilon_l}\left(T_g^4 - T_f^4\right) + H_f + L_f \qquad \text{(Eq. 2)}$$

$$F_g = \left(1-\sigma_f\right)\left[I_s\left(1-\alpha_g\right)+\varepsilon_g I_{ir}-\varepsilon_g\sigma T_g^4\right]-\frac{\sigma_f\varepsilon_g\varepsilon_f\sigma}{\varepsilon_l}\left(T_g^4-T_f^4\right)+H_g+L_g+k\,\frac{\partial T_g}{\partial z}$$ (Eq. 3)

where σ_f is the canopy fractional coverage; I_s and I_{ir} are the short and long-wave radiation (Wm-2), respectively; α_f and α_g are the foliage and substrate albedos; ε_f and ε_g are the substrate and foliage emissivity; ε_l is equal to $\varepsilon_g+\varepsilon_f-\varepsilon_f\varepsilon_g$; H_f and H_g are the sensible heat fluxes of the foliage and substrate, respectively, while L_f and L_f are the corresponding latent heat fluxes (Wm^{-2}); k is the substrate thermal conductivity ($Wm^{-1}K^{-1}$); and z is the substrate depth (m). The elements considered on the right side of Eq. 2 represent the incoming shortwave radiation, the incoming longwave radiation from the sky, the outgoing longwave radiation from the foliage, the interexchange of longwave radiation between the substrate and the vegetation, the convective heat flux and the latent heat flux in the foliage layer. This last element represents the transpiration of the plants. At the same time, the elements considered on the right side of Eq. 3 represent the incoming shortwave radiation, the incoming longwave radiation from the sky, the outgoing longwave radiation from the substrate, the interexchange of longwave radiation between the substrate and the vegetation, the convective heat flux, the latent heat flux in the foliage layer and the conductive heat flux through the substrate. The latent heat flux represents the evaporation of the water in the substrate. Of the total of evaluated studies, 10 of 17 models consider only energy balance and no mass balance (Nayak 1982, Del Barrio 1998, Gaffin 2005, Takebayashi 2006, Sailor 2008, Jim & He 2010, Tabares & Srebric 2011, Wang 2013, Chen 2015 and Quezada-García 2017).

There are also several models that incorporate the development of mass balance to the two energy balances mentioned above (Lazzarin 2005, Alexandri & Jones 2007, Ouldboukhitine 2011, Tabares et al 2012, Djedjig et al. 2012, Heidarinejad 2015, and Tiana et al. 2015). For example, Alexandri & Jones (2007) describe the mass transfer in the substrate according to the following equations.

$$\frac{d\omega_g}{dt} = \frac{\partial}{\partial z}\left(K_g \left(\frac{\partial \psi_p}{\partial z} + 1\right)\right) = \frac{\partial}{\partial z}\left(D_g \frac{\partial \omega_g}{\partial z} + K_g\right)$$
(Eq. 4)

$$K_g = K_{g,s}\left(\frac{\omega_g}{\omega_{g,s}}\right)^{2b+3} \quad \text{(Eq. 5)}$$

$$D_g = -\frac{b\, K_{g,s}\, \psi_{p,s}}{\omega_{g,s}}\left(\frac{\omega_g}{\omega_{g,s}}\right)^{b+2} \quad \text{(Eq. 6)}$$

where ω_g is VWC of the substrate ($m^3\ m^{-3}$); $\omega_{g,s}$ is the maximum VWC that a given substrate type can hold ($m^3\ m^{-3}$); ψ_p is the moisture potential of substrate tension (cm); $\psi_{p,s}$ is the moisture potential when substrate is saturated (cm); K_g is the hydraulic conductivity of the substrate ($m\ s^{-1}$); $K_{g,s}$ is the hydraulic conductivity of the substrate at saturation ($m\ s^{-1}$); D_g is the diffusion coefficient of water through the substrate ($m^2\ s^{-1}$); b is a coefficients depending of the substrate type; t is the time (s); and z is the substrate depth (m).

2.6 Vegetative roof models implemented in building energy tools

Currently, only two simulation programs have implemented vegetative roof models, these software are EnergyPlus and DesignBuilder.

2.6.1 EnergyPlus

EnergyPlus is a free energy simulation tool developed by the U.S. Department of Energy (DOE). This software makes energy analyses and thermal loads simulations. Despite of being very capable software, this program has not a user-friendly graphical interface (Energyplus.net, 2017).

This software has implemented the model developed by Sailor (2008) and currently is implementing the Tabares et al. (2012) vegetative roof model. The vegetative roofs inputs considered are:

- Height of the plants (m)
- LAI (-)
- Leaf reflectivity (-)
- Leaf emissivity (-)
- Minimum stomatal resistance (s m^{-1})
- Maximum VWC at saturation (m^3 m^{-3})
- Minimum residual VWC (m^3 m^{-3})
- Initial VWC (m^3 m^{-3})

Additionally, the user must select between the simple and the advanced moisture diffusion calculation method. The difference between the two methods is that the simple

considers a linear variation of the VWC through the substrate, while the advanced method implements finite differences.

The advantage of this software is the diverse variety of outputs offered to the user such as substrate and foliage surface temperatures, volumetric water content of the substrate and evapotranspiration rates.

2.6.2 DesignBuilder

DesignBuilder uses as solver engine EnergyPlus, thus both programs have certain similarities (Designbuilder.co.uk, 2017). For example, this program considers the same inputs that EnergyPlus and since 2016 allows the user to select the moisture diffusion calculation method.

The advantage of this software is that it has a user-friendly graphical interface. However, this program does not offer specific vegetative roofs outputs and due to its dependence to EnergyPlus the only model available is the one developed by Sailor (Sailor, 2008).

2.7 Validations of the vegetated roof models

As for the validation of the model, Table 3 presents the calculated outputs considered for the validation, and cities with their respective climates where the validation was carry out. The Figure 9 and the Tables 4 and 5 have been developed according to the literature survey in Table 3.

2.7.1 Climates used for validation

Developing an analysis of the climatic data considered for the development and validation of the models, it was observed how the 55.5% of the models were made for humid subtropical and oceanic climate. Figure 9 presents the number of models developed for different climates according to Köppen-Geiger classification.

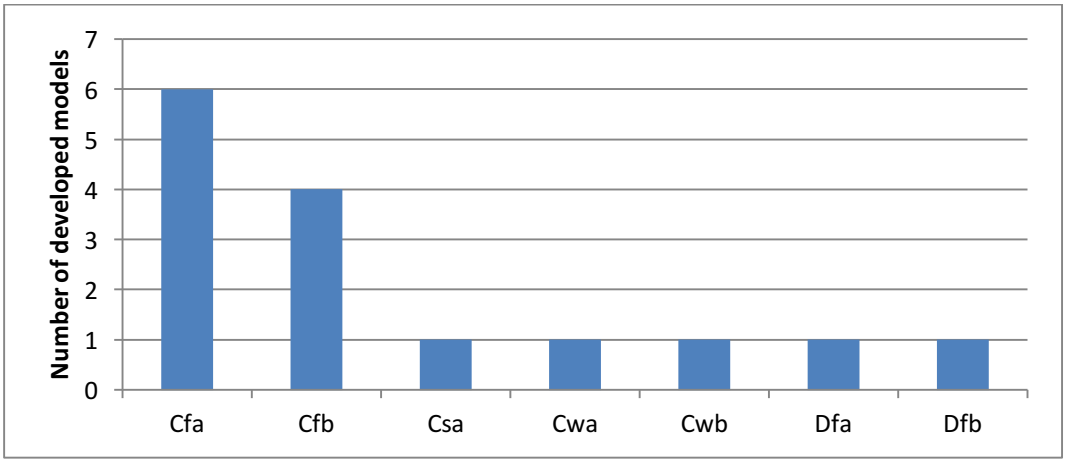

Figure 9: Number of model developed according to Köppen-Geiger climate classification. Cfa: Humid subtropical, Cfb: Oceanic, Csa: Hot summer Mediterranean, Cwa: Dry Winter subtropical, Cwb: Subtropical highland, Dfa: Humid continental, Dfb: Subarctic

Table 4 indicates the cities where the validations were performed, the average annual temperature (°C) of the city and its amount of annual precipitation (mm). In this table were not considered the models of Nayak (1982) and Tabares & Srebric (2011), due to the first one was not validated, while the second one was validated in steady state conditions.

Table 4: Köppen climate classification of the cities considered for the vegetative roof models validation.

Authors	City	Climate	Köppen	Average annual Temperature (°C)	Precipitation per year (mm)
Lazzarin 2005	Vicenza	Humid subtropical	Cfa	13.3	967
Takebayashi 2006	Kobe	Humid subtropical	Cfa	15.7	1400
Sailor 2008	Orlando	Humid subtropical	Cfa	22.0	1260
Wang 2013	Princeton	Humid subtropical	Cfa	11.1	1175
Chen 2015	Taipei City	Humid subtropical	Cfa	22.0	2574
Quezada 2017	Guangzhou	Humid subtropical	Cfa	22.2	1720
Alexandri & Jones 2007	Cardiff	Oceanic	Cfb	10.3	991
Ouldboukhitine 2011	La Rochelle	Oceanic	Cfb	12.6	762
Djedjig 2012	La Rochelle	Oceanic	Cfb	12.6	762
Heidarinejad 2015	Cardiff	Oceanic	Cfb	10.3	991
Del Barrio 1998	Athens	Hot-Summer Mediterranean	Csa	18.1	397
Jim & He 2010	Hong Kong	Dry winter subtropical	Cwa	22.6	2152
Tiana 2015	Antananariv	Subtropical highland	Cwb	18.4	1317
Tabares 2012	Chicago	Humid continental	Dfa	10.0	918
Gaffin 2005	State College	Subarctic	Dfb	9.5	985

Table 4 presents that no validated models were developed for the semiarid climates, such as Bsk, classification according to Köppen-Geiger classification. Santiago of Chile corresponds to this climate. This city has an average annual temperature of 14.6 °C and an annual precipitation of 359 mm. The city with the precipitation data that fits the most is Athens (Del Barrio 1998). While the cities with the average annual temperature data that fit the most are the Vicenza (Lazzarin 2005) and Kobe (Takebayashi 2006). However, its precipitation values are between 3 and 4 times higher than that of Santiago.

For this reason, there is no certainty that the developed vegetative roof models are good energy performance estimators for other climates than where they were validated. Therefore, it is not possible to assert that models implemented in energy simulation tools provide accurate results of the building energy impact of vegetated roof technology.

2.7.2 Outputs considered for validation

In the literature, many studies assert that vegetative roofs are capable of improving the energy performance of buildings. This is estimated by calculating surface temperatures and heat fluxes through the roof but not actual energy consumption. Table 5 presents the outputs considered in each model of vegetative roof considered for this study. Despite the literature review shows that studies ensure that vegetative roof improves the energy performance of buildings, these models have only been validated by surface temperatures, heat flows through the roof, evapotranspiration rates, net radiation above the roof, and by the VWC of the substrate. Also, there are a few models that have not been validated against experimental data (Nayak 1982, Del Barrio 1998, Takebayashi 2006, Tiana et al. 2015).

Table 5: Output considered for validation of vegetative roof models.

Surface temperature	**ET**	**Heat flux**	**Net radiation**	**VWC**	**Not validated**
Nayak 1982 Alexandri 2007 Sailor 2008 Tabares 2011 Ouldboukhitine 2011 Tabares 2012 Wang 2013 Chen 2015 Heidarinejad 2015 Quezada 2017	Lazzarin 2005	Jim & He 2010 Tabares 2011 Tabares 2012 Chen 2015	Jim & He 2010 Tabares 2011 Tabares 2012 Wang 2013	Alexandri 2007 Wang 2013	Nayak 1982 Del Barrio 1998 Takebayashi 2006 Tiana 2015

Since these models have not been validated by energy consumption, there is no certainty that vegetative roof models are good energy building performance estimators. Therefore, it is not possible to assert that vegetative roof models implemented in energy simulation programs provide accurate results of the energy performance of these technologies.

2.8 Conclusions

Given the high energy costs in the building sector, it has become a necessity to find solutions that reduce its energy consumption. One of these solutions is the implementation of vegetative roofs. However, to fully obtain the benefits of this technology is important to count with accurate models that assist developers to design vegetative roofs.

This paper provides an overview of the vegetative roof models developed for the energy and thermal performance of buildings. 18 models developed between 1982 and 2017 were considered for this review in order to analyze their equations, the assumptions considered, the outputs obtained, and the output data and climate considered for their validation. The purpose of this study is to understand how these models work and to obtain information that indicates if these models can be used to design properly vegetative roofs for the semi-arid climate of Santiago de Chile.

The conclusions of this research paper are as follows:

1. The number of papers of vegetative roof modelling has increased mainly in the recent years. The 55.6% of the vegetated roof models have been developed between 2010 and 2017.
2. The 33.3% of the vegetative roofs models have been developed for humid subtropical climate and 22.2% for oceanic climate. No model has been validated for semiarid climates.
3. Since the validation of vegetative roof models has been developed for specific climates there is no way to ensure its correct performance for other climates.

Thus, there is no way to assert the correct performance of simulation tools that incorporate these models.

4. Only the 11.1% (two models) of the developed vegetative roof models have been implemented on simulation programs.
5. The 55.5% of the developed vegetative roof models has been validated with the substrate surface temperature. While the 22.2% has not been validated. The remaining models have been validated against experimental data fot conductive heat fluxes through the roof, evapotranspiration rates, net radiation above the vegetative roof surface and volumetric water content of the substrate.
6. Although the literature ensured that vegetative roofs improve the energy performance of buildings, no model has been validated by experimental measurements of energy consumption, nor substrate surface temperature calculated considering the couple of the vegetative roof model to a building model.
7. The 50% of the developed vegetative roof models only considers energy balance. The remaining 50% of the models consider energy and mass balance.
8. Only the 27.7% of the developed vegetative roof models considers the thermal inertia of the substrate.
9. Despite the well-known relationship between the volumetric water content of the substrate and its thermal properties, the 55.5% of studies considers them as constant values.

3. INFLUENCE OF VEGETATION, SUBSTRATE, AND THERMAL INSULATION OF AN EXTENSIVE VEGETATED ROOF ON THE THERMAL PERFORMANCE OF RETAIL STORES IN SEMIARID AND MARINE CLIMATES

This chapter corresponds to the published paper "Influence of vegetation, substrate, and thermal insulation of an extensive vegetated roof on the thermal performance of retail stores in semiarid and marine climates" added in reference (Vera et al. 2017).

3.1 Abstract

Buildings play an important role in electricity energy use and greenhouse generation. Vegetated roofs, so-called green roofs, offers many benefits beyond energy savings. Among different building types, retail stores with flat and large roof/walls ratio, offers a match for this technology. Despite this potential in retail stores the literature review shows a lack of studies on the influence of vegetated roofs' design parameters on the thermal and energy performance of retail stores. This study performs a parametric analysis to evaluate the influence of the main green roof design parameters on the thermal performance of a big-box retail stores. The selected climates are semiarid climates of Albuquerque (USA) and Santiago (Chile) and the marine climate of Melbourne (Australia) to inform engineers and architects design of vegetated roofs that fully use their thermal benefits. Based on the analyzed roofs, this study finds that: (1) thermal insulation shows significantly larger influence on the stand-alone retail's heating loads than the thermal properties of the substrates and LAI of vegetation and (2)

vegetation can be an effective alternative to insulation on reducing cooling loads due to the evapotranspiration of the vegetation-substrate system and canopy's shading effects. Thus, vegetated roofs cannot replace insulation to if the desire is to mainly reduce heating loads.

3.2 Introduction

In recent years, cities are using more land to accommodate the increasing population and migration from rural areas to the cities (Antrop 2004). This worldwide phenomenon is increasing the demand for new buildings as well as land, water, and energy. The demand may increase even more in the future because of the economic growth of undeveloped and developing regions such as Africa (Valipour 2014, Valipour 2015). In particular, the building sector represents 32% of the global energy use in 2010 and causes one-third of the greenhouse gas emissions (Lucon et al. 2014, OECD/IEA 2013). Therefore, building energy efficiency plays a key role to limit the global warming and mitigate the impacts of climate change. Vegetated roofs, so-called green roofs, are claimed to reduce the cooling and heating building energy consumption by decreasing the heat flux through the roof due to: (1) shading produced by the canopy, (2) evapotranspiration of the plant-substrate biophysical system, (3) additional thermal resistance and thermal inertia due to the thermal properties of the substrate (Jaffal et al. 2012). Several authors have reported other benefits of vegetated roof such as water runoff quantity and quality control (i.e. Berndtsson 2010, Getter et al. 2007, Vijayaraghavan 2016, Teemusk et al. 2007), carbon sequestration and particle matter capture (i.e. Getter et al. 2009, Li et al. 2010, Speak et al. 2012), urban heat island effect

reduction (i.e. Alexandri & Jones 2008, Karachaliou et al. (2016) Takebayashi & Moriyama 2007), sound absorption (i.e. Vijayaraghavan 2016, Van Renterghem & Botteldooren2011), increase of new habitats for species (i.e. Brenneisen 2006, Brenneisen 2003, Williams et al. 2014) and larger durability of rooftops (i.e. Teemusk &Mander 2009).

Based on these benefits, several countries have boosted the implementation of vegetated roofs on new building constructions (Vijayaraghavan 2016): in Toronto (Canada), all new buildings having a roof surface greater than 2000 m2 must have between 20-60% of vegetated roofs; in Tokyo (Japan), all new buildings must have at least 20% of vegetated surfaces on their rooftops (Chen 2013); in Portland (USA), all the new city-owned buildings must be built with at least 70% of vegetated roofs on their roof surfaces (Townshend 2007); and in Basel (Switzerland), all the new or renovated flat roofs have to be covered with at least 15% of vegetation (Townshend 2007). Despite the advancement of vegetated roof research to quantify green roof benefits, the design of the vegetated roof technology is still significantly based on the aesthetic point of view, thus the aforementioned benefits are not potentiated (Berndtsson 2010, Vijayaraghavan 2014).

Several studies have quantified the impact vegetated roofs have on building energy performance. For example, Ascione et al. (2013) finds cooling energy savings between 1 and 11% from using a vegetated roof in a 1-story office building in different warm European climates and cooling energy saving up to 7% in cold climates of Europe. A similar study (Sailor et al. 2012) evaluates the impact of vegetated roof on the energy

consumption of a 3-story office building and a 4-story apartment building in different US cities. Another study compares the thermal performance of a supermarket in Athens, Greece with concrete slab roof and a vegetated roof (Foustalieraki et al. 2016). They find that the supermarket with the vegetated roof showed a reduction of cooling and heating loads up to 18.7% and 11.4%, respectively. In contrast, (Julia et al. 2013) finds no annual energy savings due to vegetated roof in mock up buildings in Pennsylvania (USA).

In terms of the impact of vegetated roofs on the thermal performance of the roof itself, the canopy and the substrate play a key role in the thermal and energy performance of the system. The canopy design parameters are: leaf area index (LAI), stomatal resistance, height of plants, leaf reflectivity and leaf emissivity. In addition substrate parameters are: thermal conductivity, heat capacity, density, and thickness. Several parametric studies evaluate the impact of some of these design parameters on the building thermal performance showing variability among them. For example, (Wong et al. 2003) shows that the variation of vegetation type, volumetric water content (VWC) and substrate thickness causes energy savings between 1 and 15% in a 5-story commercial building in Singapore. In a Mediterranean climate, Theodosiou (2003) shows that LAI is the most important parameter that influences the thermal performance of the vegetated roof because LAI increases its cooling capacity by means of evapotranspiration. Another study indicates that LAI is the most important parameter that effects the energy performance of the buildings studied in US cold climates, while higher substrate depth reduces the heating energy consumption. However, most

vegetated roof models have not been validated in winter conditions (Sailor et al. 2012). Similarly, Vera et al. (2015) finds that cooling loads of a supermarket in a semiarid climate are significantly influenced by LAI, whereas heating loads are mainly influenced by the substrate thermal properties.

Most new buildings have insulated facades and rooftops. Nevertheless, there is a lack of studies on how this layer affects the thermal and energy benefits of vegetated roofs on buildings. For example, a study in the Mediterranean climate, Theodosiou (2003) concludes that the lack of insulation increases the cooling capabilities of vegetated roofs in summer. Also in a Mediterranean climate, Silva et al. (2016) shows cooling energy demand of a room with an insulated vegetated roof is slightly larger than that for a traditional roof. Jaffal et al. (2012) finds energy savings between 10% and 48% for insulated and uninsulated vegetated roofs of a single-family house in the Oceanic climate of La Rochelle (France), respectively, in comparison with conventional roofs. Likewise, Niachou et al. (2001) shows energy savings up to 2%, 7% and 48% for high-insulated, moderate insulated and non-insulated vegetated roofs, respectively, for an office building located in the Mediterranean climate of Athens (Greece). Another study concludes that the modest building energy savings obtained with vegetated roofs were caused by the high level of thermal insulation of the roofing system (Sailor et al. 2012). In an experimental study, Zhao et al. (2014) evaluates the vegetated roof thermal performance for four U.S climate zones and concluded that the insulation layer limited the impact of the vegetated roof have on reducing heat flux through the roof. Finally, an experimental study evaluates the influence of an insulation layer on the cooling energy

consumption of houses with vegetated roof in the subtropical climate of Hong Kong (Jim 2014). Depending on the plant species, the cooling energy consumption varies between 5% lower and 18.3% higher for an uninsulated vegetated roof than the insulated scenario.

Previous studies evaluate energy savings in different types of buildings due to the incorporation of vegetated roofs. Among building, big-box retail stores have a large roof surface and only one or two stories. Thus, it matches vegetated roof ideal building geometry to obtain highest benefits. Retailers are implementing strategies to reduce operational cost due to the increased competition. In particular, the profit margin of retail stores is very low, thus operation cost savings can produce important profit increments as energy related costs account for a significant portion of the operational costs (Richman & Simpson 2016). Jamieson (2014) reports energy consumption reduction by 15% increases profit margin of retailers from 4% to 4.75%. Additionally, Jamieson et al. (2016) shows that big-box retail stores in US can reduce energy consumption up to 20-30%. Energy consumption profiles vary significantly between food and non-food retail stores because of the use of refrigeration. In Canada, the average energy intensity use of food and non-food retail stores is around 805 and 388 kWh/m2·year, respectively; while in US, the energy consumption is 549 and 172 kWh/m2·year in food and non-food retail stores, respectively (EPA 2008). Finally, energy consumption associated to HVAC is 20% of the total energy use in food retailers, while it is 40% in non-food retailers (Jamieson 2014).

Despite this potential in retail stores, previous studies have either focused to a particular roof design, particular location, or looking only at the reduce heat flux or surface temperature. In addition, the aforementioned literature review shows a lack of studies looking at the influence of vegetated roofs' design parameters such as LAI, and substrate properties not only in the roof heat fluxes, but also on the thermal and energy performance of retail stores. Moreover, most of studies do not involve semiarid and marine climates that are cooling dominated climates with a significant heating season. Since vegetated roofs have significant potential benefits in retail stores and semiarid and marine climates, this paper performs a parametric analysis to evaluate the influence vegetated roof design parameters have on the cooling and heating loads of a big-box retail stores. The selected climates are semiarid climates of Albuquerque (USA) and Santiago (Chile) and the marine climate of Melbourne (Australia). This study contributes to inform engineers and architects what important design variables they most consider when designing vegetated roofs to obtain their thermal benefits.

3.3 Methodology

3.3.1 Roofing systems and vegetated roofs characteristics

This study is mostly based on building simulation results but also includes preliminary experimental data. Thermal building simulations are performed in EnergyPlus version 8.6.0, which incorporates a vegetated roof model (Sailor 2008). It uses the Stand-Alone Retail Prototype building model according to ANSI/ASHRAE/IES Standard 90.1 – 2013 (Deru et al. 2011, DOE 2013). This prototype building is part of a set of building

models that represents approximately 70% of the commercial buildings in the U.S. and provide a consistent baseline to evaluate the building energy consumption.

The prototype building model has 17 different versions according to the 17 U.S. climate zones. This study considers the Stand-Alone Retail prototype building for 4B climate zone, corresponding to a semiarid climate. For comparison purposes, the same buildings model is used in Albuquerque and Santiago (Semarid climate) and Melbourne (Maritime climate). Table 6 shows the geographical coordinates and climatological classification of these cities.

Table 6: Latitude, longitude, meters above sea level (masl) and Köppen-Geiger climate classification of the cities.

City	Latitude	Longitude	Altitude (masl)	Köppen Classification	Description
Albuquerque	35°20 N	106°37 W	1619	Bsk	Semi-arid cool climate
Santiago	33°30 S	70°42 W	520	Bsk	Semi-arid cool climate
Melbourne	37°39 S	144°49 W	119	Cfb	Marine west coast climate

The parametric analysis is based on this prototype building model, and only the composition of the roof is changed according to the traditional and vegetated roofing systems indicated in Figure 10 and considering the variation of LAI, substrate properties, and the level of roof insulation as shown in Table 7. The other characteristics of the building (e.g. facades composition, internal loads and its schedules of occupation) remained unchanged to observe the effect of changing the roofing system only.

Table 7: Roof parameters considered for the parametric analysis

Parameter	Values			
Substrate	Lightweight substrate (LW)		Heavyweight substrate (HW)	
Leaf area index of vegetation	0.1 (bare soil)	1.0	3.0	5.0
Roof structure material	Concrete (C)		Metal Sheet (M)	
Insulation levels (mm)	0		50	100

The characteristics of the construction materials and vegetated roofs are shown in Tables 8 and 9. The analyzed green roofs have a substrate thickness of 15cm and plant height of 30cm, typically of extensive green roofs. Substrates and plants radiative properties are also typical and based on previous studies (Zhao et al. 2014). Likewise, saturation moisture content is based on previous studies (Zhao et al. 2014, Sailor & Hagos 2011, and Sailor et al. 2008). Substrate thermal properties are selected based on the ranges for dry (0.15-0.3 W/mK) and wet substrates (0.5-1.2W/mK) as shown in the literature (Zhao et al. 2014, Sailor & Hagos 2011, Sailor et al. 2008). Lightweight substrate represents a more porous substrate (lower density) and lower thermal conductivity. Although the difference in thermal conductivity from the two analyze substrates is about a factor of 4, the thermal diffusivity is very close in both cases. It is worthy to mention that due to a limitation of EnergyPlus green roof model (Sailor 2008), the thermal properties of the substrate remain constant although its water moisture content (VWC) varies over time in reality. Table 10 shows the irrigation schedule used in this study that considers a rate of 4.2 mm/h. This schedule was selected with the idea to keep the vegetated roof within the field volumetric moisture content. Also considers this schedule allows implementing a same baseline between the different scenarios. In order to create this schedule was considered to provide more

water to the green roof during the hottest season of the year. For this reason, in summer there is greater irrigation due to the higher evapotranspiration losses.

Table 8: Thickness and thermal properties of the roof material layers

Construction material	Thickness (m)	Thermal conductivity ($W\ m^{-1}\ K^{-1}$)	Density ($kg\ m^{-3}$)	Specific Heat ($J\ kg^{-1}\ K^{-1}$)	Thermal Diffusivity ($m^2\ s^{-1}$)
Concrete	0.15	1.6	2500	840	7.62×10^{-7}
Metal Sheet	0.002	45	7850	480	1.19×10^{-5}
Insulation (Polyurethane)	0.05-0.1	0.028	35	1590	5.03×10^{-7}
Heavyweight Substrate (HW)	0.15	0.85	1639	1800	2.88×10^{-7}
Lightweight Substrate (LW)	0.15	0.208	730	1100	2.59×10^{-7}

Table 9: Vegetated roof constant parameters values

Height of Plants	0.3 (m)
Leaf Reflectivity	0.22
Leaf Emissivity	0.95
Minimum Stomatal Resistance	300 ($s\ m^{-1}$)
Roughness	Medium Rough
Saturation Volumetric Moisture Content of the substrate layer	0.5 ($m^3\ m^{-3}$)
Residual Volumetric Moisture Content of the substrate layer	0.001 ($m^3\ m^{-3}$)
Initial Volumetric Moisture Content of the substrate layer	0.3 ($m^3\ m^{-3}$)
Moisture Diffusion Calculation Method	Simple

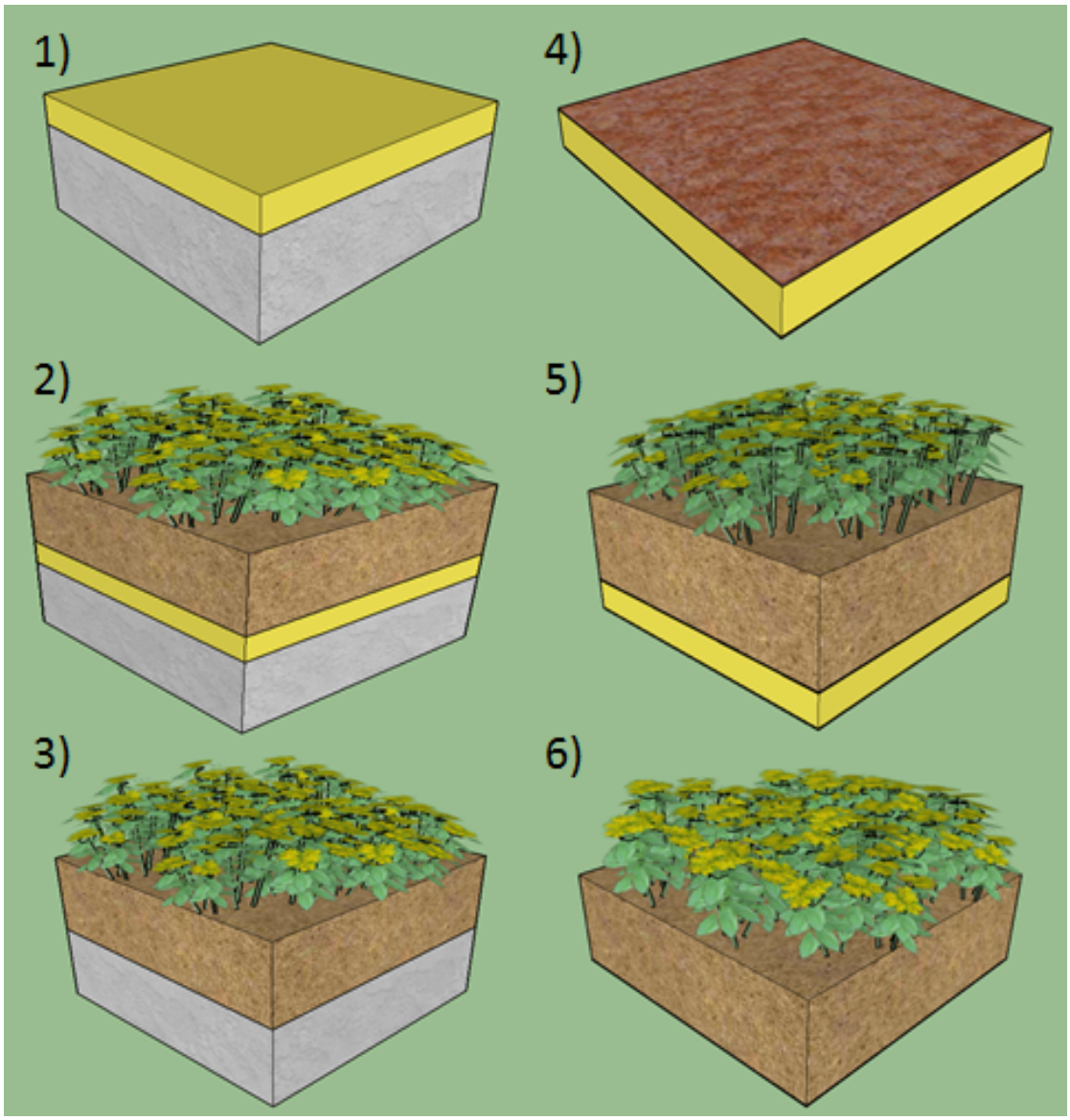

Figure 10: Traditional roofing systems in retail stores: 1) Insulated concrete slab, 4) Insulated metal deck. Vegetated roofing systems: 2) Vegetated roof upon an insulated concrete slab, 3) Vegetated roof upon an uninsulated concrete slab, 5) Vegetated roof upon an insulated metal deck, 6) Vegetated roof upon an uninsulated metal deck

Table 10: Irrigation schedule set throughout the year (irrigation schedule in parentheses are for cities in the Northern Hemisphere).

Month	Wednesday	Saturday	Other days
Jan – Feb – Dec (Jun – Jul – Aug)	8:00-10:00 hrs / 13:00 – 15:00 hrs / 19:00 – 21:00 hrs	8:00-10:00 hrs / 13:00 – 15:00 hrs / 19:00 – 21:00 hrs	Off
Mar – Nov (May – Sep)	8:00-10:00 hrs / 13:00 – 15:00 hrs / 19:00 – 21:00 hrs	8:00-9:00 hrs / 13:00 – 14:00 hrs / 19:00 – 20:00 hrs	Off
Apr – May – Aug-Sep – Oct (Mar – Apr – Oct – Nov)	8:00-9:00 hrs / 13:00 – 14:00 hrs / 19:00 – 20:00 hrs	8:00-9:00 hrs / 13:00 – 14:00 hrs / 19:00 – 20:00 hrs	Off
Jun – Jul (Jan – Feb – Dec)	8:00-9:00 hrs / 13:00 – 14:00 hrs / 19:00 – 20:00 hrs	Off	Off

3.3.2 Substrate moisture diffusion model

EnergyPlus allows users to choose between two moisture diffusion methods for the substrate: simple or advanced. The simple model is the original Ecoroof model based on a constant diffusion trough the substrate. While the advanced method is a newer model that redistributes the VWC according to Schaap and van Genuchten model (Schaap et al. 2006). Since there are no studies about the behavior of these two moisture diffusion methods, several simulations were performed for selecting the proper moisture diffusion model using Santiago weather data. Figure 11 shows the VWC of the vegetated roof with the advanced (straight blue line) and simple (dotted red line) methods for a building in the city of Santiago with no irrigation and no precipitation. Results from the advanced model are unrealistic, since there is no irrigation or precipitation during

January in Santiago weather file. In contrast, the simple model shows a more realistic trend, as the substrate dries out due to the lack of moisture entering the roof. This and other tests show that there are some issues with the advanced method, thus, this study uses the simple method.

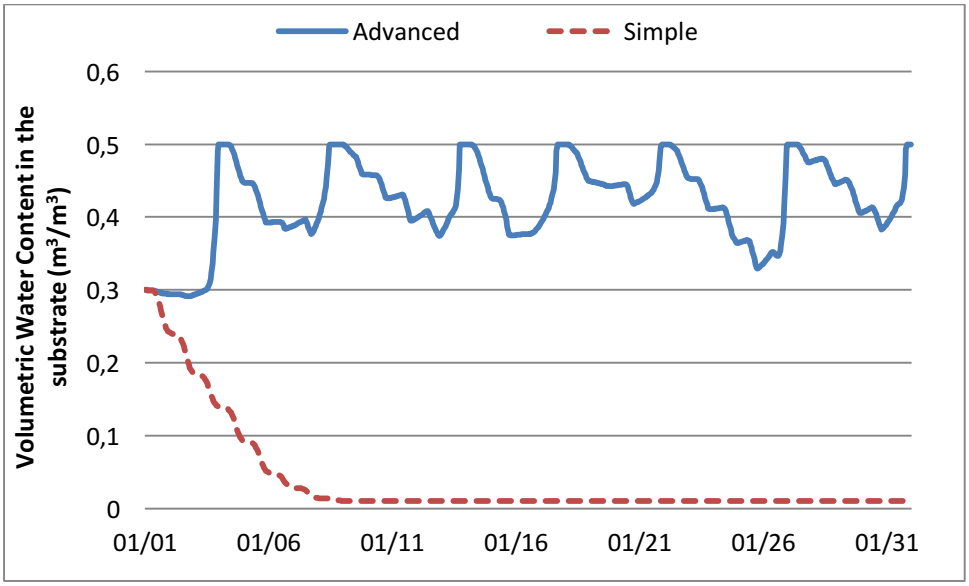

Figure 11: Substrate volumetric water content (VWC) in January (southern hemisphere) with advanced and simple moisture diffusion methods, and no irrigation schedule.

3.3.3 Numerical model of the vegetated roof

EnergyPlus vegetated roof model (Sailor 2008) is based on the Fast All-season Soil STrenght (Frankestein & Koenig 2004, Frankestein & Koenig 2004), the Biosphere Atmosphere Transfer Scheme (Dickison et al. 1993) and the Simple Biosphere (Sellers et al. 1986) models.

The vegetated roof model consists on a single vegetation layer (Eq. 7) above the surface of a substrate layer (Eq. 8). These equations allow calculating the canopy (T_f) and substrate surfaces (T_g) temperatures (in Kelvin) that are used by EnergyPlus to calculate the heat flux through the whole roofing system.

$$F_f = \sigma_f \left[I_s(1-\alpha_f) + \varepsilon_f I_{ir} - \varepsilon_f \sigma T_f^4\right] + \frac{\sigma_f \varepsilon_g \varepsilon_f \sigma}{\varepsilon_l}\left(T_g^4 - T_f^4\right) + H_f + L_f \quad \text{(Eq. 7)}$$

$$F_g = \left(1-\sigma_f\right)\left[I_s(1-\alpha_g) + \varepsilon_g I_{ir} - \varepsilon_g \sigma T_g^4\right] - \frac{\sigma_f \varepsilon_g \varepsilon_f \sigma}{\varepsilon_l}\left(T_g^4 - T_f^4\right) + H_g + L_g + k\,\frac{\partial T_g}{\partial z} \quad \text{(Eq. 8)}$$

where σ_f is the canopy fractional coverage; I_s and I_{ir} are the short and long-wave radiation (W m-2), respectively; α_f and α_g are the foliage and substrate albedos; ε_f and ε_g are the substrate and foliage emissivity; ε_l is equal to $\varepsilon_g + \varepsilon_f - \varepsilon_f \varepsilon_g$; H_f and H_g are the sensible heat fluxes of the foliage and substrate, respectively, while L_f and L_f are the corresponding latent heat fluxes (W m-2); k is the substrate thermal conductivity (W m-1 K-1); and z is the substrate depth (m).

3.4 Results and analysis

3.4.1 Experimental heat fluxed through vegetated roofs

Three vegetated roofs are also investigated via field measurements at the Laboratory of Vegetated Infrastructure of Buildings at Pontificia Universidad Católica de Chile located in Santiago during December 20th and 21st, 2016 (summer days). Figure 12 shows the instrumented roofs: (1) an uninsulated concrete slab with substrate but no

vegetation, (2) an uninsulated concrete slab with vegetated roof, and (3) and insulated lightweight metal roof with vegetated roof. All roofs have the same substrate type. Installed heat flux sensors (model HFP-01 Hukseflux) are located between the slab and the substrate. Table 11 shows three vegetated roof components, which are very similar to the parametric analysis performed in this study. Figure 13 shows the uninsulated concrete slab without vegetation (but with substrate) has the largest heat gains during daytime, peaking at 10 Wh/m2, while the same roof with vegetation have heat losses during typical working hours of retail stores (8 AM – 10 PM). This demonstrates plants can reduce incoming heat flux and overall reduce cooling loads. Figure 12 also shows that the insulated lightweight metal roof with vegetation presents only heat losses through the roof, but they lose less heat after 4 PM than that for the uninsulated concrete slab with vegetation. Although these two cases are not completely comparable to the retail store, these results evidence that thermal insulation might limit the thermal benefits of vegetated roof and the following section will have more in-depth numerical simulations.

Figure 12: Panoramic view of the evaluated vegetated roof at Laboratory of Vegetated Infrastructure of Buildings (Chile)

Table 11: Components of vegetated roofs evaluated experimentally

Roof Type	Roof structure	Insulation thickness	Substrate thickness	Vegetation
Uninsulated concrete slab without vegetation	Normal concrete slab 150 mm	0 mm	170 mm	None (LAI = 0)
Uninsulated concrete slab with vegetation	Normal concrete slab 150 mm	0 mm	170 mm	Grass: festuca (LAI ~ 3)
Insulated lightweight metal with vegetation	Lightweight metal deck	50 mm	170 mm	Grass: festuca (LAI ~ 3)

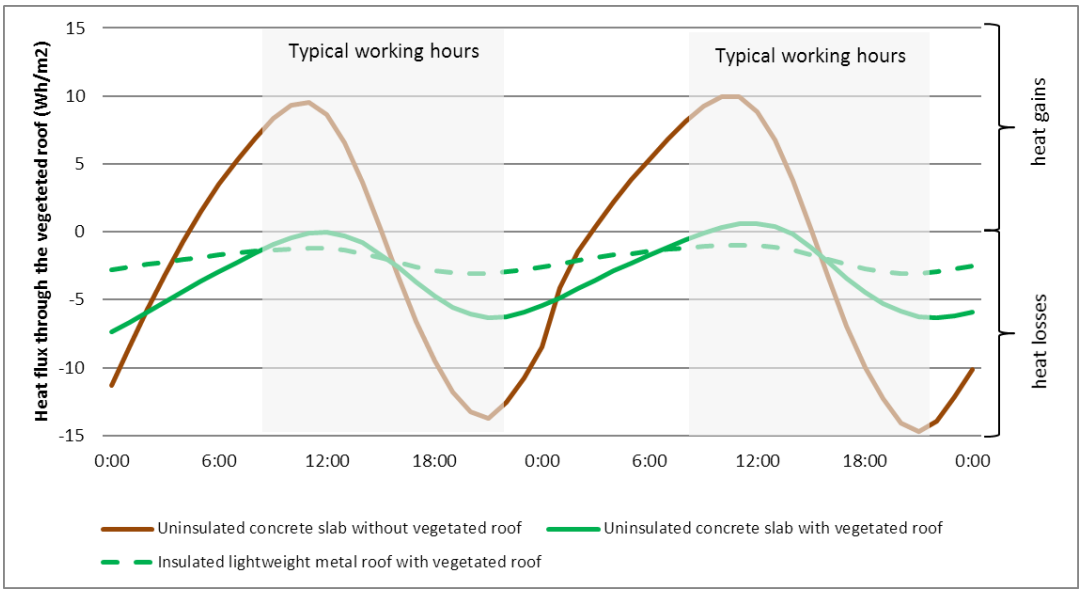

Figure 13: Heat fluxes through vegetated roofs of a typical summer day in Santiago (Chile).

3.4.2 Simulation results

The main results shown in this paper correspond to the cooling and heating loads. This section presents and analyzes the results about the impacts LAI, substrate properties and the level of insulation has on cooling and heating loads for two roofing structures in Albuquerque, Santiago, and Melbourne.

3.4.2.1 Influence of the leaf area index

Table 12 shows the effect LAI has on heating and cooling loads for uninsulated concrete slab (C) and lightweight metal (M) roofs for Albuquerque (Alb), Santiago (Stgo), and Melbourne (Melb). LAI values of 0.1 and 5 represent range of potential values for vegetated roofs and the percentage difference is highlighted with a gray background. Higher LAI values can lower or increase heating loads depending on the weather: for Santiago and Melbourne, the average seasonal solar radiation and wind speed are lower, below 300 W/m2 and 1-2 m/s, respectively. For this reason by increasing the LAI the vegetated roof works as a barrier that decreases the heating losses through the roof. In contrast, Albuquerque has higher average winter solar radiation (670 W/m2) and wind speed (3-4 m/s). This is important since at low solar radiation, the shading effect due to higher LAI is not as important as when there is higher irradiance. Higher irradiance and wind speed also contributes to higher evapotranspiration as shown in Figure 14. All three selected cities follow the same trend, but Albuquerque case seems to be more sensitive to changes in LAI. For this reason, increasing the value of LAI increases the heating loads in Albuquerque while decreases heating loads in Santiago and Melbourne.

Table 12 also shows the corresponding values for cooling, the value of LAI increases the cooling loads in the three cities. This is consequence of higher evapotranspiration and shading at higher LAI that diverts incoming solar heat gains through the roof during warmer seasons. Figure 15 shows the average substrate surface temperature for Santiago for all analyzed roofs. In summer, higher solar radiation causes higher evapotranspiration while higher shading causes lower substrate surface temperature, thus cooling loads are reduced.

It is also important to consider the values shown in Table 12. For example, in Melbourne an uninsulated vegetated roof with LAI value of 0.1 and a lightweight substrate has heating loads 82% less than the same roof with heavyweight substrate. In contrast, roofs with heavyweight substrate have lower cooling loads (about 24% and 22%) than roofs with lightweight substrate. Thus, substrate selection should also be a design factor to consider, but the following section provides more in-depth analysis.

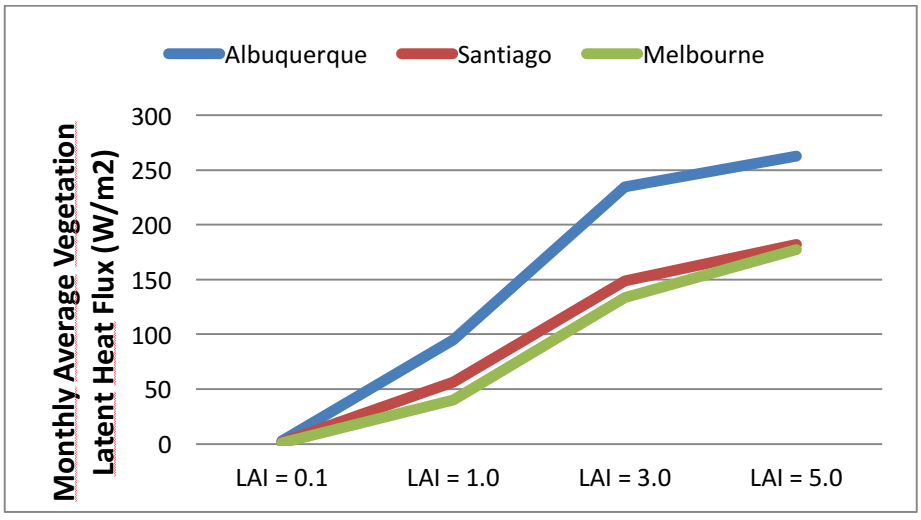

Figure 14: Average vegetation latent heat flux (W/m2) for different LAI values at 2 pm in Albuquerque (January), Santiago (July) and Melbourne (July) for metal roof.

Table 12: Effect of LAI on annual heating and cooling loads for uninsulated concrete slab (C) and metal roofs (M)

		Heating Loads (kWh/m^2·year)				Cooling Loads (kWh/m^2·year)			
Roof structure and location	**Substrate Type**			**LAI 5.0 - LAI 0.1**				**LAI 5.0 - LAI 0.1**	
		LAI 0.1	**LAI 5.0**	**Diff.**	**%**	**LAI 0.1**	**LAI 5.0**	**Diff.**	**%**
C - Alb	LW	4.77	6.70	1.93	29	68.17	56.64	-11.54	-20
C - Alb	HW	17.79	18.81	1.02	5	66.75	57.72	-9.04	-16
M – Alb	LW	12.30	11.75	-0.55	-5	77.84	61.02	-16.82	-28
M – Alb	HW	33.82	27.72	-6.11	-22	78.24	59.72	-18.52	-31
C – Stgo	LW	2.39	2.21	-0.18	-8	47.52	41.32	-6.20	-15
C – Stgo	HW	14.52	9.10	-5.42	-60	51.66	42.57	-9.09	-21
M – Stgo	LW	5.55	4.47	-1.08	-24	37.49	34.00	-3.49	-10
M – Stgo	HW	29.43	16.42	-13.01	-79	41.47	32.60	-8.87	-27
C – Melb	LW	1.94	1.87	-0.07	-4	45.58	41.45	-4.13	-10
C - Melb	HW	11.33	7.95	-3.38	-43	34.42	31.18	-3.24	-10
M – Melb	LW	4.33	3.64	-0.69	-19	49.92	43.65	-6.27	-14
M - Melb	HW	24.29	14.39	-9.90	-69	38.76	29.77	-9.00	-30

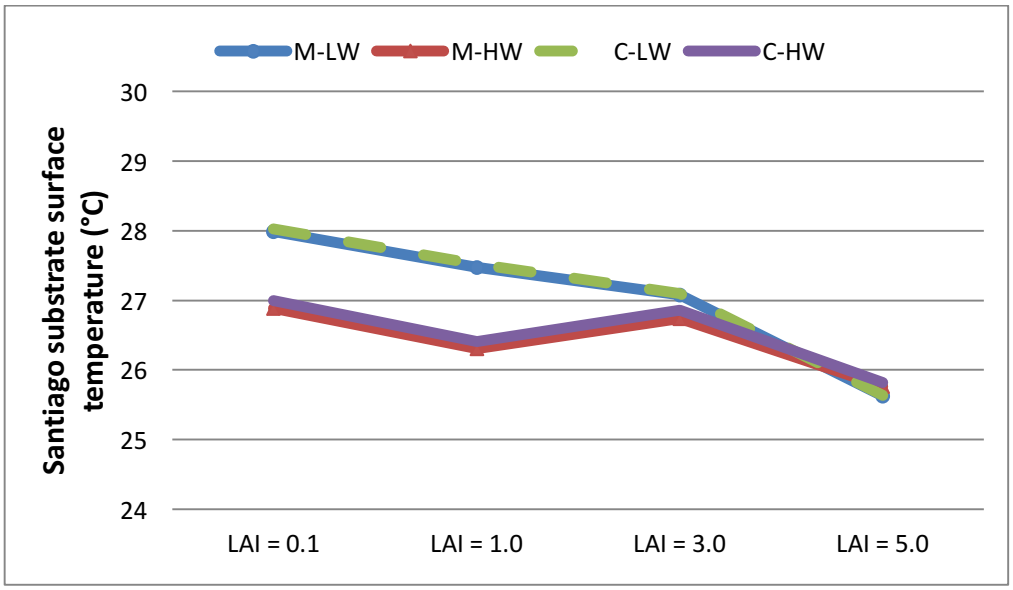

Figure 15: Average substrate temperature of the uninsulated metal (M) and concrete (C) vegetated roof with light (LW) and heavy (HW) substrates at different values of leaf area index for Santiago (January).

3.4.2.2 Influence of the substrate

Table 13 shows the impact the substrate type – lightweight (LW) and heavyweight (HW) – has on the thermal performance of the vegetated roof. Heating loads reduction ranges from 58% to 77% for an uninsulated roof and 4% to 10% for an insulated roof. In contrast, an uninsulated vegetated roof lightweight substrate has about 33% and 47% smaller cooling load than a vegetated roof with heavyweight substrate. These results are mainly explained by the lower thermal conductivity of the lightweight which is four times smaller than that for heavyweight substrate, an important factor for winter, where temperature oscillations tend to be lower than in summer. Nevertheless, both substrates have similar thermal diffusivities (Table 8) which means both substrates have similar rates of heat transfer across them for cases when transient effects are more important, such in summer, with larger daily temperature oscillations. In summer there is no significant difference between cooling loads for uninsulated vegetated roof with the two substrate types. This is explained due to the similar thermal diffusivity of the substrates and large temperature oscillations. On the contrary, in winter there is a significant difference in the heating loads between uninsulated vegetated roofs with light and heavyweight substrate. Since there are lower temperature oscillations in winter, the thermal conductivity shows larger influence than the thermal mass on the heat transfer through the substrate.

Table 13: Annual heating and cooling loads variations due to changes on green roof substrate – lightweight (LW) and heavyweight (HW) – with concrete slab (C) and metal (M) roofs

(1): Insulation thickness (mm)

Roof structure – City	(1)	Heating Loads (kWh/m^2·year)				Cooling Loads (kWh/m^2·year)			
		LW LAI 5.0	HW LAI 5.0	HW – LW		LW LAI 5.0	HW LAI 5.0	HW – LW	
				Diff.	%			Diff.	%
C - Alb	0	6.70	18.81	12.11	64	56.64	57.72	1.08	2
M - Alb	0	11.75	27.72	15.97	58	61.02	59.72	-1.31	-2
C - Stgo	0	2.21	9.10	6.89	76	41.32	34.00	-7.31	-22
M - Stgo	0	4.47	16.42	11.96	73	42.57	32.60	-9.97	-31
C - Melb	0	1.87	7.95	6.08	77	41.45	31.18	-10.27	-33
M - Melb	0	3.64	14.39	10.76	75	43.65	29.77	-13.88	-47
C - Alb	50	2.31	2.56	0.24	9	61.80	61.82	0.02	0
M - Alb	50	3.44	3.69	0.25	7	64.12	64.17	0.05	0
C - Stgo	50	0.92	0.96	0.04	4	51.11	51.35	0.24	0
M - Stgo	50	1.21	1.28	0.07	5	53.53	53.36	-0.16	0
C - Melb	50	0.86	0.96	0.10	10	52.36	49.99	-2.37	-5
M – Melb	50	1.19	1.29	0.10	7	53.64	52.45	-1.18	-2

Table 13 shows metal roofs are more sensible than concrete roofs to the selection of substrate type. This is due to the differences in thermal mass between metal and concrete roofs, having the concrete roof significant more mass and higher thermal resistance than the metal roof. For this reason, an uninsulated metal green roof is more sensitive to variations of the thermal properties of the substrate. For vegetated roofs with 50 mm of insulation, the effect of the substrate on the heating load is lower while for cooling loads is negligible as observed in Table 13. The following section will look at this more carefully.

3.4.2.3 Influence of thermal insulation

Tables 14 and 15 show the role thermal insulation has on the thermal performance of the stand-alone retail building with vegetated roofs. Uninsulated vegetated roofs have higher heating loads than insulated vegetated roofs for both concrete and metal roofing systems. These results show that vegetated roofs cannot replace the thermal insulation in heated dominated climates. However, similar values of heating loads can be achieved using a substrate with low thermal conductivity.

Table 14: Annual heating loads of vegetated roofs and a traditional insulated roofing system. (1): Traditional Insulated Roof (5cm of insulation); (2): Uninsulated Green Roof (LAI 5.0)

Annual Heating Loads (kWh/m2·year)									
Roof structure-city	**Substrate**	**(1)**	**(2)**	**Diff.**	**%**	**(1)**	**(2)**	**Diff.**	**%**
C – Alb	LW	4.52	6.70	2.18	32	4.52	2.31	-2.21	-95
C – Alb	HW	4.52	18.81	14.29	76	4.52	2.56	-1.96	-77
M – Alb	LW	8.94	11.75	2.82	24	8.94	3.44	-5.50	-160
M – Alb	HW	8.94	27.72	18.78	68	8.94	3.69	-5.25	-142
C – Stgo	LW	1.37	2.21	0.84	38	1.37	0.92	-0.45	-49
C – Stgo	HW	1.37	9.10	7.72	85	1.37	0.96	-0.41	-43
M – Stgo	LW	3.32	4.47	1.15	26	3.32	1.21	-2.11	-175
M – Stgo	HW	3.32	16.42	13.10	80	3.32	1.28	-2.04	-160
C – Melb	LW	1.14	1.87	0.73	39	1.14	0.86	-0.28	-32
C – Melb	HW	1.14	7.95	6.81	86	1.14	0.96	-0.18	-19
M – Melb	LW	2.46	3.64	1.18	32	2.46	1.19	-1.27	-106
M – Melb	HW	2.46	14.39	11.93	83	2.46	1.29	-1.17	-91

In contrast with heating, Table 15 shows that, while there are important differences depending on the climate, vegetated roofs are effective at reducing cooling loads and the uninsulated vegetated roofs achieve lower cooling loads than the insulated roofs. For example, cooling load of the uninsulated vegetated roof with concrete slab and heavy

substrate (C-Alb-HW) is 4.1 kWh/m2·year lower than the insulated vegetated roof in Albuquerque and 18.81 kWh/m2·year lower in Melbourne.

Vegetated roofs upon the insulated lightweight metal roof reduce the cooling loads between 18% and 23%. Since many buildings in developing countries are uninsulated, vegetated roofs could be an important approach to reduce cooling loads.

Table 15: Annual cooling loads for vegetated roofs and traditional insulated roofing systems. TRS: Traditional Insulated Roof (5cm of insulation); (1): Uninsulated Green Roof (LAI 5.0); (2): Insulated Green Roof (LAI 5.0 and 5 cm of insulation).

Cooling Loads (kWh/m^2·year)									
Roof structure – city	Substrate	TRS	(1)	LAI 5.0 -TRS		TRS	(2)	LAI 5.0 –TRS	
				Diff.	%			Diff.	%
C – Alb	LW	60.29	56.64	-3.65	-6	60.29	61.80	1.51	2%
C – Alb	HW	60.29	57.72	-2.57	-4	60.29	61.82	1.53	2%
M – Alb	LW	77.99	61.02	-16.97	-28	77.99	64.12	-13.87	-22%
M – Alb	HW	77.99	59.72	-18.27	-31	77.99	64.17	-13.82	-22%
C – Stgo	LW	47.14	41.32	-5.82	-14	47.14	51.11	3.97	8%
C – Stgo	HW	47.14	34.00	-13.14	-39	47.14	51.35	4.21	8%
M – Stgo	LW	63.12	42.57	-20.55	-48	63.12	53.53	-9.59	-18%
M – Stgo	HW	63.12	32.60	-30.52	-94	63.12	53.36	-9.76	-18%
C – Melb	LW	50.59	41.45	-9.14	-22	50.59	52.36	1.77	3%
C – Melb	HW	50.59	31.18	-19.41	-62	50.59	49.99	-0.60	-1%
M – Melb	LW	64.33	43.65	-20.68	-47	64.33	53.64	-10.69	-20%
M – Melb	HW	64.33	29.77	-34.56	-116	64.33	52.45	-11.88	-23%

Likewise, increasing the vegetated roof's thermal insulation from 50 mm to 100 mm increases the cooling loads and reduces the heating loads as shown Table 16. Increasing the thermal insulation levels decouples the indoor from the outdoor environment, reducing the ability of the vegetated roof to remove heat from the building. Thus, from only a cooling perspective, there are no benefits from continuously adding insulation.

Table 16: Annual heating and cooling loads for different insulated vegetated roofs

(1): Insulation Thickness (50 mm); (2): Insulation Thickness (100 mm)

		Heating Loads ($kWh/m^2 \cdot year$)				Cooling Loads ($kWh/m^2 \cdot year$)			
Roof structure – city	**Substrate**	**(1)**	**(2)**	**100 mm – 50 mm**		**(1)**	**(2)**	**100 mm – 50 mm**	
				Diff.	**%**			**Diff.**	**%**
C - Alb	LW	2.31	1.85	-0.46	-24.9	61.80	62.84	1.04	1.7
C - Alb	HW	2.56	1.89	-0.67	-35.5	61.82	63.53	1.71	2.7
M – Alb	LW	3.44	2.65	-0.79	-29.8	64.12	65.3	1.18	1.8
M – Alb	HW	3.69	2.68	-1.01	-37.7	64.17	65.65	1.48	2.3
C – Stgo	LW	0.92	0.85	-0.07	-8.2	51.11	54.39	3.28	6.0
C – Stgo	HW	0.96	0.86	-0.1	-11.6	51.35	53.73	2.38	4.4
M – Stgo	LW	1.21	1.04	-0.17	-16.3	53.53	56.59	3.06	5.4
M – Stgo	HW	1.28	1.04	-0.24	-23.1	53.36	56.8	3.44	6.1
C – Melb	LW	0.86	0.84	-0.02	-2.4	52.36	53.46	1.1	2.1
C - Melb	HW	0.96	0.84	-0.12	-14.3	49.99	53.06	3.07	5.8
M – Melb	LW	1.19	1.05	-0.14	-13.3	53.64	56.26	2.62	4.7
M - Melb	HW	1.29	1.06	-0.23	-21.7	52.45	55.14	2.69	4.9

3.4.2.4 Heat flux through the roofing system

In order to understand the difference in the cooling loads between the insulated and uninsulated vegetated roofs, the heat fluxes across the roofing systems are shown in Figure 16. This figure shows heat fluxes through the uninsulated metal roof with lightweight substrate (dotted lines) and heavy substrate (straight lines) and different LAI values (0.1, 1, 3 and 5) for two typical summer days in Santiago. The heat fluxes through the roof significantly decrease with higher LAI values due to the increase of the evapotranspiration and shading. Roofs with light substrates have lower heat fluxes than with heavy substrate due to lower thermal conductivity. Peak heat flux reduction is about 20 W/m2 when comparing a vegetated roof without and with plants having a LAI

equal to 5. For the light substrate, reduction is about 5 W/m2. Figure 16 also shows building internal loads are a reference of the magnitude and timing of other heat gains.

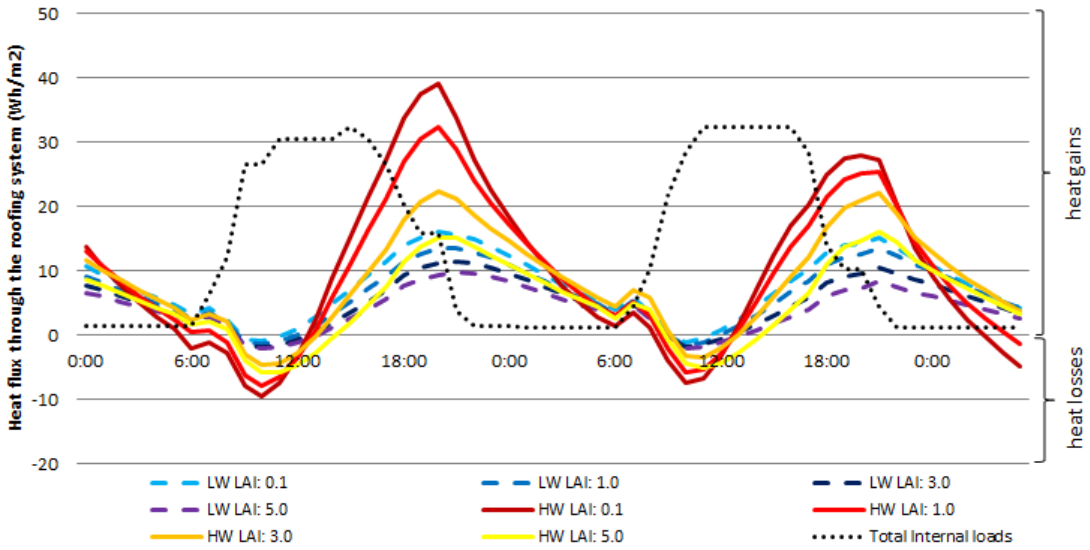

Figure 16: Total internal loads and roof heat flux for uninsulated vegetated roofs for lightweight metal roof during January 19-21 in Santiago (summer)

Figure 17 shows the roof's heat gains and losses through insulated lightweight metal roof (dotted lines) and through uninsulated lightweight metal roof with HW substrate (straight lines) for LAI values of 0.1, 1, 3 and 5. The insulation layer of 50 mm causes a significant drop of heat gains through the roof, and make the building less susceptible to LAI changes, as the insulation layer is serving as a thermal break between the green roof and the building.

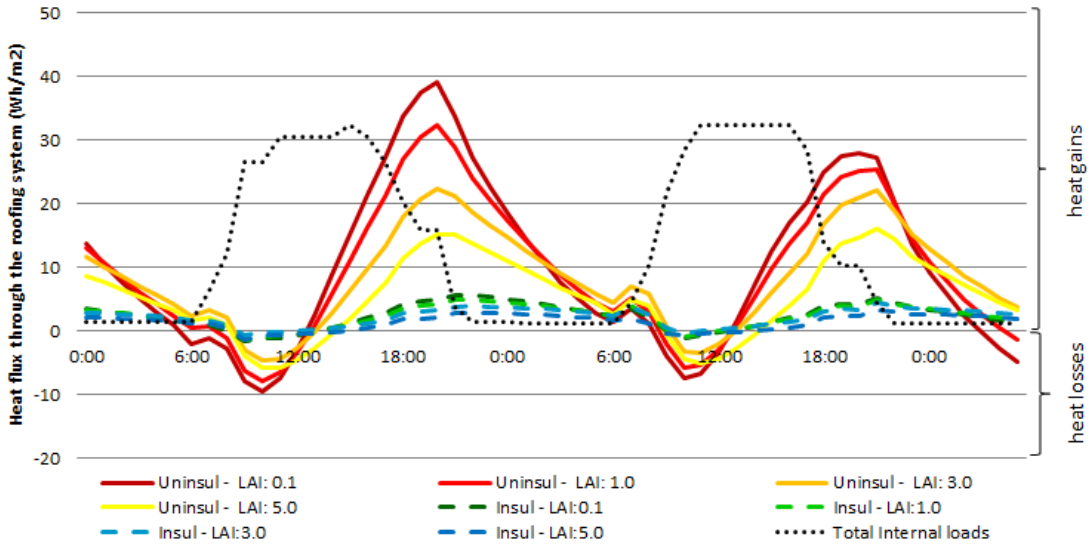

Figure 17: Total internal loads and roof heat flux for roofs for uninsulated and insulated vegetated lightweight metal roof with HW during January 19-21 in Santiago (summer)

Figures 16 and 17 show vegetation not only significantly reduces heat gains due to evapotranspiration and shading effects, but also allows dissipating (negative fluxes) the internal heat gains during daytime (from 6 AM to 1 PM), period of time that matches with peak period of internal loads. In addition, as the building envelope loads decreases, internal gains increase. Thus a technology that could remove these internal gains without using electricity would be beneficial. Vegetated roofs could potentially do that, if evapotranspiration is increased by using plants with lower stomatal resistance.

3.5 Conclusions and recommendations

Retail stores energy efficiency strategies are driven by the very low profit margin of around 4%; vegetated roofs can increase energy savings in this type of buildings because of the large roofing area and no more than 2 stories. Therefore, this study evaluates the influence leaf area index (LAI), substrate properties, and roof's thermal insulation has on the thermal performance of a stand-alone retail building. The study is performed in three cities: Albuquerque (USA), Santiago (Chile) and Melbourne (Australia). The two first cities present semiarid climate conditions, while Melbourne has a marine coast climate condition. Two traditional roofing systems (lightweight metal steel roof deck (M) and concrete slab (C)), two substrates (LW and HW), four different LAI levels (0.1, 1.0, 3.0, 5.0) and three different levels of insulation (0, 50 and 100 mm) were studied. The main conclusions, based on the analyzed building and weather files, obtained in this study are:

- Vegetation is more effective than insulation on reducing cooling loads due to the evapotranspiration of the vegetation-substrate system and canopy's shading effect. Actually, uninsulated vegetated roofs not only reduce roof's solar heat gains but also allow internal heat gains dissipate through the roof during period of peak internal heat gains. In addition, thermal insulation can decrease the vegetated roof's ability to reduce cooling loads.
- Thermal insulation shows significantly larger influence on the stand-alone retail's heating loads than the thermal properties of the substrates and LAI of

vegetation. Thus, vegetated roofs cannot replace insulation to reduce heating loads.

- The effect of the substrate's thermal properties on the heating loads is directly related to the substrate's thermal conductivity. However, substrate influence on the cooling loads depends on its thermal diffusivity. This explains the fact that lightweight substrate (LW) and heavyweight substrate (HW) have very similar cooling loads but very different heating loads.
- Uninsulated lightweight metal roofs are more sensitive in comparison with uninsulated concrete slab to variations in the vegetated roofs parameters. This is because the concrete slab already provides thermal inertia to the roofing system. On the contrary, the thermal behavior of both roofing systems is similar when both are insulated
- Despite the similar Köppen classification between Albuquerque and Santiago both cities have different behaviors on their weather conditions due to this cannot be assumed that vegetated roof will have the same performance in places with the same weather classification.

4. IMPLEMENTATION, EVALUATION AND VALIDATION OF TWO TRANSIENT HEAT AND MASS TRANSFER MODELS IN MATLAB FOR SEMIARID CLIMATES AND HUMID CONTINENTAL CLIMATES

4.1 Abstract

Given the high energy cost in the building sector, it has become a necessity to find solutions that reduce its energy consumption. One of these solutions is the implementation of vegetative roofs. Two vegetative roofs models already have been implemented in simulation software to assist developers to design vegetative roofs. However, to fully obtain the benefits of this technology is important to ensure that these models can accurately represent vegetative roof in climates where they have not been validated.

This paper presents the implementation, evaluation and validation of the vegetated roof models developed by Sailor (2008) and Tabares & Srebric (2011). Due to the original versions of these model do not consider thermal inertia, it was incorporated with the method of finite differences. The models were evaluated comparing the simulated results against experimental data of real vegetated roof. The experimental data embraces two different climates, two different vegetation species and two different substrates. The purpose of this study is to evaluate the accuracy of the results obtained with these models and to obtain information that indicates if these models can be used to design properly vegetative roofs for the semi-arid climates.

The simulation's results show that these vegetated roof models are able to accurately represent the behavior of three vegetative roofs located in Santiago of Chile, and one vegetative roof installed in a commercial building in Chicago. The RMSD obtained with experimental data Chicago is 2.51°C for Tabares model, and 3.53°C for Sailor model. The maximum RMSD obtained with experimental data Santiago is 2.08 °C for Tabares model, and 2.29°C for Sailor model. To represent accurately the behavior of the vegetated roof is fundamental to measure the substrate and vegetation parameters, in order to use them as inputs for the models.

4.2 Introduction

Vegetative roofs – so called green roofs- are building roofing systems that partially or completely covered incorporate vegetation on its outermost layer, which aims to improve the energy and thermal performance of the roof and the building.

There are several studies that analyze the influence of vegetative roof on energy performance of buildings. These studies also refer to the main mechanisms used by vegetative roofs to achieve this decrease in energy consumption (Berardi 2014, Castleton 2010, Fioretti 2010, Tabares-Velasco 2009). These may include:

- Thermal inertia of the substrate: The substrate contributes with thermal mass that helps to stabilize the indoor temperatures. For this reason, there is a reduction of the peak loads.
- Shading of vegetation: Vegetation provides a layer that shades the substrate. For this reason, the radiation absorbed by the roof and its surface temperature are lower. This contributes to reduce the heat fluxes through the roof towards the

interior of the building, and therefore its cooling loads. Weng (2014) showed that 60% of the radiation that reaches the vegetative roof is absorbed by the vegetation and used for the evapotranspiration process, whereas 20% is reflected, thus transmitting only 20% to the substrate.

- Evapotranspiration: This process considers the evaporation of the water contained in the substrate and the water used by the plants in their transpiration process. This means the water present on the roof turns into water vapor thus absorbing energy. As a result, this process cools the surface of the vegetative roof, decreasing the heat flux towards the interior of the building.
- Thermal insulation of the substrate: The implementation of an extra material layer decreases the U-value of the roofing system. As a result, reductions of the heat fluxes through the roof can be achieved. This phenomenon depends directly on the type of substrate considered and its moisture content.

Due to the aforementioned, vegetative roofs are complex envelope systems, which have great potential to influence the energy performance of buildings. As result of all the parameters of the vegetated roof that impact on the building energy consumption it is not trivial to design vegetated roofs.

18 vegetative roof models have been developed since 1982. However, it is not possible to assert an accurate calculation of the thermal performance of vegetated roofs with these models. This gap is generated for several reasons: (1) Not all the developed vegetative roof models consider the effects of thermal inertia; (2) none of these models have been evaluated for other different conditions that the validation climate; (3) only

two of the total developed models have been implemented in the building energy simulation tools called EnergyPlus; (4) despite this implementation, this simulation tools does not provide an open source code in order to check and understand how the vegetated roof model are being considered, acting mainly as a black box; and (5) an exhaustive literature review did not find a study that simultaneously implemented, evaluated and validated more than one model in two different climates against field experimental data.

The purpose of this study is to obtain a validated tool that allows designing properly vegetative roofs for the semiarid climates. In order to achieve this, two vegetative roof models (Sailor 2008 and Tabares & Srebric 2011) has been implemented in MATLAB considering the effect of thermal inertia through finite difference method. The validation of these models has been done through the comparison of the simulated results against experimental data of three real vegetative roofs located in Santiago of Chile, and one real vegetative roof installed in a commercial building in Chicago. The experimental data embraces two different climates, two different vegetation species and two different substrates.

4.3 Vegetated roofs modelling

4.3.1 Sailor green roof model

The vegetative roof model developed by Sailor (Sailor 2008) is based on the Fast All-season Soil STrenght (Frankestein & Koenig 2004, Frankestein & Koenig 2004), the Biosphere Atmosphere Transfer Scheme (Dickison et al. 1993) and the Simple

Biosphere (Sellers et al. 1986) models. This vegetated roof model is currently the only model implemented in the building energy simulation tool EnergyPlus.

The following 5 sub sections explains (1) the substrate and vegetation energy budget developed by the model; (2) the implementation of the vegetation shading effect; (3) the evapotranspiration (ET) calculation considered in the model; (4) the stomatal resistance calculation considered in the model; and (5) the relation between the substrate's thermal properties and the volumetric water content (VWC) in the substrate.

4.3.1.1 Substrate and vegetation energy budget

The vegetated roof model consists on a single vegetation layer (Eq. 9) above the surface of a substrate layer (Eq. 10). These equations allow calculating the canopy (T_f) and substrate surfaces (T_g) temperatures (in Kelvin) that are used by EnergyPlus to calculate the heat flux through the whole roofing system.

$$F_f = \sigma_f \left[I_s\left(1-\alpha_f\right) + \varepsilon_f I_{ir} - \varepsilon_f \sigma T_f^4\right] + \frac{\sigma_f \varepsilon_g \varepsilon_f \sigma}{\varepsilon_l}\left(T_g^4 - T_f^4\right) + H_f + L_f \quad \text{(Eq. 9)}$$

$$F_g = \left(1-\sigma_f\right)\left[I_s\left(1-\alpha_g\right) + \varepsilon_g I_{ir} - \varepsilon_g \sigma T_g^4\right] - \frac{\sigma_f \varepsilon_g \varepsilon_f \sigma}{\varepsilon_l}\left(T_g^4 - T_f^4\right) + H_g + L_g + k\,\frac{\partial T_g}{\partial z} \quad \text{(Eq. 10)}$$

where σ_f is the canopy fractional coverage; I_s and I_{ir} are the short and long-wave radiation (Wm-2), respectively; α_f and α_g are the foliage and substrate albedos; ε_f and ε_g are the substrate and foliage emissivity; ε_l is equal to $\varepsilon_g + \varepsilon_f - \varepsilon_f \varepsilon_g$; H_f and H_g are the sensible heat fluxes of the foliage and substrate, respectively, while L_f and L_g are

the corresponding latent heat fluxes (Wm-2); k is the substrate thermal conductivity (Wm-1K-1); and z is the substrate depth (m).

4.3.1.2 Shading by the vegetation

The use of a vegetation layer above the roof provides shades to the substrate below the plants. For this reason the surface temperature of the substrate and the radiation absorbed by the roof are lower compared to conventional roofs. This contributes to reduce the heat fluxes through the roof towards the interior of the building, and therefore its cooling loads.

In this model, the shading effect is considering by the implementation of a fractional coverage factor in the energy balance (σ_f). This factor diminishes the amount of incoming shortwave radiation in the substrate layer. This factor also affects the amount of longwave radiation reflected between the substrate and the vegetation.

4.3.1.3 Evapotranspiration

The evaporation of the substrate and the transpiration of the plant are calculated directly from the latent heat flux calculations for the substrate (Eq. 11) and vegetation (Eq. 12) layers and the latent heat of vaporization of the water.

$$L_g = C_{e,g}\, l_g\, \rho_{af}\, W_{af} \left(q_{af} - q_g\right) \quad \text{(Eq. 11)}$$

$$L_f = l_f\, LAI\, \rho_{af}\, C_f\, W_{af}\, r'' \left(q_{af} - q_{f,sat}\right) \quad \text{(Eq. 12)}$$

where $C_{e,g}$ is the bulk transfer coefficient; l_g and l_f are the latent heat of vaporization at the ground and vegetation surfaces (J kg^{-1}), respectively; ρ_{af} is the density of air at the instrument height (kg m^{-3}); W_{af} is the wind speed within the vegetation (m s^{-1}); r'' is

the vegetation surface wetness factor and represents the combined effect of aerodynamic and stomatal resistances to vapor diffusion (s m^{-1}); q_{af}, q_g and $q_{f,sat}$ are the mixing ratios at the vegetation-air interface, at ground surface, and the saturation mixing ratio at the vegetation surface temperature, respectively; while L_f and L_f are the corresponding latent heat fluxes (W m-2).

4.3.1.4 Stomatal resistance

The transpiration of the plant is the process of water loss through plant respiration. It is controlled by the opening and closing of the stomata on the leaf surfaces. The resistance to the diffusion of water vapor from the leaf surface to the atmosphere is called stomatal resistance. It depends of factors such as solar radiation, volumetric water content (VWC) of the substrate and vapor pressure difference between the ambient air and the leaf interior. Eq. 13 represents the stomatal resistance calculation in the model.

$$r_s = \frac{r_{s,min}}{LAI} f_{Is} f_\theta f_3 \quad \text{(Eq. 13)}$$

where $r_{s,min}$ is the minimum stomatal resistance of the plant (s m^{-1}); LAI is the leaf area index of the vegetation; f_{Is} is the multiplying factor for radiation effect; f_θ is the multiplying factor for VWC on stomatal resistance; and f_3 is the additional multiplying factor for stomatal resistance and has a value of 1 for any kind of vegetation except for trees.

4.3.1.5 Substrate thermal properties variation

The vegetative roof model considers the variation of the substrate thermal properties based on the current VWC of the substrate and generalized sensitivity functions. Sailor & Hagos (2011) in prior laboratory measurements explored the variation of these properties with VWC for eight different substrates. His results found that diffusivity and conductivity varied linearly with the VWC in the substrate, thus saturated substrates show 40% higher specific heat capacity and twice the thermal conductivity than that of the dry samples. The results show that increment of the VWC decrease linearly the substrate albedo. Also in the study, the density of the substrate was calculated directly from the density of the dry soil and the density of water.

The available version of the Sailor's vegetative roof model that is incorporated in EnergyPlus does not consider the variation of these properties with the VWC. The one-dimensional heat conduction with varying substrate's thermal properties is complicated due to the use of conduction transfer functions (CTF). This method does not allow the properties to vary in response to the moisture content of the substrate because the CTF is calculated at the beginning of the simulation and it remains constant to avoid stability issues.

4.3.2 Tabares and Srebric green roof model

The vegetative roof model developed by Tabares considered a vegetative roof without plants and then considered a vegetative roof with plants. Then these two models are combined into a model partially-covered vegetative roof model.

4.3.2.1 Substrate and vegetation energy budget

The vegetated roof model consists on a single vegetation layer (Eq. 14) above the surface of a substrate layer (Eq. 15). Equations 14 and 15 allow calculating the vegetation and substrate surfaces temperatures (in Kelvin) that are used to calculate the heat flux through the whole roofing system.

$$E_f = -R_{sh\_f} + Q_{conv\_f} + Q_{ir\_f} + Q_T + -Q_{ir\_sp} \quad \text{(Eq. 14)}$$

$$E_s = -R_{sh\_s} - Q_{ir_{sp}} + Q_{conv\_s} + Q_{ir\_scov} + Q_E + Q_{cond} \quad \text{(Eq. 15)}$$

where R_{sh_f} and R_{sh_s} are the incoming solar radiation into the vegetation and substrate layers (Wm-2), respectively; Q_{conv_f} and Q_{conv_s} are the convective heat fluxes in the vegetation and substrate (Wm-2), respectively; Q_{ir_f}, Q_{ir_scov} and Q_{ir_sp} are the long-wave radiation between the vegetation and the environment, the substrate and the environment, and between the substrate and the vegetation (Wm-2), respectively; Q_E and Q_T are the substrate evaporation and plants transpiration heat fluxes (Wm-2), respectively; Q_{cond} is the conductive heat fluxes through the substrate (Wm-2).

4.3.2.2 Shading by the vegetation

In this model, the shading effect is considering by the implementation of the extinction coefficient of the plant (k_s). This factor diminishes the amount of incoming shortwave radiation into the substrate layer, intercepting it in the vegetation layer. This parameter is used to calculate the sort-wave transmittance of the vegetation layer according to the Eq. 16.

$$\tau_{plants,solar} = e^{-k_s\, LAI} \quad \text{(Eq. 16)}$$

where $\tau_{plants,solar}$ is the short-wave transmittance of the plants; k_s is the extinction coefficient; and LAI is leaf area index of the vegetation.

4.3.2.3 Evapotranspiration

The evaporation of the substrate and the transpiration of the plant are calculated directly from the latent heat flux calculations for the substrate (Eq. 17) and vegetation (Eq. 18) layers and the corresponding values of latent heat of vaporization of the water.

$$Q_E = \frac{\rho\, C_p}{\gamma\,(r_{subs}+r_a)}\,(e_{subs} - e_{air}) \quad \text{(Eq. 17)}$$

$$Q_T = LAI\,\frac{\rho\, C_p}{\gamma\,(r_s+r_a)}\left(e_{s,plants} - e_{air}\right) \quad \text{(Eq. 18)}$$

where C_p is the specific heat of air (J $kg^{-1}K^{-1}$); γ is the psychrometric constant; ρ is the density of air (kg m^{-3}); r_{subs} is the substrate resistance to evaporation (s m^{-1}); r_a is the aerodynamic resistance to mass transfer (s m^{-1}); r_s is the stomatal resistance of the vegetation (s m^{-1}); LAI is the leaf area index of the plant; e_{air}, e_{subs} and $e_{s,plants}$ are the vapor pressure in the air, the saturated vapor pressure at the soil temperature, and the saturated vapor pressure at the vegetation temperature (kPa).

4.3.2.4 Stomatal resistance

Eq. 19 represents the stomatal resistance calculation in the model.

$$r_s = \frac{r_{s,min}}{LAI}\, f_{solar}\, f_{VPD}\, f_{VWC}\, f_{temperature} \quad \text{(Eq. 19)}$$

where $r_{s,min}$ is the minimum stomatal resistance of the plant (s m^{-1}); LAI is the leaf area index of the vegetation; f_{solar} is the multiplying factor for solar radiation; f_{VPD} is the multiplying factor for vapor pressure deficit; f_{VWC} is the multiplying factor for VWC in the substrate; and $f_{temperature}$ is the multiplying factor for the temperature of the plant.

4.3.2.5 Substrate thermal properties variation resistance

Similarly to Sailor's vegetative roof model, the model developed by Tabares considers the variation of the substrate thermal properties based on the current VWC of the substrate and generalized sensitivity functions. The conductive heat transfer through the green roof substrate is calculated by the Fourier's Law, and the thermal conductivity is considered according to Eq.20.

$$k_{substrate} = a_1 + a_2 \times VWC \quad \text{(Eq. 20)}$$

where $k_{substrate}$ is the thermal conductivity of the substrate (W m^{-1} K^{-1}); the values of a_1 and a_2 vary depending on the substrate type. For substrates based on expanded clay $a_1 = 0.16 - 0.24$ and $a_2 = 0.30 - 0.51$; for substrates based on pumice $a_1 = 0.17$ and $a_2 = 1.1$; and for substrates based on expanded shale $a_1 = 0.2$ and $a_2 = 1.4$.

The Tabares vegetative roof model is currently being incorporated to EnergyPlus. Due to this simulation tools considers the CTF method, even if thermal properties of the substrate vary with the VWC the CTF remains constant to avoid stability issues in the simulation.

4.4 Thermal inertia implementation

The models developed by Sailor (2008) and Tabares & Srebic (2011) are steady state vegetated roof models. For this reason it is necessary to incorporate the thermal inertia to the models implementation. In order to consider the variation of the VWC, the finite difference method was used to accurately represent the thermal inertia of the substrate. The discretization of the roof considered several nodes depending on the number of layers and its thermal properties. Despite the number of nodes, 4 equations where considered in the model according to the possible cases: the top surface of the substrate (Eq. 21), the internal nodes of a layer (Eq. 22), the interface between two layers of different materials (Eq. 23), and the inner face of the roof (Eq. 24).

Due to Eq. 21 represents the top node of the substrate surrounded by the vegetation and the environment, it is considered the evaporative heat flux, the convective heat fluxes, the incoming solar radiation, and the exchange of long-wave radiation.

$$T\,(1,n+1) = \left(-2\cdot Q_E\cdot dxdt + 2\cdot R_{sh-s}\cdot dxdt + 2\cdot k\cdot T(2,n+1)dt + 2\cdot h_{r-scov}\cdot T_{sky}(n+1)dxdt + 2\cdot T_{ext}(n+1)\cdot {}^{1}/_{R_{cov}}\cdot dxdt + 2\cdot h_{r-sp}\cdot T_f(n+1)\,dxdt + C_p\cdot\rho\cdot T(1,n)\cdot dx^2\right) \;/\; \left(2\cdot dxdt\left(h_{r-scov} + h_{r-sp} + {}^{1}/_{R_{cov}}\right) + 2\cdot k\cdot dt + C_p\cdot\rho\cdot dx^2\right) \quad \text{(Eq. 21)}$$

$$T\,(i,n+1) = \frac{\left(\frac{(C_p\cdot\rho\cdot dx)}{T(1,n)\cdot dt} + \frac{\left(k\cdot T(i-1,n+1) + k\cdot T(i+1,n+1)\right)}{dx}\right)}{\left(\frac{(C_p\cdot\rho\cdot dx)}{dt} + \frac{(k+k)}{dx}\right)} \quad \text{(Eq. 22)}$$

$$T\,(i,n+1) = \frac{\left(2\cdot\left(k\cdot T(i-1,n+1)\cdot dx_{lay2}dt + k_{lay2}\cdot T(i+1,n+1)\cdot dxdt\right) + C_{p-fac}\cdot T(i,n)\right)}{\left(2\cdot\left(k\cdot dx_{lay2}dt + k_{lay2}\cdot dxdt\right) + C_{p-fac}\right)}$$

(Eq. 23)

$$T\,(i,n+1) = T_{int}$$ (Eq. 24)

where T is the temperature of the layer at different nodes (K); T_{sky} is the temperature of the sky (K); T_{ext} is the temperature of the air (K); T_f is the temperature of the vegetation; T_{int} is the temperature at the bottom of the roof (K); Q_E is the evaporative heat flux (W m^{-2}); R_{sh-s} is the incoming solar radiation (W m^{-2}); k is the thermal conductivity of the substrate (W m^{-1} K^{-1}); h_{r-scov} is the exchange of long-wave radiation between the substrate and the air (W m^{-2}); h_{r-sp} is the exchange of long-wave radiation between the substrate and the plants (W m^{-2}); $1/R_{cov}$ is the resistance of the substrate to the convective heat fluxes (W^{-1} m^2 K); C_p is the specific heat of the layer (J kg^{-1}K^{-1}); ρ is the density of the layer (kg m^{-3}); C_{p-fac} is the resultant specific heat of the interface, where $C_{p-fac} = C_{p-lay1}\cdot {dx_{lay1}}^2\cdot dx_{lay2}\cdot\rho_{lay1} + C_{p-lay2}\cdot {dx_{lay2}}^2\cdot dx_{lay1}\cdot\rho_{lay2}$; dx is the depth differential (m); and dt is the time differential (s). The subscript lay specifies the layer considered.

In Eq. 24 the value considered for T_{int} is an input to the model, and depending if the model considers the structural material layer or just the substrate, it can be the inner surface temperature of the roof or the bottom temperature of the substrate.

These equations assume that the thermal inertia is neglected in the vegetation layer. Also, an assumption considered for the implementation is the homogeneous distribution of the VWC in the substrate. Thus the thermal properties of the substrate layer do not vary with the depth level, but they do vary through different time steps.

4.5 Validation

After the models were implemented in MATLAB, the next step is the validation of the results. The validation process consists of compare the simulated substrate surface temperature results with field experimental data of vegetated roofs located in Chicago and Santiago of Chile. To evaluate the results the root mean square deviation (RMSD) was considered. This represents the average value of the difference between the simulation results and the experimental data, and it is calculate according to Eq. 25.

$$RMSD = \sqrt{\frac{\sum_{t=1}^{n}\left(x_{1,t}-x_{2,t}\right)^2}{n}} \quad \text{(Eq.25)}$$

where x_1 is the simulated substrate surface temperature (°C); x_2 is the measured substrate surface temperature (°C); and n is the quantity of data compared.

While it would be valuable to compare heat flux predictions to observations, the data comparison were limited to surface substrate temperatures. The simulation results yielded surface temperature predictions that closely matched the measured data.

4.5.1 Chicago experimental measurements

For an initial evaluation of the models implemented in MATLAB field data recorded in a vegetative roof installed on a commercial building in Chicago (USA) during summer

weather conditions was used. The experimental data was provided by Professor Paulo Tabares, because it was used by him for the dynamic validation of his model (Tabares et al. 2012).

According to Köppen classification, Chicago can be considered as a Humid Continental climate (Dfa). This city has an average annual temperature of 10°C and 918 mm of precipitation per year.

4.5.1.1 Vegetated roof description

The instrumented green roof is located in a commercial building in Chicago, Illinois. The total area of the roof is about 14,000 m2 and about half of that roof area is covered with a green roof. From top to bottom, the vegetative roof consists of: (1) a vegetation layer of sedum, (2) 7.5 cm substrate layer, (3) two layers of polypropylene fabric layers, (4) 2.5 cm of thick foam drainage/protection board, and (5) 0.2 cm waterproof membrane layer. The substrate used was based on expanded clay and has a dry bulk density of 650 kg/m3, bulk density at the maximum water-holding capacity of 1130 kg/m3, and a maximum volumetric water-holding capacity of 49.6% (Tabares et al. 2012).

4.5.1.2 Results

The installation was thoroughly monitored, providing months of useful data for comparison. All data were recorded at 15 min intervals. The month of July of 2007 was modelled in order to evaluate the vegetated roof performance. However the results presented correspond to days between July 6th and July 16th.

The inputs considered in the simulation correspond to: (1) the experimental weather data conditions; (2) the experimental substrate's bottom surface temperature; (3) the experimental vegetation and substrate parameters; and (4) the VWC of the substrate.

To compare the results was necessary to replicate in MATLAB the substrate and vegetation experimental characteristics to properly implement the vegetated roof models. Table 17 presents the parameters considered for the evaluation of both models. At the same time, it also presents the results obtained and its correspond RMSD.

Table 17: Simulation parameter values, simulation period and RMSD between simulated substrate surface temperature and measured substrate surface temperature for Chicago experimental data.

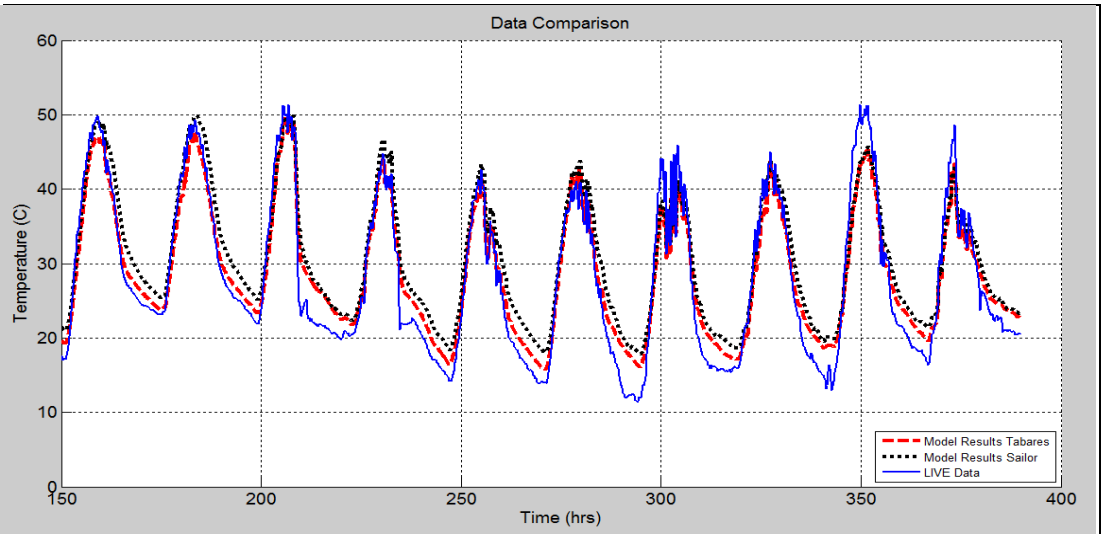

RMSD (°C) obtained in simulation										Simulation Period
Tabares			Sailor							July 6th 2007
2.51			3.53							July 16th 2007
Vegetation parameters and VWC considered as inputs										
LAI	2	Min stomatal resistance (s/m)	700	Vegetation coverage (%)	83	VWC range	0.15 – 0.41	Plant specie	Sedum	
Substrate parameters considered as inputs										
Thickness (m)	0.076	Thermal conductivity (W/m K)	0.25	Heat Capacity (J/kg K)	1400	Density (kg/m3)	850			

The results show a good agreement of both models with the experimental data. It is observed that both models present a better adjustment of the results during the time intervals of high solar radiation and high air environmental temperature, compared to the adjustment reached during night-time. Overall, it is observed that both models represent in good form the high thermal oscillation of the substrate temperature that occurred in reality.

However, the implemented model of Tabares is the one that best represents the behavior of the Chicago data; because its RMSD is lower (2.51 °C) than that for Sailor model (3.53°C).

4.5.2 Santiago experimental measurements

Along with the experimental data of Chicago, the models are also evaluated with experimental data recorded in the city of Santiago of Chile. According to Köppen classification, Santiago can be considered as a semiarid climate (Bsk). This city has an average annual temperature of 14.6°C and 359 mm of precipitation per year.

The experimental data were recorded at the Laboratory of Vegetative Infrastructure of Building (LIVE, for the acronym in spanish), located on the San Joaquín Campus of the Pontificia Universidad Católica de Chile.

4.5.2.1 LIVE Laboratory description

The laboratory building consists of 4 modules with high level of thermal insulation in their walls and floors. For this reason, the facade can be assumed as adiabatic (except by the roof). This implies that all variations of temperature and consumption inside the

laboratory are due to the heat transfer through the roof, which corresponds to a vegetative roof.

In the following figure, module D corresponds to a lightweight steel roof deck composed by two metal sheets of 2 mm with 5 cm of insulation, while modules A, B and C correspond to concrete slabs of 15 cm. Modules B, C and D have a floor surface of 5x5 m^2, whereas module A has an area of 7x5 m^2.

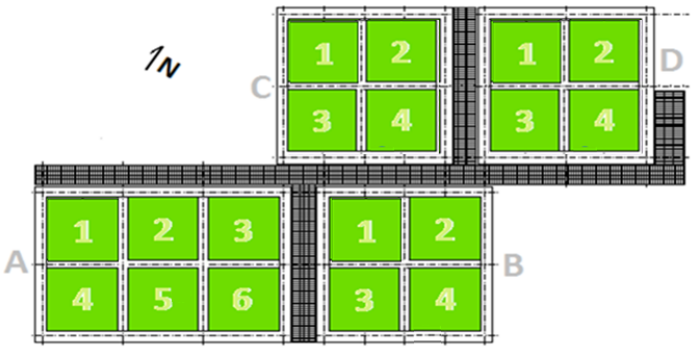

Figure 18: Laboratory layout. Floorplan.

To ensure the correct operation of the vegetative roof it is composed (from inside to outside) by: (1) Support structure that depending on the module can be concrete slab or insulated lightweight metal roof deck; (2) a waterproofing layer; (3) a drainage layer; (4) a root barrier; (5) a filter layer; (6) a substrate composed by 1/3 part of humus, 1/3 part of garden soil and 1/3 part of perlite (measures in volume); and (7) a vegetation that depending on the module can be grass and a mix of sedum.

The substrate's thickness is 15 cm for the modules with concrete slab, and 7 cm for the modules with insulated lightweight metal roof. As for the vegetation, the module A considers sedum; the modules C and D consider grass; and the module B do not considered it.

The thermal and biophysical performance of the roof and the weather conditions are measured by:

- Environmental air temperature
- Environmental relative humidity
- Wind speed
- Incoming solar radiation
- Incoming long wave radiation
- Precipitations
- Foliage temperature
- Substrate temperature
- Volumetric water content in the substrate
- Irrigation flow rate

The interior of the laboratory is considered to keep the indoor temperature at 20.5 ° C. The HVAC system uses cool water for cooling and resistances for heating. This air conditioning system includes fans in order to homogenize the interior environment.

4.5.2.2 Data Collection Methodology

To record all the data, there are 4 Agilent Technologies data acquisition systems, with three multiplexers each. These multiplexers allow connecting simultaneously several sensors to the dataloggers, in order to record all the measurements at the same time steps. Table 18 shows the sensors installed, while Table 19 shows the distribution of thermocouples in each module cubicle.

Table 18: Sensors and instruments available for the 4 laboratory modules.

Sensor	Brand	Model	Quantity
Flowmeter	BadgerMeter	PTFE 3/4	4
Datalogger	Agilent Technologies	34972A	4
Multiplexer	Agilent Technologies	34901A	12
Weather station	Decagon		1
Pyrgeometer	Kipp&Zonen	CGR4	1
Heat flux	Hukseflux	HFP01	18
Resistance temperature detector (RTD)	Omega	P-M-1/10-1/4-6-0-P-15	4
Pyranometer	Kipp&Zonen	CMA4	1
Thermocouples	PelicanWire	T	144
Volumetric water content	Decagon	GS3	18
Air temperature and relative humidity	Vaisala	HMP60	4

Table 19: Distribution of thermocouples in each module cubicle.

Location	Quantity
Substrate	4
Vegetation	1
Air	1
Outside face of the concrete slab/lightweight metal roof	1
Inside face of the concrete slab/lightweight metal roof	1

4.5.2.3 Measurement of substrate temperature

The temperatures of both the substrate and the roofing structure will be measured using type T thermocouples. These will be installed in the top surface of roofing structure, while in the substrate they will be buried with a spacing of 5 cm between each other. It means these will be buried at 5 cm, 10 cm, 15 cm, and so on. The surface temperature of

the substrate will be measured with a thermocouple buried a few millimeters below the surface.

4.5.2.4 Time step

The time step measurement will be 10 seconds. Greater time steps do not allow obtaining smoothed curves during the implementation of the mathematical models of vegetative roofs.

4.5.2.5 Results

The laboratory was thoroughly monitored, providing months of useful data for comparison. Specifically, multiple temperature sensors were installed to measure substrate and roof surface temperatures. In addition, local weather conditions were measured by a suite of weather station instruments. All data were recorded at 10 second intervals, but analyzed at 15 min intervals. We modeled 2 weeks of vegetated roof performance (February 11th, 2017 to February 16th, 2017, and March 14th, 2017 to March 19th, 2017) by using as input data the substrate and vegetation characteristics experimentally measured. These parameters were the minimum stomatal resistance of the plant; the LAI of the vegetation; the percentage of vegetation coverage (shading); and the substrate thickness. The thermal properties of the substrate remains constant due to the almost constant amounts of VWC, and by not having experimental measurements of how these properties varied with the VWC. Of these parameters the minimum stomatal resistance of the plant, the percentage of vegetation coverage, and the heat capacity and density of the substrate were estimated; while LAI of the

vegetation, the substrate thickness, the VWC, and the substrate thermal conductivity was experimentally measured. The density and heat capacity of the substrate remains constant due to: (1) the high VWC in the substrate; and (2) by not having experimental measurements of how these properties varied with the VWC.

Tables 20 to Table 25 present the parameters considered for the evaluation of both models. At the same time, it also presents the simulation period and the results obtained.

Table 20: Simulation parameter values and RMSD between simulated substrate surface temperature and measured substrate surface temperature experimental data for LIVE module A between February 11th and February 16th.

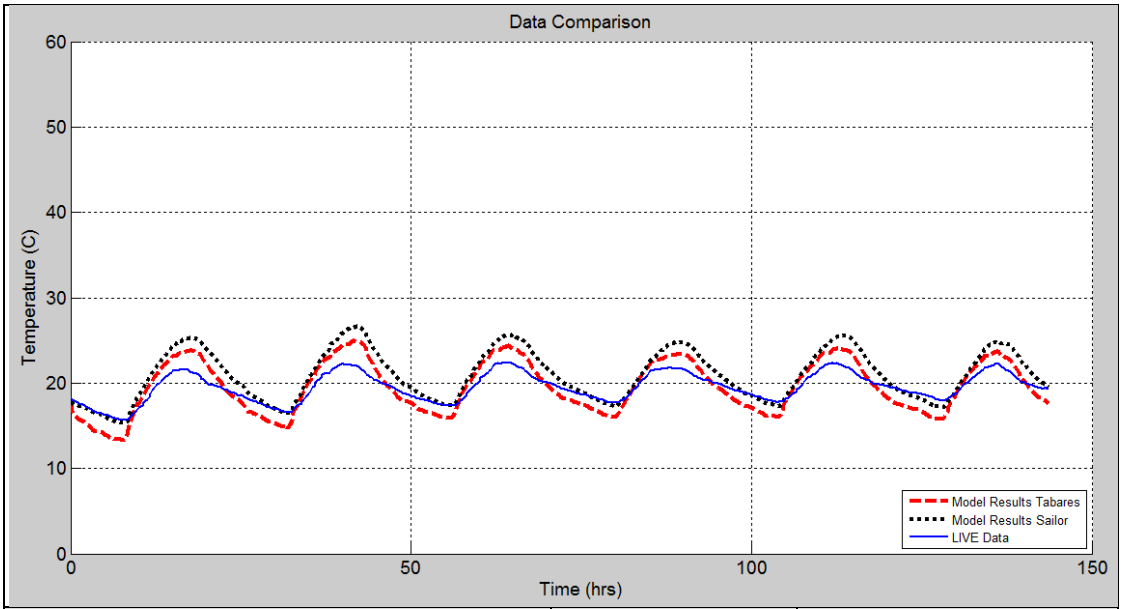

RMSD (°C) obtained in simulation		**Laboratory Module**	**Simulation Period**
Tabares	Sailor	A	February 11th 2017 February 16th 2017
1.4673	2.0161		

Vegetation parameters and VWC considered as input									
LAI	4	Min stomatal resistance (s/m)	500	Vegetation coverage (%)	95	VWC range	0.46 – 0.48	Plants specie	Sedum

Substrate parameters considered as input							
Thickness (m)	0.15	Thermal conductivity (W/m K)	0.8	Heat Capacity (J/kg K)	2700	Density (kg/m3)	950

Table 20 shows the comparison of simulated substrate surface temperature against the experimental measured data for the week of February 11th of 2017 for LIVE module A. While Table 21 presents the same comparison in the module A for the week of March 14th of 2017. This module corresponds to a vegetated roof above an uninsulated concrete slab roof. The vegetation considered is a mix of sedum species.

Table 21: Simulation parameter values and RMSD between simulated substrate surface temperature and measured substrate surface temperature experimental data for LIVE module A between March 14th and March 19th.

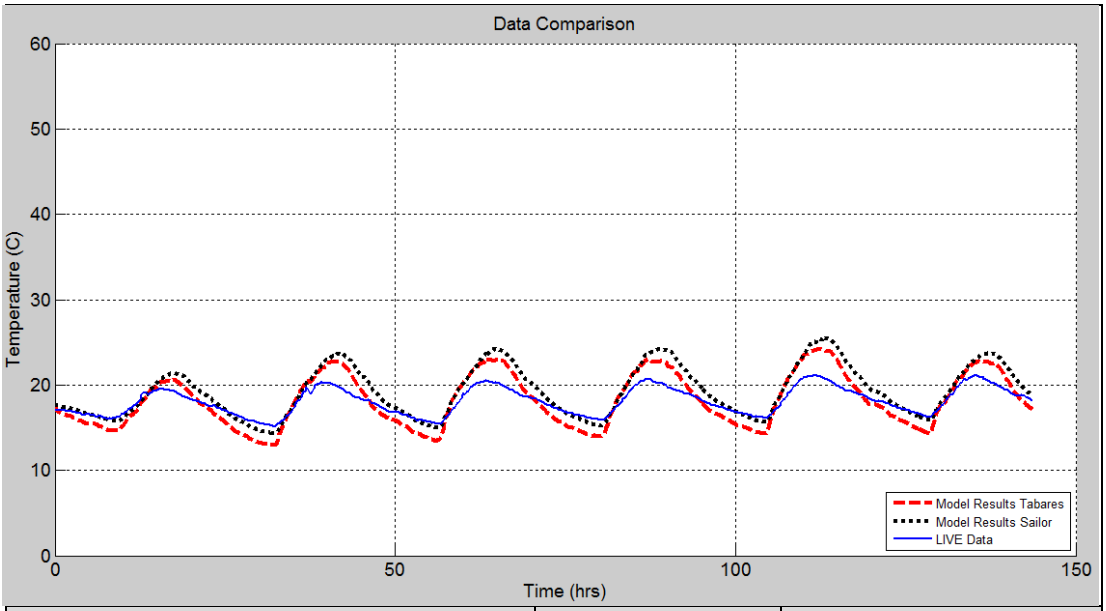

RMSD (°C) obtained in simulation		**Laboratory Module**	**Simulation Period**
Tabares	Sailor	A	March 14th 2017 March 19th 2017
1.5772	1.9163		

Vegetation parameters and VWC considered as input									
LAI	4	Min stomatal resistance (s/m)	500	Vegetation coverage (%)	95	VWC range	0.47 – 0.50	Plant specie	Sedum

Substrate parameters considered as input							
Thickness (m)	0.15	Thermal conductivity (W/m K)	0.8	Heat Capacity (J/kg K)	2700	Density (kg/m3)	950

Table 22 shows the comparison of simulated substrate surface temperature against the experimental data for the week of February 11th of 2017 for LIVE module C. This module corresponds to a vegetated roof above an uninsulated concrete slab roof. The vegetation considered corresponds to festuca specie grass.

Table 22: Simulation parameter values and RMSD between simulated substrate surface temperature and measured substrate surface temperature experimental data for LIVE module C between February 11th and February 16th.

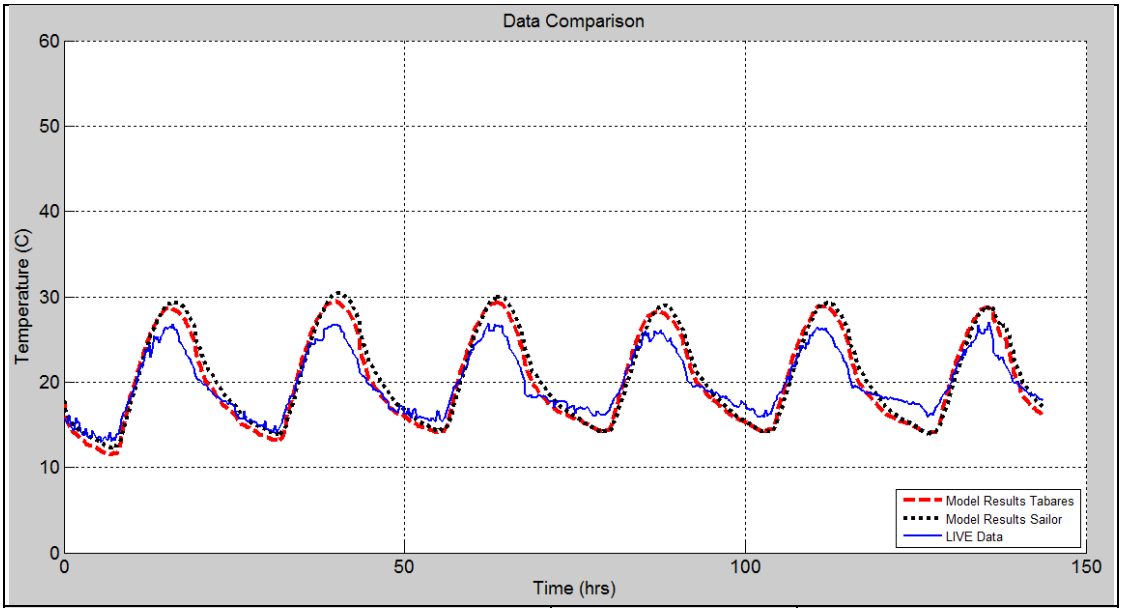

RMSD (°C) obtained in simulation		**Laboratory Module**	**Simulation Period**
Tabares	Sailor	C	February 11th 2017 February 16th 2017
1.9232	2.3542		

Vegetation parameters and VWC considered as input									
LAI	2	Min stomatal resistance (s/m)	200	Vegetation coverage (%)	100	VWC range	0.50 – 0.51	Plant specie	Festuca grass

Substrate parameters considered as input							
Thickness (m)	0.15	Thermal conductivity (W/m K)	0.8	Heat Capacity (J/kg K)	2700	Density (kg/m3)	950

Table 23 shows the comparison of simulated substrate temperature against the experimental data for the week of March 14th of 2017. This module corresponds to a vegetated roof above an uninsulated concrete slab roof. The vegetation considered corresponds to festuca specie grass.

Table 23: Simulation parameter values and RMSD between simulated substrate surface temperature and measured substrate surface temperature experimental data for LIVE module C between March 14th and March 19th.

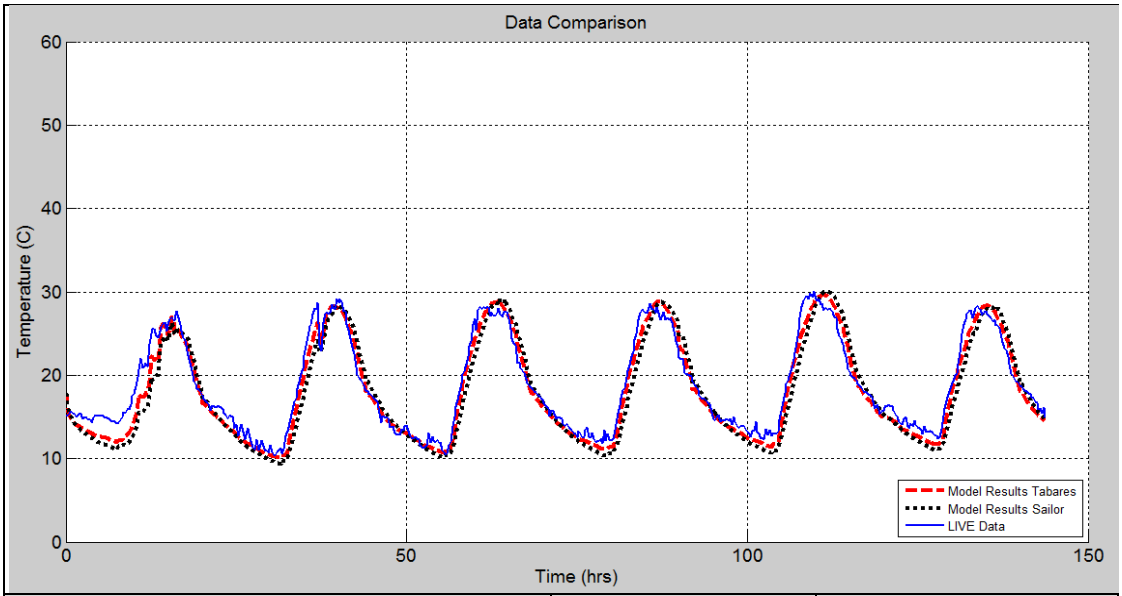

RMSD (°C) obtained in simulation		**Laboratory Module**	**Simulation Period**
Tabares	Sailor	C	March 14th 2017 March 19th 2017
1.3963	2.2911		

Vegetation parameters and VWC considered as input									
LAI	2	Min stomatal resistance (s/m)	200	Vegetation coverage (%)	100	VWC range	0.52-0.52	Plant specie	Festuca grass

Substrate parameters considered as input							
Thickness (m)	0.15	Thermal conductivity (W/m K)	0.8	Heat Capacity (J/kg K)	2700	Density (kg/m3)	950

Table 24 shows the comparison of the simulated substrate temperature against the experimental data for the week of February 11th of 2017 for LIVE module D. This module corresponds to a vegetated roof above an insulated lightweight metal roof deck. The vegetation considered corresponds to festuca specie grass.

Table 24: Simulation parameter values and RMSD between simulated substrate surface temperature and measured substrate surface temperature experimental data for LIVE module D between February 11th and February 16th.

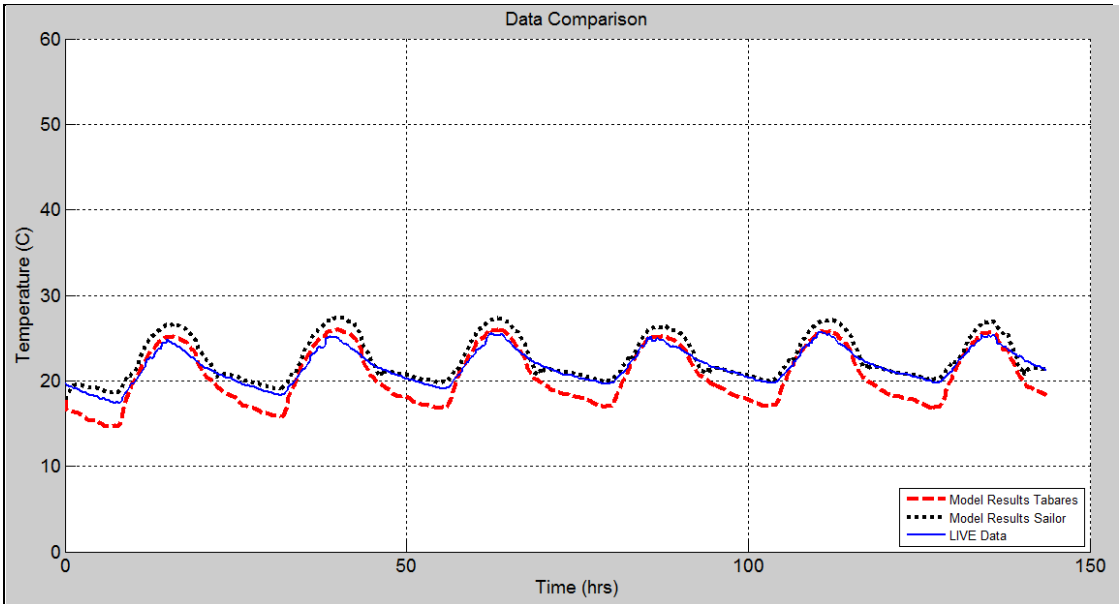

RMSD (°C) obtained in simulation		**Laboratory Module**	**Simulation Period**
Tabares	Sailor	D	February 11th 2017 February 16th 2017
1.8297	1.2673		

Vegetation parameters and VWC considered as input									
LAI	2	Min stomatal resistance (s/m)	200	Vegetation coverage (%)	100	VWC range	0.49-0.49	Plant specie	Festuca grass

Substrate parameters considered as input							
Thickness (m)	0.07	Thermal conductivity (W/m K)	0.8	Heat Capacity (J/kg K)	2700	Density (kg/m3)	950

Table 25 presents the comparison of simulated substrate surface temperature against the experimental data for the week of March 14th of 2017 for LIVE module D. This module corresponds to a vegetated roof above an insulated lightweight metal roof deck. The vegetation considered corresponds to festuca specie grass.

Table 25: Simulation parameter values and RMSD between simulated substrate surface temperature and measured substrate surface temperature experimental data for LIVE module D between March 14th and March 19th.

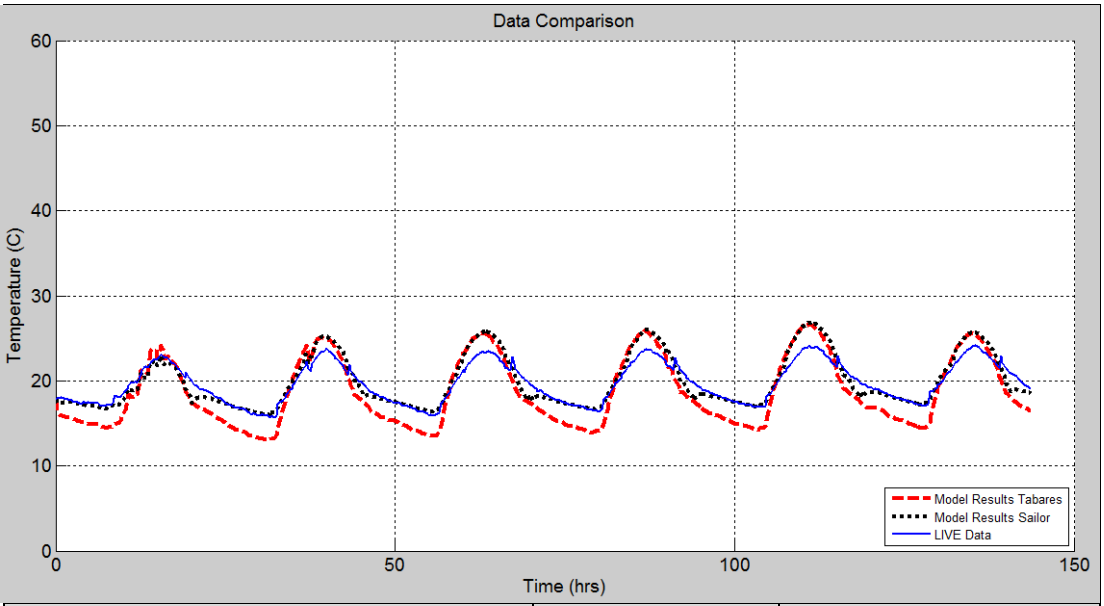

RMSD (°C) obtained in simulation										**Laboratory Module**	**Simulation Period**
Tabares			Sailor							D	March 14th 2017 March 19th 2017
2.0821			1.1350								
Vegetation parameters and VWC considered as input											
LAI	2	Min stomatal resistance (s/m)	200	Vegetation coverage (%)	100	VWC range	0.50-0.50	Plant specie	Festuca grass		
Substrate parameters considered as input											
Thickness (m)	0.07	Thermal conductivity (W/m K)	0.8	Heat Capacity (J/kg K)	2700	Density (kg/m3)	950				

4.6 Discussion

The results show that the models present patterns that coincide in good agreement with the experimental data both for Chicago and for Santiago. The results of the LIVE modules A and C show that the implemented model of Tabares is the one that best represents the behavior of the vegetated roof substrate's surface temperature data, because its RMSD is lower than that for Sailor model. The RMSD obtained with Tabares' model is: (1) 1.46°C in February and 1.57 °C in March for the module A; and (2) 1.92°C in February and 1.39 °C in March for module C. While the RMSD obtained with Sailor's model is: (1) 2.01°C in February and 1.91 °C in March for the module A; and (2) 2.35°C in February and 2.29 °C in March for module C. On the contrary, the implemented model of Sailor is the one that best represents the behavior of the vegetated roof substrate's surface temperature data in module D, because its RMSD is lower (1.26°C in February and 1.13 °C in March) than that for Tabares model (1.83°C in February and 2.08 °C in March).

The results presented in Tables 20, 21, 24 and 25 show that Tabares' vegetated roof model obtains a better performance during day-time; whereas Sailor's vegetated roof model shows better performance overnight. These results also show a greater thermal oscillation compared to the field experimental data. While, Tables 22 and 23 show that Tabares' vegetated roof model and Sailor's vegetated roof model obtain a very similar performance both for the day-time and overnight in comparison to the experimental data. The simulated substrate's surface temperature results not only represent and accurate thermal oscillation, but also the maximum and minimum temperatures reached.

The following three Figures present the experimental environmental data of Chicago and Santiago considered in the previous simulations.

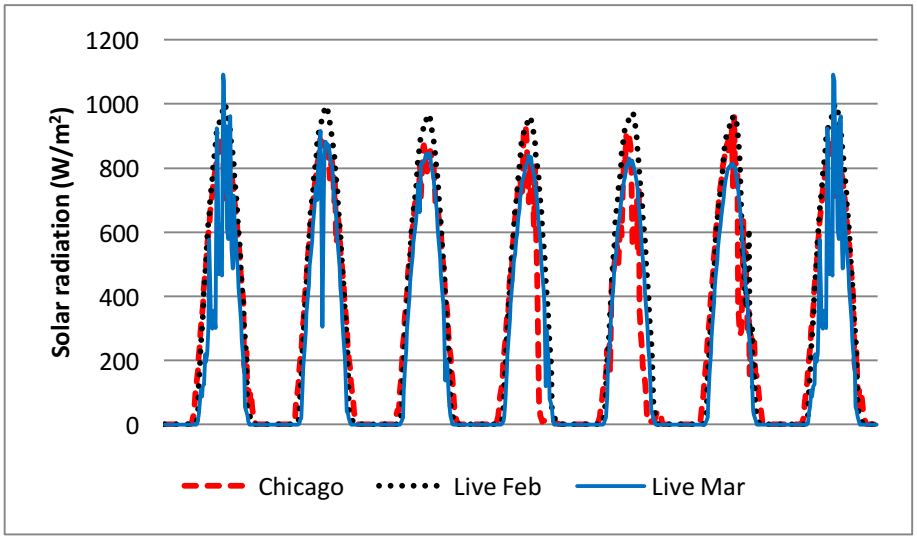

Figure 19: Measured solar radiation (W/m^2) for the simulated weeks in Chicago and Santiago.

The substrate's surface temperatures of Chicago reach an approximate thermal oscillation of 30°C; while the maximum and minimum thermal oscillations reached in Santiago are 20°C (module C) and 10°C (module A), respectively. The solar radiations presented in Figure 19 show a very similar behavior between the data measured in Chicago and Santiago, reaching similar maximum values. Thus, the thermal oscillation simulated in the models can not be attributed to the solar radiation data. On the other hand, Figures 20 and 21 present significantly higher air temperature values and wind speed values for Chicago than that of Santiago, respectively. Higher air temperature values lead to higher substrate's surface temperature temperatures; while higher winds speed values during night-time lead to lower substrate's surface temperature due to the

increased heat losses by convection. Figure 21 shows that during night-time the wind speed in Chicago can be 4 m/s higher than the wind speed in Santiago.

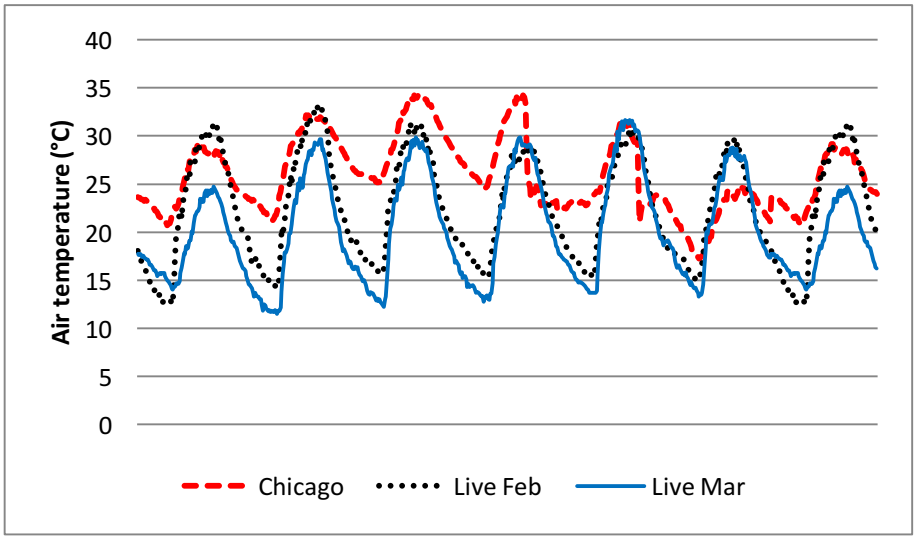

Figure 20: Measured air temperature (°C) for the simulated weeks in Chicago and Santiago.

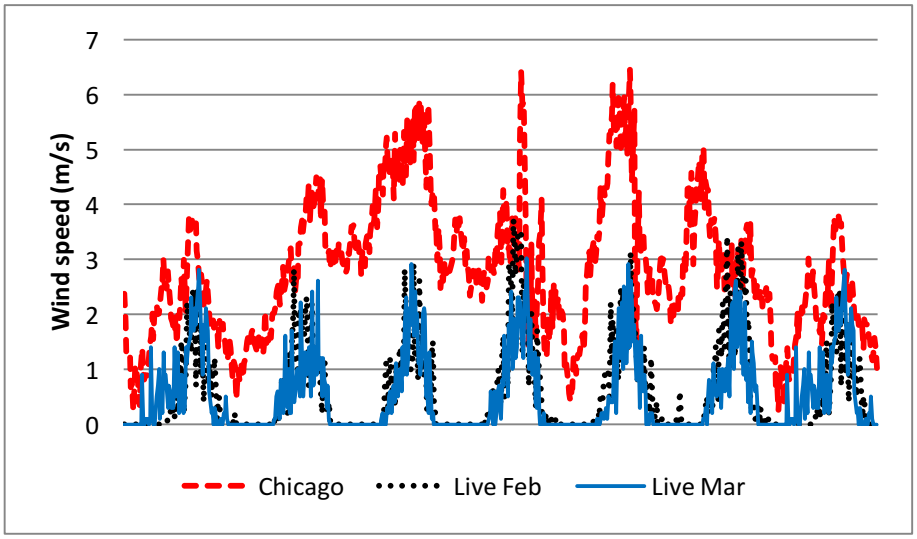

Figure 21: Measured wind speed (m/s) for the simulated weeks in Chicago and Santiago.

As for the LIVE laboratory results, the more accurate visual agreement is obtained in the module C; while the second more accurate results correspond to module D. These both modules have the same vegetation specie in common, which correspond to Festuca (grass). In comparison with the sedum species, the grass has a more homogeneous distribution in the vegetated roofs' surface. For this reason, the thermal performance of a vegetated roof with this type of vegetation can be more accurately represented with the implemented models. Also, Wolf (1960) and Starry et al. (2014) indicate that succulent vegetation species such as sedum develop crassulacean acid metabolism (CAM). This is a process whereby plants collect and store carbon dioxide (CO2) via the formation of malic acid at night, and metabolize it the following day with stomates closed, reducing plant water loss by evapotranspiration (ET). For this reason, considerate the stomatal resistance calculation of the sedum in the same way than that the grass can lead to less accurate results of the vegetated roof's thermal behavior.

4.7 Conclusions

The vegetated roofs are an envelope building technology whose use has become more widespread in the last decade. For this reason, several heat and mass transfer vegetated roof models have been developed in order to simulate the thermal performance of this roofing system. Two of these models already have been implemented in building energy simulation tools to assist developers to design vegetative roofs. However, to fully obtain the benefits of this technology is important to ensure that these models can accurately represent vegetative roof in climates where they have not been validated.

This study presents the implementation, evaluation and validation using MATLAB of the vegetated roof models developed by Sailor (2008) and Tabares & Srebric (2011). The original versions of these models were developed in steady-state, thus the implementation incorporated the thermal inertia by the method of finite differences. The models were evaluated comparing the simulated results against experimental data of three real vegetated roofs located in Santiago (Chile) and one in Chicago (USA). The field data considers two different vegetation species (a mix of sedum and festuca grass) and two different substrates. The purpose of this study is to evaluate the accuracy of the results obtained with these models in order to indicate if these models can be used to design properly vegetative roofs for the semi-arid climates.

The conclusions of this paper are as follows:

1. The simulation's results show that the implemented vegetated roof models are able to accurately represent the behavior of three vegetative roofs located in Santiago of Chile, and one vegetative roof installed in a commercial building in Chicago.
2. Tabares' vegetated roof model obtains a better performance during day-time; whereas Sailor's vegetated roof model shows more accurate thermal performance overnight.
3. The implemented model of Tabares is the one that best represents the thermal performance of the substrate's surface temperature data of vegetated roof above uninsulated concrete slab roofs. On the contrary, the implemented model of Sailor is the one that best represents the behavior of the substrate's surface

temperature data in vegetated roof installed above insulated lightweight metal roof decks.

4. Both implemented vegetated roof models present a more accurate agreement with the experimental data in vegetative roof with high thermal oscillation on the substrate's surface temperature.

5. COUPLING TWO DYNAMIC HEAT AND MASS TRNASFER MODELS FOR SEMIARID CLIMATES IMPLEMENTED IN MATLAB WITH ENERGYPLUS SIMULATION SOFTWARE

5.1 Abstract

Several countries have boosted the implementation of vegetated roofs on new building constructions based on the energy and thermal benefits that this technology provides to the buildings. In order to achieve these benefits, several heat and mass transfer vegetative roof models have been developed since 1982. The simulation results provided by these models indicate that vegetated roofs improve the buildings' energy performance. However, none of these models has been validated with experimental measurements of energy consumption or against substrate´s surface temperature experimental data considering the vegetative roof model coupled to building simulation software, in order to assert the savings in buildings' energy consumption.

This paper presents the coupling, evaluation and validation of the vegetated roof models (Sailor 2008, and Tabares & Srebric 2011) implemented in MATLAB with a building model developed in EnergyPlus. The coupled vegetated roof models were evaluated and validated comparing the simulated results against experimental data of three real vegetated roofs located in Santiago (Chile). The field data considers two different vegetation species (a mix of sedum and festuca grass) and two different roof structures (an uninsulated concrete slab and an insulated lightweight metal roof deck). The results present that the implemented models acceptably simulate the behavior of the evaluated vegetative roofs. The results also indicate that the mainly vegetative roof parameters

that influence the building energy consumption are the leaf area index (LAI), the vegetation fractional coverage, and the thermal properties of the substrate. Finally, the results also conclude that the presence of a thermal insulation layer on the roofing system diminishes the influence of the vegetated roofs' parameters on the buildings energy performance; corroborating results presented in the literature.

5.2 Introduction

Vegetative roofs – so called green roofs- are roofing systems where the roof of a building is partially or completely covered with vegetation and substrate. Between the structural support and the substrate, the constructive system may be composed by a waterproofing membrane; a root barrier; a drainage layer; and geotextile filter (Berardi et al. 2014). Usually, vegetated roofs are classified in three types: extensive, intensive and semi-intensive. An extensive vegetated roof is characterized by a thin substrate layer (less than 15 cm), small plants, simple and minimal maintenance. Intensive roofs have a heavier and thicker substrate layer (above 20 cm), require more complicated maintenance, structural reinforcement, and support a wider variety of plants and trees. Semi-intensive roofs present intermediate characteristics (Berardi et al. 2014).

Several vegetated roof studies present the benefits that can be achieved by the implementation of this roofing technology. Among the benefits can be mentioned: Mitigation of air pollution (Alexandri & Jones 2017; Oberndorfer 2007; Getter et al. 2009; and Zhang et al. 2012); improve the water management by improving the runoff quality and reducing the rainwater runoff (Berndtsson 2010; Sun et al. 2013; and Chen 2014); exterior noise absorption (Van Renterghem et al. 2013; and Van Renterghem &

Botteldooren 2014); decrease the urban heat island effect (Kolokotsa et al. 2013; Lehmann 2014; and Santamouris 2014); and reduce the building energy consumption by improving the environmental temperature (Kumar & Kaushik 2005; and Erdemir & Ayata 2017) and decreasing the thermal loads (Wong et al. 2003, Kumar & Kaushik 2005, Alexandri & Jones 2007, Sailor 2008, Vera et al. 2015 Squier & Davidson 2016, and Erdemir & Ayata 2017).

Based on these benefits, several countries have boosted the implementation of vegetated roofs on new building constructions (Vijayaraghavan 2016): in Toronto (Canada), all new buildings having a roof surface greater than 2000 m2 must have between 20-60% of vegetated roofs; in Tokyo (Japan), all new buildings must have at least 20% of vegetated surfaces on their rooftops (Chen 2013); in Portland (USA), all the new city-owned buildings must be built with at least 70% of vegetated roofs on their roof surfaces (Townshend 2007); and in Basel (Switzerland), all the new or renovated flat roofs have to be covered with at least 15% of vegetation (Townshend 2007). Despite the advancement of vegetated roof research to quantify green roof benefits, the design of the vegetated roof technology is still significantly based on the aesthetic point of view, thus the aforementioned benefits are not potentiated (Berndtsson 2010, Vijayaraghavan 2014).

In order to provide guidance in design to potentiate the previous benefits, several heat and mass transfer vegetative roof models have been developed since 1982. However, none of these models has been validated by experimental measurements of energy consumption or by substrate´s surface temperature experimental data considering the

vegetative roof model coupled to building simulation software. Moreover, none of these developed models involve semiarid climates on their validation. These climates are cooling dominated with a significant heating season. Since vegetated roofs have significant potential benefits in saving buildings energy consumption in semiarid climates, this paper performs the coupling, evaluation and validation in semiarid climates of the two vegetated roof models implemented in MATLAB with a building model developed in EnergyPlus. This study contributes to engineers and architects to understand the thermal performance of vegetated roof in semiarid climates, what are their mainly parameters that influence the building energy performance and how the thermal insulation affects the vegetative roofs energy performance.

5.3 Coupling Sailor and Tabares vegetated roof models implemented in MATLAB with EnergyPlus

In the previous chapter two transient vegetative roof models have been implemented in MATLAB and then validated against experimental data showing agreement ranges for an acceptable to excellent between the simulated substrate temperature and experimental measured data. In order to carry out the building energy performance evaluation, it is needed to couple both models with EnergyPlus. The coupling of both programs has been performed through the toolbox MLE+.

5.3.1 MLE+ toolbox

MLE+ is an open-source MATLAB/Simulink toolbox for co-simulation with the building energy simulator EnergyPlus (Mlab.seas.upenn.edu, 2017). This software was

designed for engineers and researchers who were familiar with MATLAB and Simulink and wanted to use these programs in building energy simulation studies.

5.3.2 IDF file – Other Side Coefficients

In order to couple both tools, it is necessary to understand how the EnergyPlus input file (IDF) works and to identify in its code a section to be linked with MATLAB. To select the section of the IDF file is necessary to find some function that allows controlling a variable to simulate the performance of a vegetative roof coupled to a building model. Vegetative roofs provide an outer layer of material whose thermal properties vary overtime. For this reason, this layer can not be considered as a simple material given the complex interactions between the plants with the substrate and with the outside environment.

Considering the outputs obtained by the vegetative roof models and the fact it is an exterior layer an EnergyPlus function must be selected to allow controlling the exterior temperature of a building envelope surface. For this reason, it is necessary to extract from MATLAB the substrate bottom temperature and consider it as a controlled outdoor condition for the exterior surface of the building roof.

Figure 22 presents the interaction between MATLAB and EnergyPlus. In (1) is calculated the bottom surface substrate temperature by MATLAB at time step *x*; then in (2) this temperature is send by MLE+ to the IDF EnergyPlus file to be considered as an input; then in EnergyPlus uses the temperature of (1) and the interior building conditions (4) to calculate the interior surface temperature of the roof (3) at time step

x+1; finally in (5) this temperature is send by MLE+ to MATLAB in order to calculate (1) at time step *x+1* considering the environmental conditions (6).

The EnergyPlus function selected to develop the previous relation is the Other Side Coefficient Surface Properties. The EnergyPlus input/output reference states that by referencing the Other Side Coefficients on a building surface, the temperature of the outer plane of the surface can be directly controlled (U.S Department of Energy, 2016).

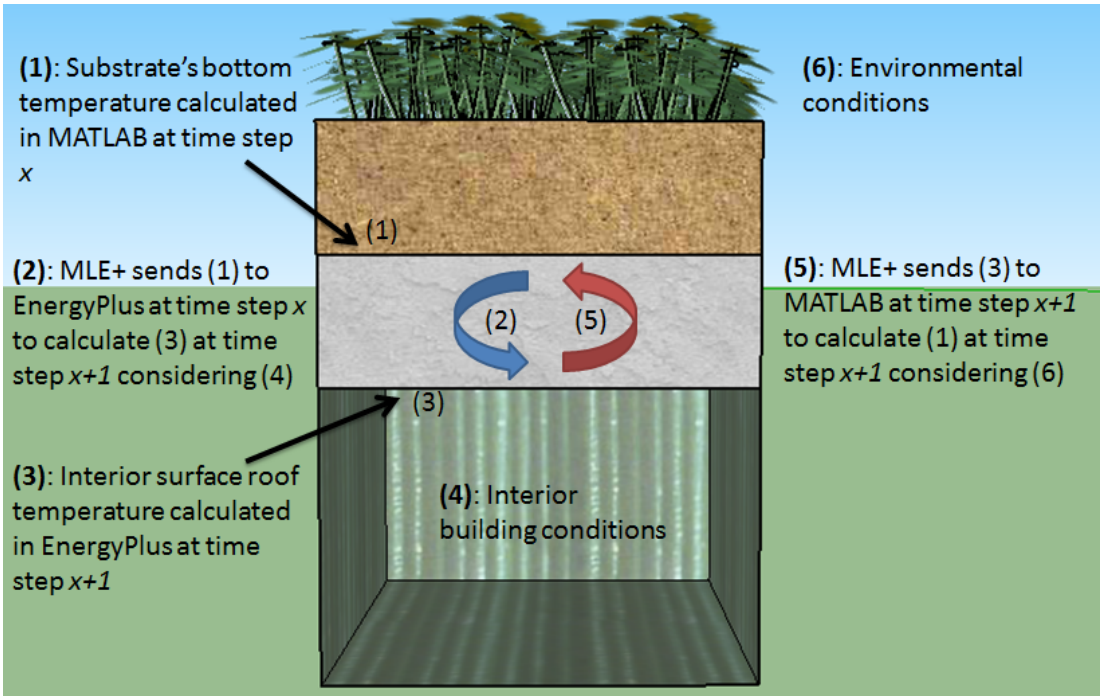

Figure 22: Interactions between the vegetative roof models implemented in MATLAB and the building module developed in EnergyPlus.

5.3.3 Coupling implementation

In order to couple both programs is necessary to understand the MLE+ code. Then, identify the vegetative roof models sections where the MLE+ code has to be added.

The MLE+ code has mainly 6 sections: (a) the initial configuration; (b) start the co-simulation; (c) read the IDF file; (d) extract the IDF output; (e) input the MATLAB output to the IDF file; and (f) stop the co-simulation.

Considering this point, (a) should be located at the beginning of the co-simulation code, because this section configures the co-simulation, and declares the weather file (epw) and the IDF file.

```
%% Create a mlepProcess instance and configure it
ep = mlepProcess;
%IDF & EPW, EPW should be in C://E+/WeatherData folder
ep.arguments = {'LabLIVE_NEW2','CHL_SANTIAGO_LIVE_FEB'};
%Timeout to end the connection between MATLAB and EnergyPlus if
the co-simulation presents problems (time in milliseconds)
ep.acceptTimeout = 30000;
% version number of communication protocol (2 for E+ 7.2.0)
VERNUMBER = 2;
```

Then the points (b), (c), (d), and (e) are entered in the main loop of the vegetative roof model, because along all the iteration made by the model must be carried out the information exchange between MATLAB and EnergyPlus. The point (b) declares the beginning of the co-simulation through the following code:

```
ep.start
```

Then, in (c) the EnergyPlus IDF file is read through the next code lines:

```
packet = ep.read;
if isempty(packet)
            error('Could not read outputs from E+.');
end
```

Then, it is extracted the EnergyPlus IDF output and is declared as an input to the MATLAB code in point (d). In this case the interior surface temperature of the building roof is considered as the input using the following script:

```
% Parse it to obtain building outputs
[flag, eptime, outputs] = mlepDecodePacket(packet);
%output must be declared in IDF file
if flag ~= 0; break; end
Tint=outputs(1)+273.15;
```

At the end of the iteration loop in MATLAB the calculated bottom surface temperature of the substrate is extracted and used as an input in EnergyPlus. This information is sent to the IDF file according to the following script.

```
SP=T(11,n)-273.15;
%MATLAB output is send to EnergyPlus
ep.write(mlepEncodeRealData(VERNUMBER, 0, n, SP));
```

Then, once the input-output exchange is completed the co-simulation is stopped using the next code line,

```
ep.stop
```

5.4 Laboratory description

In order to validate the results obtained by the coupled models with MLE+, simulated results for the substrate surface temperature were compared with field data from three real vegetative roofs. The experimental data considered were collected at the Laboratory of Vegetative Infrastructure of Buildings (LIVE, for the acronym in spanish), located on the San Joaquín Campus of the Pontificia Universidad Católica of Chile.

The laboratory building consists of 4 modules with high level of thermal insulation in their walls and floors. For this reason, the facade can be assumed as adiabatic (except by the roof). This implies that all variations of temperature and consumption inside the

laboratory are due to the heat transfer through the roof, which corresponds to a vegetative roof.

In the following figure, module D corresponds to a lightweight steel roof deck composed by two metal sheets of 2 mm with 5 cm of insulation, while modules A, B and C correspond to concrete slabs of 15 cm. Modules B, C and D have a floor surface of 5x5 m^2, whereas module A has an area of 7x5 m^2.

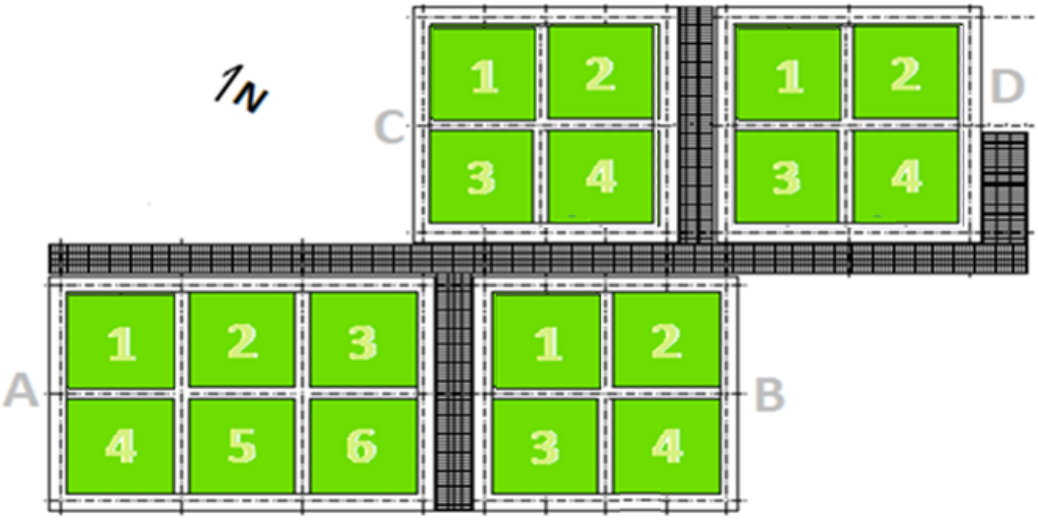

Figure 23: Laboratory layout. Floorplan.

To ensure the correct operation of the vegetative roof it is composed (from inside to outside) by: (1) Support structure that depending on the module can be concrete slab or insulated lightweight metal roof deck; (2) a waterproofing layer; (3) a drainage layer; (4) a root barrier; (5) a filter layer; (6) a substrate composed by 1/3 part of humus, 1/3 part of garden soil and 1/3 part of perlite (measures in volume); and (7) a vegetation that depending on the module can be grass and a mix of sedum.

The substrate's thickness is 15 cm for the modules with concrete slab, and 7 cm for the modules with insulated lightweight metal roof. As for the vegetation, the module A considers sedum; the modules C and D consider grass; and the module B do not considered it.

The interior of the laboratory is considered to keep the indoor temperature at 20.5 ° C. The HVAC system uses cool water for cooling and resistances for heating. This air conditioning system includes fans in order to homogenize the interior environment.

5.5 Validation

Once the co-simulation is implemented, the next step is the validation of the results. To perform this validation the root mean square deviation (RMSD) between the simulated substrate's surface temperature and experimental measurements was considered. This represents the average value of the difference between the simulation results and the experimental data, and it is calculate according to Eq. 26.

$$RMSD = \sqrt{\frac{\sum_{t=1}^{n}\left(x_{1,t}-x_{2,t}\right)^2}{n}} \quad \text{(Eq.26)}$$

where x_1 is the simulated substrate surface temperature (°C); x_2 is the measured substrate surface temperature (°C); and n is the quantity of data compared.

5.5.1 Results

In order to carry out the simulations, the substrate exterior surface temperature and the HVAC cooling loads are analyzed. In this chapter, the exterior surface temperature of the substrate is calculated in MATLAB considering as inputs the experimental environment conditions and the interior building conditions calculated in EnergyPlus; while in chapter 4, the exterior surface temperature of the substrate calculated in MATLAB depends of the experimental environment conditions and the bottom surface temperature of the substrate experimentally measured but not the building's interior conditions.

5.5.1.1 Substrate surface temperature

The laboratory was thoroughly monitored, providing months of useful data for comparison. Specifically, multiple temperature sensors were installed to measure substrate and roof surface temperatures. In addition, local weather conditions were measured by a suite of weather station instruments. All data were recorded at 10 second intervals, but analyzed at 60 min intervals. We modeled 2 weeks of vegetated roof performance (February 10th, 2017 to February 17th, 2017, and March 13th, 2017 to March 20th, 2017) by using as input data the substrate and vegetation characteristics experimentally measured. These parameters were the minimum stomatal resistance of the plant; the LAI of the vegetation; the percentage of vegetation coverage (shading); and the substrate thickness. The thermal properties of the substrate remains constant due to the almost constant amounts of VWC, and by not having experimental

measurements of how these properties varied with the VWC. Of these parameters the minimum stomatal resistance of the plant, the percentage of vegetation coverage, and the heat capacity and density of the substrate were estimated; while LAI of the vegetation, the substrate thickness, the VWC, and the substrate thermal conductivity was experimentally measured. The density and heat capacity of the substrate remains constant due to: (1) the high VWC in the substrate; and (2) by not having experimental measurements of how these properties varied with the VWC.

Tables 24 to Table 29 present the parameters considered for the evaluation of both models. At the same time, it also presents the simulation results compared with the experimental data.

Table 26 shows the comparison of simulated substrate surface temperature against the experimental measured data for the week of February 10th of 2017 for LIVE module A. This module corresponds to a vegetated roof above an uninsulated concrete slab roof and considers a mix of sedum species as vegetation.

Table 26: Simulation parameter values and RMSD between simulated substrate surface temperature and measured substrate surface temperature experimental data for LIVE module A between February 10th and February 17th.

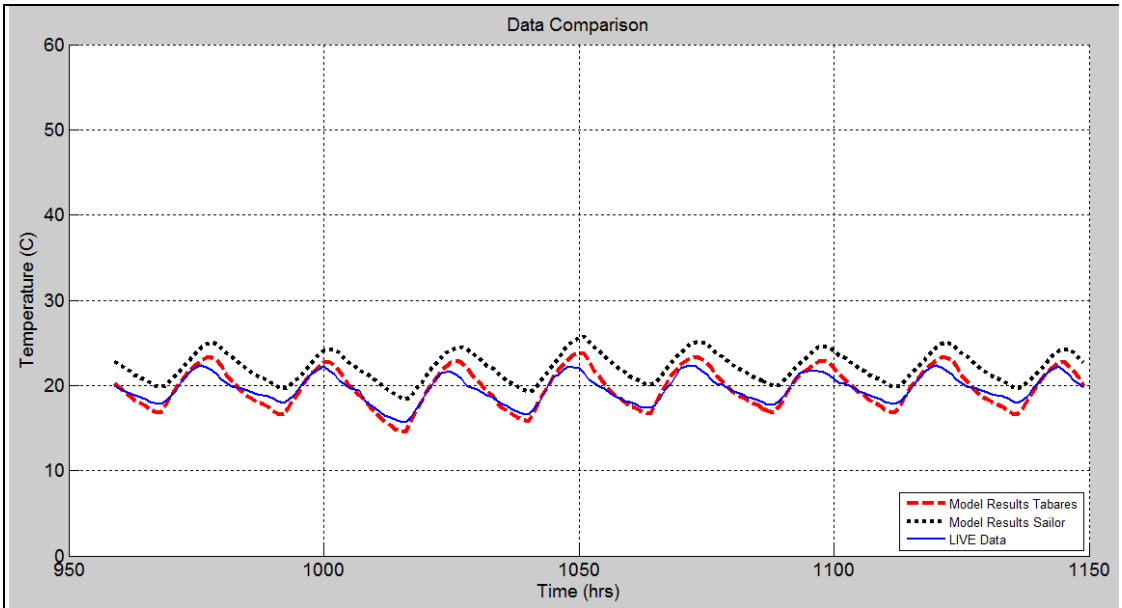

RMSD (°C) obtained in simulation		**Laboratory Module**	**Simulation Period**
Tabares	Sailor	A	February 10th 2017 February 17th 2017
0.8532	2.6796		

Vegetation parameters and VWC considered as input									
LAI	4	Min stomatal resistance (s/m)	500	Vegetation coverage (%)	95	VWC range	0.46 – 0.48	Plant specie	Sedum

Substrate parameters considered as input							
Thickness (m)	0.15	Thermal conductivity (W/m K)	0.8	Heat Capacity (J/kg K)	2700	Density (kg/m3)	950

Table 27 presents the same comparison in the module A for the week of March 13th of 2017.

Table 27: Simulation parameter values and RMSD between simulated substrate surface temperature and measured substrate surface temperature experimental data for LIVE module A between March 13th and March 12th.

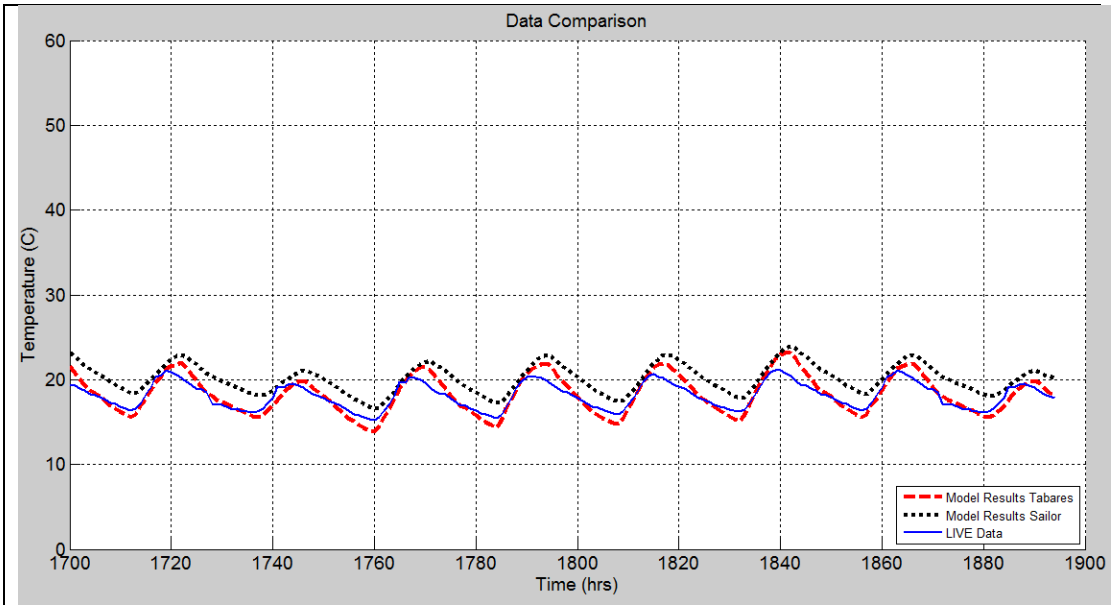

RMSD (°C) obtained in simulation		Laboratory Module	Simulation Period
Tabares	Sailor	A	March 13th 2017 March 20th 2017
0.9728	2.1398		

Vegetation parameters and VWC considered as input									
LAI	4	Min stomatal resistance (s/m)	500	Vegetation coverage (%)	95	VWC range	0.47 – 0.50	Plant specie	Sedum

Substrate parameters considered as input							
Thickness (m)	0.15	Thermal conductivity (W/m K)	0.8	Heat Capacity (J/kg K)	2700	Density (kg/m3)	950

Table 28 shows the simulated substrate surface temperature obtained and the substrate temperature experimentally measured data in the module C for the week of February 10th of 2017. This module corresponds to a vegetated roof above an uninsulated concrete slab roof. The vegetation considered corresponds to festuca specie grass.

Table 28: Simulation parameter values and RMSD between simulated substrate surface temperature and measured substrate surface temperature experimental data for LIVE module C between February 10th and February 17th.

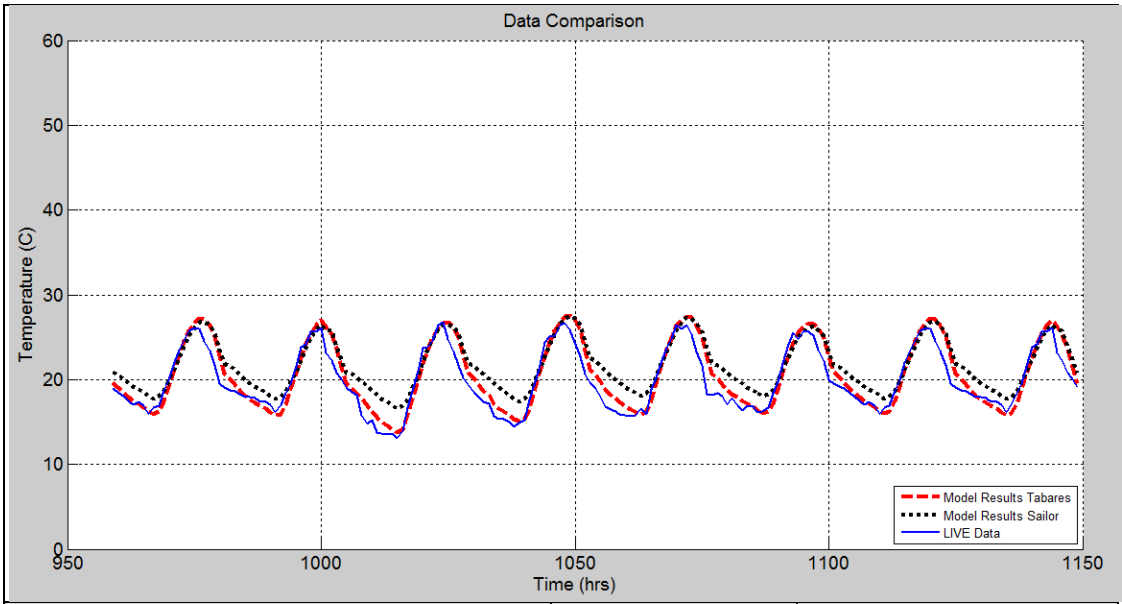

RMSD (°C) obtained in simulation		**Laboratory Module**	**Simulation Period**
Tabares	Sailor	C	February 10th 2017 February 17th 2017
1.4657	2.3544		

Vegetation parameters and VWC considered as input									
LAI	2	Min stomatal resistance (s/m)	200	Vegetation coverage (%)	100	VWC range	0.50 – 0.51	Plant specie	Festuca grass

Substrate parameters considered as input							
Thickness (m)	0.15	Thermal conductivity (W/m K)	0.8	Heat Capacity (J/kg K)	2700	Density (kg/m3)	950

Table 29 presents the same comparison in the module C but for the week of March 13th of 2017.

Table 29: Simulation parameter values and RMSD between simulated substrate surface temperature and measured substrate surface temperature experimental data for LIVE module C between March 13th and March 20th.

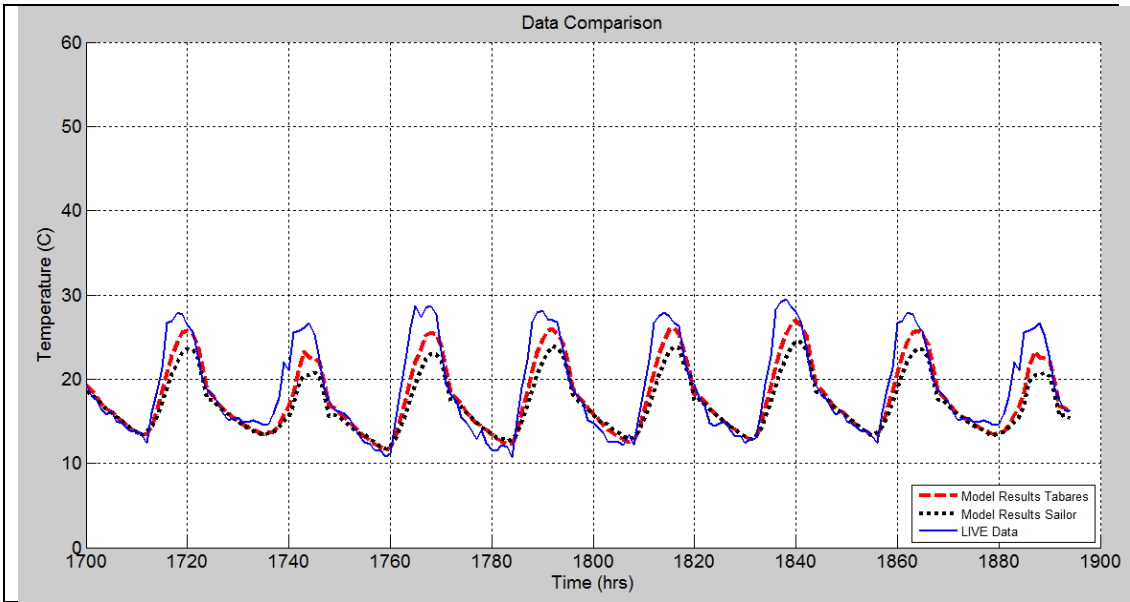

RMSD (°C) obtained in simulation		Laboratory Module	Simulation Period
Tabares	Sailor	C	March 13th 2017 March 20th 2017
2.3479	3.4		

Vegetation parameters and VWC considered as input									
LAI	2	Min stomatal resistance (s/m)	200	Vegetation coverage (%)	100	VWC range	0.52-0.52	Plant specie	Festuca grass

Substrate parameters considered as input							
Thickness (m)	0.15	Thermal conductivity (W/m K)	0.8	Heat Capacity (J/kg K)	2700	Density (kg/m3)	950

Table 30 presents the same analysis between the simulated substrate surface temperature and the substrate temperature experimentally measured data developed for the module D in the week of February 10th of 2017. This module corresponds to a vegetated roof above an uninsulated concrete slab roof. The vegetation considered corresponds to festuca specie grass.

Table 30: Simulation parameter values and RMSD between simulated substrate surface temperature and measured substrate surface temperature experimental data for LIVE module D between February 10th and February 17th.

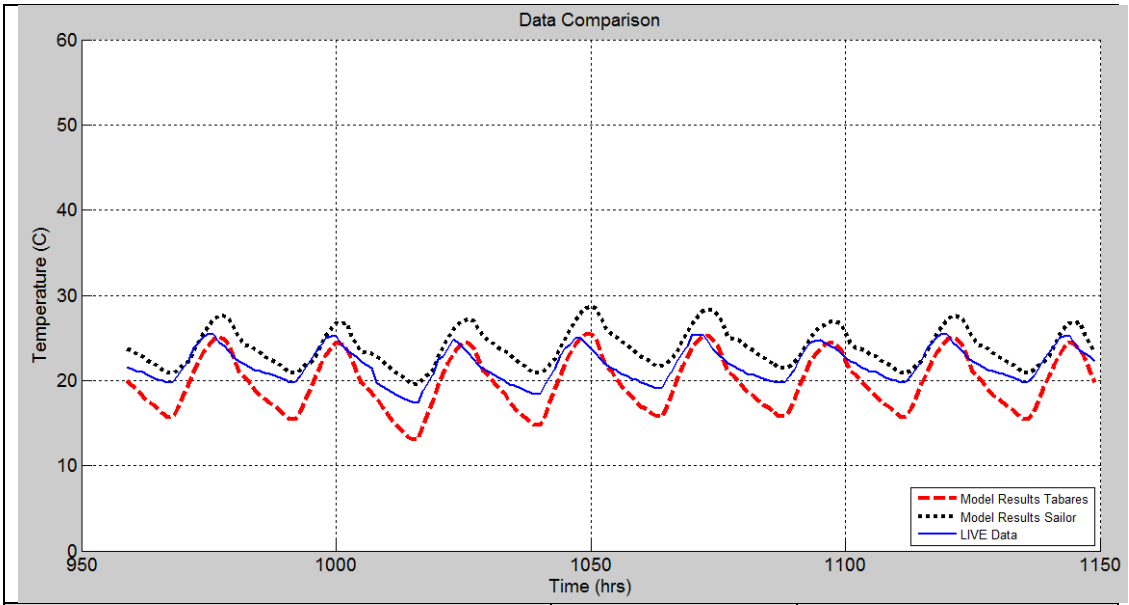

RMSD (°C) obtained in simulation		Laboratory Module	Simulation Period
Tabares	Sailor	D	February 11th 2017 February 16th 2017
2.5082	2.5191		

Vegetation parameters and VWC considered as input									
LAI	2	Min stomatal resistance (s/m)	200	Vegetation coverage (%)	100	VWC range	0.49-0.49	Plant specie	Festuca grass

Substrate parameters considered as input							
Thickness (m)	0.07	Thermal conductivity (W/m K)	0.8	Heat Capacity (J/kg K)	2700	Density (kg/m3)	950

Table 31 shows the same results of the module D but in the week of March 13th of 2017.

Table 31: Simulation parameter values and RMSD between simulated substrate surface temperature and measured substrate surface temperature experimental data for LIVE module D between March 13th and March 20th.

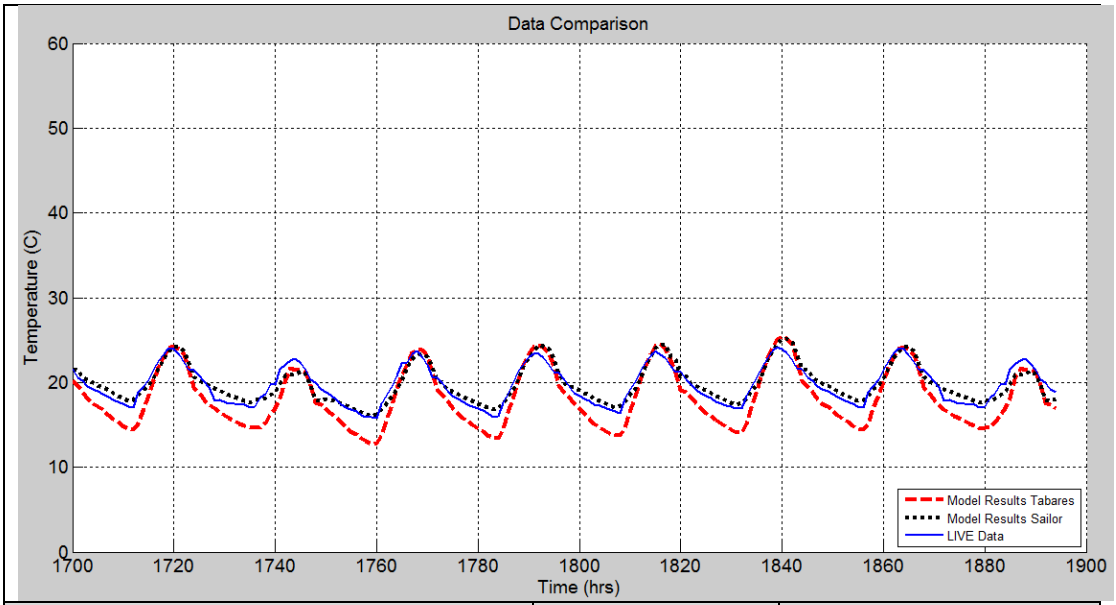

RMSD (°C) obtained in simulation		**Laboratory Module**	**Simulation Period**
Tabares	Sailor	D	March 13th 2017 March 20th 2017
1.9800	0.8660		

Vegetation parameters and VWC considered as input									
LAI	2	Min stomatal resistance (s/m)	200	Vegetation coverage (%)	100	VWC range	0.50-0.50	Plant specie	Festuca grass

Substrate parameters considered as input							
Thickness (m)	0.07	Thermal conductivity (W/m K)	0.8	Heat Capacity (J/kg K)	2700	Density (kg/m3)	950

The results show that the models present patterns that coincide in good agreement with the laboratory experimental data of Santiago. The results of the LIVE modules A and C show that the implemented model of Tabares is the one that best represents the behavior of the vegetated roof substrate's surface temperature data, because its RMSD is lower than that for Sailor model. The RMSD obtained with Tabares' model is: (1) 0.85°C in

February and 0.97 °C in March for the module A; and (2) 1.46°C in February and 2.34°C in March for module C. While the RMSD obtained with Sailor's model is: (1) 2.67°C in February and 2.14 °C in March for the module A; and (2) 2.35°C in February and 3.4 °C in March for module C. On the contrary, the implemented model of Sailor is the one that best represents the behavior of the vegetated roof substrate's surface temperature data in module D, because its RMSD is lower (0.86 °C in March) than that for Tabares model (1.98 °C in March). The RMSD for the module D in February is similar between both models (2.51 °C for Tabares and 2.52°C for Sailor).

The results presented in Tables 26, 27, 30 and 31 show that Sailor' vegetated roof model obtains a better range thermal oscillation agreement with the experimental data; however for module A and for module D in February, the model presents an approximate delay of 2.5°C against the experimental field data.

5.5.1.2 HVAC ideal loads

Once the temperatures were corroborated with the experimental data, an analysis of the cooling loads was carried out for each simulated module. For this a simple HVAC system was implemented in EnergyPlus in order to calculate the ideal thermal loads in each module.

The HVAC ideal loads schedule considered is on 24/7 and the temperature set point was 20.5°C. An equipment of 120W was considered in the inside of the building module in order to simulate the laptop and datalogger used to monitor the installed sensors.

Table 32 presents the cooling loads for each module for the two weeks evaluated in the previous section. The results show a similar behavior between the models of Tabares

and Sailor. Despite the aforementioned, the Sailor model presents higher cooling loads compared to Tabares model. These results are obtained due to the higher substrate surface temperatures reached by the Sailor model in comparison to Tabares model.

Table 32: Simulated ideal cooling loads in each LIVE module during one week of February and one week of March.

	Module	Sailor (Wh/m2)	Tabares (Wh/m2)
February	A	913.29	761.58
	C	920.35	914.38
	D	2269.31	1900.08
March	A	780.02	552.24
	C	351.87	479.09
	D	1477.37	1374.54

The results also show that the implementation of thermal insulation on the roof increase the cooling loads. Due to the high insulation level on the roof, the internal loads are retained at the interior of the building, increasing the cooling thermal loads in order to reach the indoor air temperature set point. Figure 24 presents the daily variation of the cooling loads consumption of each module.

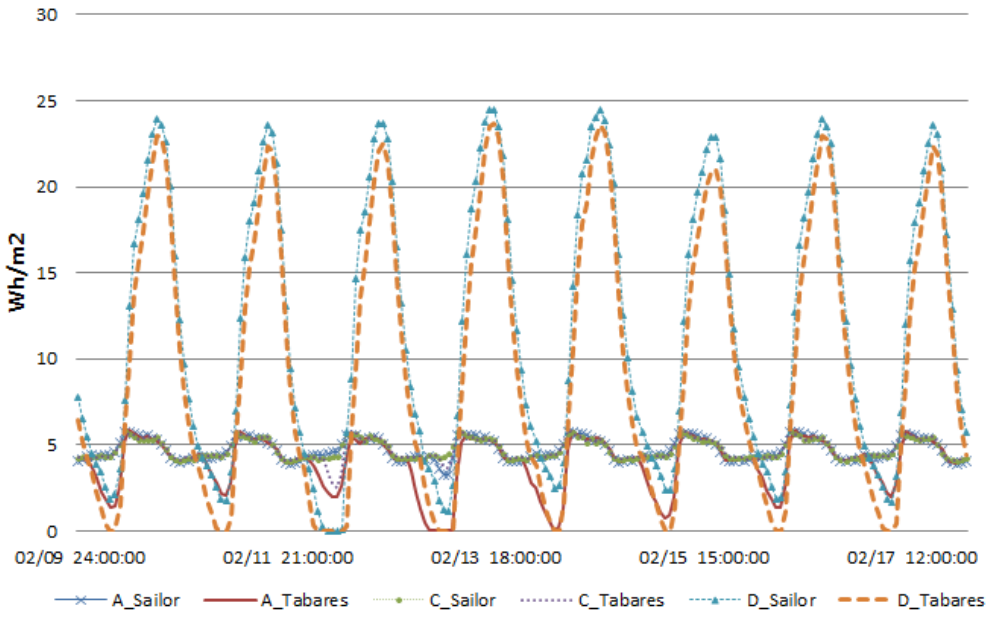

Figure 24: Simulated cooling loads for each LIVE module between February 10th and February 17th

Figure 24 show during day-time cooling thermal loads 4.5 times higher for the module D than that for modules A and C, reaching values of 24 Wh/m^2. During night-time, modules A and C due to the uninsulated roof and the thermal mass of the roofing system present slightly higher cooling loads by 4 Wh/m2 than that for module D; which has an insulated lightweight metal roof deck.

5.6 Discussion

A sensitive analysis was conducted to: (1) identify the main parameters that influence the thermal and energy performance of the vegetative roofs, and (2) evaluate these results against the chapter 3and literature studies.

In order to develop the analysis several simulation were performed and their results were compared with a base case. The base case composition considers: LAI value of

3.0; height of the vegetation of 0.2 m; minimum stomatal resistance value of 300 s/m; plant coverage factor of 75%; substrate's thermal conductivity value of 1.0 W/mK; substrate's heat capacity of 2000 J/kgK; and substrate's density equals to 1000 kg/m^3.

Table 33 shows that the higher variations in the results are obtained due to the LAI of the vegetation and the plant coverage. The variation between LAI 1.0 and LAI 5.0 is 133.9 Wh/m2, while the variation of the plant coverage is 60.32 Wh/m2.

The influence of LAI is supported by several papers in the literature. Theodosiou (2003) indicates that in Mediterranean climates, the LAI is the parameter that most influence has on the thermal performance of vegetated roofs, due to the relation between LAI and the evaporative cooling by means of evapotranspiration. Similarly, Sailor et al. (2012) show that for US cold climates, LAI is the most important vegetated roofs' parameter that affects the buildings' energy performance. Also, Vera et al. (2015) present that LAI significantly influences the cooling loads of a supermarket in a semiarid climate.

Then the next two parameters that mainly influence on the cooling loads are the thermal properties of the substrate. The variation of the heat capacity and the density is 40.89 Wh/m2, while the variation reached by the thermal conductivity if 22.63 Wh/m2.

Table 33 also shows a different behavior between the Sailor and Tabares model. Due to the higher temperature calculated by the Sailor model in comparison to Tabares model the variation between the vegetation and substrate parameters is almost negligible. The results show that using the same inputs two different vegetative roof models can represent different building's energy performance.

Table 33: Influence of vegetation and substrate parameter on the cooling loads (Wh/m2) for Tabares and Sailor model between March 13th and March 20th

	Tabares			**Sailor**		
Base case	772.86			915.86		
Parameters of Vegetation	***Wh/m2***	***Δ***	***%***	***Wh/m2***	***Δ***	***%***
LAI = 1.0	865.59	-92.73	-12.00	914.47	1.38	0.15
LAI = 5.0	731.69	41.18	5.33	916.85	-0.99	-0.11
Height = 0.1 m	772.86	0.00	0.00	915.11	0.75	0.08
Height = 0.3 m	772.86	0.00	0.00	916.16	-0.30	-0.03
Stomatal Resistance = 100 s/m	758.82	14.05	1.82	915.86	0.00	0.00
Stomatal Resistance = 500 s/m	776.22	-3.36	-0.43	915.86	-0.01	0.00
Plant coverage = 50%	811.63	-38.77	-5.02	903.33	12.52	1.37
Plant coverage = 100%	751.32	21.54	2.79	905.15	10.70	1.17
Parameters of Substrate	***Wh/m2***	***Δ***	***%***	***Wh/m2***	***Δ***	***%***
Thermal conductivity = 0.5 W/mK	760.29	12.58	1.63	914.88	0.98	0.11
Thermal conductivity = 1.5 W/mK	782.93	-10.07	-1.30	916.00	-0.14	-0.02
Heat capacity = 1000 J/kg K	800.06	-27.20	-3.52	915.95	-0.10	-0.01
Heat capacity = 3000 J/kg K	759.17	13.69	1.77	915.22	0.63	0.07
Density = 500 kg/m3	800.06	-27.20	-3.52	915.95	-0.10	-0.01
Density = 1500 kg/m3	759.17	13.69	1.77	915.22	0.63	0.07

The different cooling loads performance simulated with the implemented models is related to the substrate's surface temperature calculated by the vegetated roof models. Figure 25 presents the simulated substrate's temperatures with Sailor's and Tabares' vegetated roof models for the sensitive analysis between March 13th and March 14th. The figure shows that the temperatures calculated by Sailor's model (dotted lines) are considerably higher than that Tabares' model (straight lines), reaching maximum

differences of nearly 15°C and mean difference of 10°C between both models (Table 34). Due to the similar high Sailor's modeled temperatures, the cooling loads shows neglected difference among the evaluated cases in Table 33.

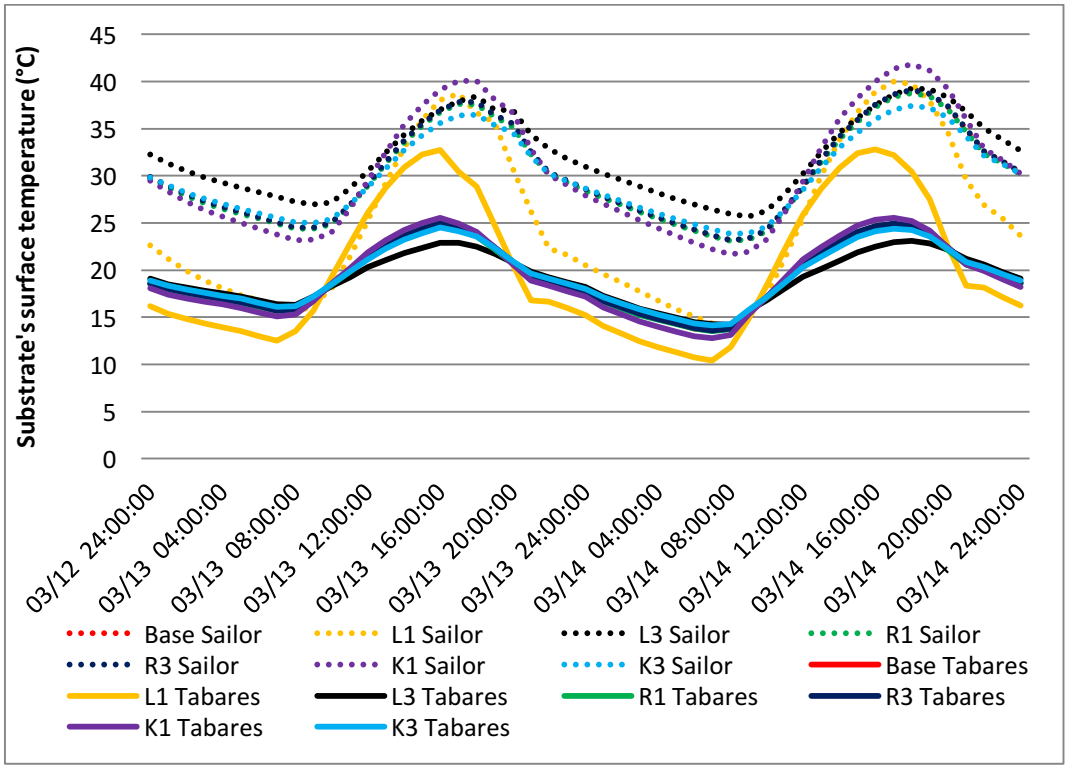

Figure 25: Simulated substrate's temperatures with Sailor's and Tabares' vegetated roof models between March 13th and March 14th. L1: LAI value of 1.0; L3: LAI value of 5.0; R1: minimum stomatal resistance of 50 s/m; R3: minimum stomatal resistance of 500 s/m; K1: substrate's thermal conductivity of 0.5 W/mK; and K3: substrate's thermal conductivity of 1.5 W/mK.

The previous sensitive analysis results show that despite of having two vegetated roof models validated against the same experimental data, it is not possible to assert similar thermal performance among them for all possible scenarios.

Table 34: Average value of the substrate's simulated surface temperature in the sensitive analysis for both implemented models.

	Substrate's temperature	
Cases	**Sailor**	**Tabares**
Base	30.57	19.74
L1	25.53	20.61
L3	32.33	19.45
R1	30.42	19.62
R3	30.63	19.77
K1	30.89	19.66
K3	30.29	19.80

Table 35 presents the same sensitivity analysis comparing the results obtained in the laboratory building with an uninsulated concrete slab roof and a lightweight metal roof deck with 5 cm of thermal insulation. The results show the lightweight metal roof obtained higher cooling loads due to the implementation of thermal insulation. For example the variation of the LAI decreased from 133.9 Wh/m2 to 48.86 Wh/m2; the plant coverage influence decrease from 60.32 Wh/m2 to 19.2 Wh/m2.As for the substrate parameters, the variation of the heat capacity and the density decreased from 40.89 Wh/m2 to 8.53 Wh/m2, while the variation reached by the thermal conductivity changed from 22.63 Wh/m2 to5.61 Wh/m2.

Table 35: Influence of vegetation and substrate parameter on the cooling loads (Wh/m2) of a building with concrete slab roof and an insulated lightweight metal roof for Tabares model between March 13th and March 20th

	Tabares					
	Concrete Slab			**Lightweight metal roof**		
Base case	772.86			1472.64		
Parameters of Vegetation	***Wh/m2***	***Δ***	***%***	***Wh/m2***	***Δ***	***%***
LAI = 1.0	865.59	-92.73	-12.00	1509.08	-36.44	-2.47
LAI = 5.0	731.69	41.18	5.33	1460.22	12.42	0.84
Height = 0.1 m	772.86	0.00	0.00	1472.64	0.00	0.00
Height = 0.3 m	772.86	0.00	0.00	1472.64	0.00	0.00
Stomatal Resistance = 100 s/m	758.82	14.05	1.82	1467.65	5.00	0.34
Stomatal Resistance = 500 s/m	776.22	-3.36	-0.43	1473.83	-1.18	-0.08
Plant coverage = 50%	811.63	-38.77	-5.02	1485.28	-12.63	-0.86
Plant coverage = 100%	751.32	21.54	2.79	1466.08	6.57	0.45
Parameters of Substrate	***Wh/m2***	***Δ***	***%***	***Wh/m2***	***Δ***	***%***
Thermal conductivity = 0.5 W/mK	760.29	12.58	1.63	1469.17	3.47	0.24
Thermal conductivity = 1.5 W/mK	782.93	-10.07	-1.30	1474.79	-2.14	-0.15
Heat capacity = 1000 J/kg K	800.06	-27.20	-3.52	1478.64	-5.99	-0.41
Heat capacity = 3000 J/kg K	759.17	13.69	1.77	1470.10	2.54	0.17
Density = 500 kg/m3	800.06	-27.20	-3.52	1478.64	-5.99	-0.41
Density = 1500 kg/m3	759.17	13.69	1.77	1470.10	2.54	0.17

These results are supported by several literature studies. For example, Niachou (2001) concludes energy savings for an office building located in Mediterranean climates up to 2%, 7% and 48% for highly-insulated, moderate insulated and non-insulated vegetated roofs, respectively. In the same climate, Theodosiou (2003) shows that in summer the lack of thermal insulation increases the cooling capabilities of vegetated roofs. Similarly, Jaffal et al. (2012) present energy savings of a single-family house in an

Oceanic climate between 10% and 48% for insulated and uninsulated vegetated roofs, respectively. Also, Vera et al. (2017) show that the presence of a thermal insulation layer reduces the influence of the vegetative roof parameters on cooling loads of stand-alone retail buildings located in semiarid climates and Marine climates.

5.7 Conclusions

The reduction of the effects of global warming has become a worldwide priority. This resulted in the need for reducing the greenhouse gas emissions. As the building sector has the major amount, it has become a necessity to find solutions that reduce its energy consumption which is generated mostly from fossil fuels such as gas, coal, and oil. One of these solutions is the implementation of vegetated roofs. These are an envelope building technology whose use has become more widespread in the last decade. For this reason, several heat and mass transfer vegetated roof models have been developed in order to simulate the thermal performance of this roofing system. Two of these models already have been implemented in building energy simulation tools to assist developers to design vegetative roofs. However, to fully obtain the benefits of this technology is important to ensure that these models can accurately represent vegetative roof in climates where they have not been validated.

This paper presents the coupling, evaluation and validation of the vegetated roof models developed by Sailor (2008) and Tabares & Srebric (2011) implemented in MATLAB with a building model developed in EnergyPlus. The coupled vegetated roof models were evaluated and validated comparing the simulated results against experimental data

of three real vegetated roofs located in Santiago (Chile). The field data considers two different vegetation species (a mix of sedum and festuca grass) and two different roof structures (an uninsulated concrete slab and an insulated lightweight metal roof deck). The purpose of this study is to evaluate the accuracy of the results obtained with these coupled models in order to indicate if these can be considered to design properly vegetative roofs for the semi-arid climates.

The conclusions of this paper are as follows:

1. Vegetation is more effective than insulation on reducing cooling loads due to the evapotranspiration of the vegetation-substrate system and canopy's shading effect.
2. The implementation of a thermal insulation layer of the roof decrease considerably the influence of the vegetative roof parameters on the cooling loads.
3. The mainly plants parameters that affects the cooling loads performance of a building are the leaf area index and the plant factor coverage. A variation from LAI value of 1.0 to 5.0 generates a variation of 133.9 Wh/m2, while the variation of the plant coverage from 50% to 100 % is about 60.32 Wh/m2.
4. The mainly substrate parameters that affects the cooling energy performance of a building are the heat capacity and the density. A variation from 1000 J/kg K to3000 J/kg K for the heat capacity, and from 500 kg/m3 to 1500 kg/m3 generates a variation of 40.89 Wh/m2.

5. Despite having two vegetated roof models validated against experimental data, these models do not obtain similar results in the sensitivity analysis performed. Thus, it is not possible to assert that vegetative roof models implemented in simulation tools such as DesignBuilder and EnergyPlus will accurately represent the performance of these technologies for other climates different than that of validation.

BIBLIOGRAPHY

Alexandri, E., Jones, P. (2007). Developing a one-dimensional heat and mass transfer algorithm for describing the effect of green roofs on the built environment: Comparison with experimental results. *Building and Environment*, 42, 2835-2849.

Alexandri, E., & Jones, P. (2008). Temperature decreases in an urban canyon due to green walls and green roofs in diverse climates. *Building and Environment*, 43(4), 480–493.

Antrop, M. (2004). Landscape change and the urbanization process in Europe, *Landscape and Urban Planning*, 67 (1–4), 9-26.

Ascione, F., Bianco, N., De' Rossi, F., Turni, G., Vanoli, G. P. (2013). Green roofs in European climates. Are effective solutions for the energy savings in air-conditioning? *Applied Energy*, 104, 845-859.

ASHRAE. (2012). ANSI/ASHRAE Standard 140-2011: Standard Method of Test for the Evaluation of Building Energy Analysis Computer Programs. Atlanta, GA: American Society of Heating, Refrigerating, and Air-Conditioning Engineers, Inc.

Berardi, U., Ghaffarianhoseini, A., Ghaffarianhoseini, A. (2014). State-of-the-art analysis of the environmental benefits of green roofs. *Applied Energy*, 115, 411-428.

Berndtsson JC. (2010). Green roof performance towards management of runoff water quantity and quality: a review. *Ecological Engineering*, 36, 351–60.

Brenneisen, S. (2006). Space for urban wildlife: Designing green roofs as habitats in Switzerland. *Urban Habitats*, 4(1), 27–36.

Brenneisen, S. (2003). The Benefits of Biodiversity from Green Roofs-Key Design Consequences, in: 1st North American Green Roof Conference: Greening Rooftops for Sustainable Communities, The CArdinal Group, Toronto, Chicago, 323-329.

Chen, C.F. (2013). Performance evaluation and development strategies for green roofs in Taiwan: a review. *Ecological Engineering*, 52, 51–58.

Chen, P., Li, Y. Lo, W., Tung, C. (2015). Toward the practicability of a heat transfer model for green roofs. *Ecological Engineering,* 74, 266-273

Chile Desarrollo Sustentable. (2017). INVESTIGADORES UC CREAN PROTOTIPOS DE CUBIERTAS VEGETALES SUSTENTABLES PARA SANTIAGO. [online] Available at: http://www.chiledesarrollosustentable.cl/noticias/noticia-

pais/investigadores-uc-crean-prototipos-de-cubiertas-vegetales-sustentables-para-santiago/ [Accessed 30 Jun. 2017].

Coutts, A., Daly, E., Beringer, J., Tapper, N.J. (2013). Assessing practical measures to reduce urban heat: Green and cool roofs. *Building & Environment*, 70, 266–276.

Del Barrio, E. P. (1998). Analysis of the green roofs cooling potential in buildings. *Energy and Buildings*, 27, 179-193.

Denardo, J. C. (2003). Green roof mitigation of stormwater and energy use. M.Sc. Thesis, Pennsylvania State University.

Deru, M., Field, K., Studer, D., Benne, K., Griffith, B., Torcellini, P., Crawley, D. (2011). U.S. Department of Energy commercial reference building models of the national building stock. Publications (E), (February 2011), 1 – 118. https://doi.org/NREL Report No. TP-5500-46861

Designbuilder.co.uk. (2017). DesignBuilder Software Ltd - Home. [online] Available at: https://www.designbuilder.co.uk/ [Accessed 11 Jun. 2017].

Dickinson, E., Henderson-Sellers, A., & Kennedy, J. (1993). Biosphere-atmosphere Transfer Scheme (BATS) Version 1e as Coupled to the NCAR Community Climate Model. NCAR Tech. Rep. NCAR/TN-3871STR, 72, (August), 77. https://doi.org/10.5065/D67W6959

Djedjig, R., Ouldboukhitine, S.-E., Belarbi, R., Bozonnet, E. (2012). Development and validation of a coupled heat and mass transfer model for green roofs. *International Communications in Heat and Mass Transfer*, 39, 752-761.

DOE. (2013). Building Energy Data Book [Online]. U.S. Department of Energy. Disponible en: http://buildingsdatabook.eren.doe.gov/

Eisenman, T. (2006). Raising the bar on green roof design. Landscape Architecture, 96 (11), 22–29.

El-Darwish, I., Gomaa, M. (2017). Retrofitting strategy for building envelopes to achieve energy efficiency. *Alexandria Engineering Journal*. In Press, Corrected Proof.

Energyplus.net. (2017). EnergyPlus | EnergyPlus. [online] Available at: https://energyplus.net/ [Accessed 11 Jun. 2017].

Erdemir, D., Ayata, T. (2017). Prediction of temperature decreasing on a green roof by using artificial neural network. Applied Thermal Engineering, 112, 1317-1325.

EPA. (2008). Sector Collaborative on Energy Efficiency Accomplishments and Next Steps, in: National Action Plan for Energy Efficiency, U.S. Environmental Protection Agency | Department of Energy, United States, 2008, pp. 80.

FAO. (1998). Crop evapotranspiration - Guidelines for computing crop water requirements. FAO Irrigation and drainage paper, 56.

Frankenstein, S., & Koenig, G. (2004a). FASST Vegetation Models. Cold Regions Research and Engineering Laboratory, (December), 56.

Frankenstein, S., & Koenig, G. G. (2004b). Fast All-season Soil STrength (FASST). Cold Regions Research and Engineering Laboratory, (September).

M. Foustalieraki, M., Assimakopoulos, M.N., Santamouris, M., Pangalou, H. (2016). Energy performance of a medium scale green roof system installed on a commercial building using numerical and experimental data recorded during the cold period of the year, Energy and Buildings.

Gaffin, S.R., Rosenzweig, C., Parshall, L., Beattie, D., Berghage, R., O'Keeffe, G., Braman, D. (2005). Energy Balance Modeling Applied to a Comparison of Green and White Roof Cooling Efficiency. Green roofs in the New York Metropolitan region research report. Retrieved August 01 2016 from http://www.statisticstutors.com/articles/debrat-green-roofs.pdf#page=17.

Getter, K. L., Rowe, D. B., & Andresen, J. A. (2007). Quantifying the effect of slope on extensive green roof stormwater retention. Ecological Engineering, 31(4), 225–231. https://doi.org/10.1016/j.ecoleng.2007.06.004

Getter, K. L., Rowe, D. B., Robertson, G. P., Cregg, B. M., & Andresen, J. A. (2009). Carbon Sequestration Potential of Extensive Green Roofs. Environmental Science & Technology, 43(19), 7564–7570. https://doi.org/10.1021/es901539x

Ghaffarianhoseini, A., Dahlan, N. D., Berardi, U., Ghaffarianhoseini, A., Makaremi, N., Ghaffarianhoseini, M. (2013). Sustainable energy performances of green buildings: A review of current theories, implementations and challenges. *Renewable and Sustainable Energy Reviews*, 25, 1-17.

Heidarinejad, G., Esmaili, A. (2015). Numerical simulation of the dual effect of green roof thermal performance. *Energy Conversion and Management*. 106, 1418-1425.

Jaffal, I., Ouldboukhitine, S., Belarbi, R. (2012). A comprehensive study of the impact of -green roofs on building energy performance. *Renewable Energy*, 43, 157-164.

Jamieson, M. (2014). A $3 Billion Opportunity: Energy Management in reatil Operations, in, Schneider Electric, http://www.schneider-electric.us/en/, 2014.

Jamieson, M., Hughes, D. (2016). A Practical Guide to Sustainability and Energy Management in Retail Environments, in, Schneider Electric, http://www.schneider-electric.us/en/

Jim, C. Y. (2014). Air-conditioning energy consumption due to green roofs with different building thermal insulation. *Applied Energy*, 128, 49-59.

Jim, C. Y., He, H. (2010). Coupling heat flux dynamics with meteorological conditions in the green roof ecosystem. *Ecological Engineering*, 36, 1052-1063.

Julia, C.D., Jarrett, A.R., Manbeck, H.B., Beattie, D.J., Berghage, R.D. (2003). Green Roof Mitigation of Stormwater and Energy Usage.

Karachaliou, P. Santamouris, M. Pangalou, H. (2016). Experimental and numerical analysis of the energy performance of a large scale intensive green roof system installed on an office building in Athens, Energy and Buildings, 114, 256-264.

Klein, P., Coffman, R. (2015). Establishment and performance of an experimental green roof under extreme climatic conditions. Science of the Total Environment, 512–513, 82–93

Kohler, M., Schmidt, M., Grimme, F.W., Laar, M., de Assuncao, P.V.L., Tavares, S. (2002). Green roofs in temperate climates and in the hot-humid tropics-far beyond the aesthetics. Environmental Management & Health, 13 (4), 382–391.

Kolokotsa, D., Santamouris, M., Zerefos, S. C. (2013). Green and cool roofs' urban heat island mitigation potential in European climates for office buildings under free floating conditions. *Solar Energy*, 95, 118-130.

Kumar, R., Kaushik, S. C. (2005). Performance evaluation of green roof and shading for thermal protection of buildings. *Building and Environment*, 40, 1505-1511.

Lazzarin, R. M., Castellotti, F., Busato, F. (2005). Experimental measurements and numerical modelling of a Green roof. *Energy and Buildings*, 37, 1260-1267.

Lehmann, S. (2014). Low carbon districts: Mitigating the urban heat island with green roof infrastructure. *City, Culture and Society*, 5, 1-8.

Leiva G, M. A., Santibañez, D. A., Ibarra E, S., Matus C, P., Seguel, R. (2013). A five-year study of particulate matter (PM2.5) and cerebrovascular diseases. *Environmental Pollution*, 181, 1-6.

Li, J., Wai, O. W. H., Li, Y. S., Zhan, J., Ho, Y. A., Li, J., & Lam, E. (2010). Effect of green roof on ambient CO2 concentration. Building and Environment, 45(12), 2644–2651. https://doi.org/10.1016/j.buildenv.2010.05.025

Lucon, O., Ürge-Vorsatz, D., Ahmed, A.Z., Akbari, H., Bertoldi, P., Cabeza, L.F., Eyre, N., Gadgil, A., Harvey, L.D.D., Jiang, Y., Liphoto, E., Mirasgedis, S., Murakami, S., Parikh, J., Pyke, C., Vilariño, M.V. (2014). Buildings. Contribution of Working Group III to the Fifth Assessment Report of the Intergovernmental Panel on Climate Change., in: Climate Change 2014: Mitigation of Climate Change. , Cambridge, United Kingdom and New York, NY, USA., 2014.

Minenergia. (2013). Balance Energético 2012 [Online]. *Ministerio de Energía de Chile*.

Mlab.seas.upenn.edu. (2017). MLE+ Matlab EnergyPlus Co-Simulation Toolbox for Energy Efficient Buildings. [online] Available at: http://mlab.seas.upenn.edu/project sites/mlep/ [Accessed 12 Jun. 2017].

Mma. (2012). Informe del Estado del Medio Ambiente 2011. *Ministerio del Medio Ambiente*. Santiago, Chile.

Nayak, J. K., Srivastava, A., Singh, U., Sodha, M. S. (1982). The relative performance of different approaches to the passive cooling of roofs. *Building and Environment*, 17, 145-161.

Niachou, A., Papakonstantinou, K., Santamouris, M., Tsangrassoulis, A., Mihalakakou, G. (2001). Analysis of the green roof thermal properties and investigation of its energy performance. *Energy and Buildings*, 33, 719-729.

Oberndorfer, E., Lundholm, J., Bass, B., Coffman, R.R., Doshi, H., Dunnett, N. (2007). Green roofs as urban ecosystems: ecological structures, functions, and services. Bioscience, 57(10), 823–833.

Oee.nrcan.gc.ca. (2017). Report to Parliament Under the Energy Efficiency Act 2005-2006. [online] Available at: http://oee.nrcan.gc.ca/publications/statistics/parliament05-06/appendix-a.cfm?graph=17&attr=0 [Accessed 27 Jun. 2017].

OECD/IEA, (2013). Transition to Sustainable Buildings: Strategies and Opportunities to 2050, in: www.iea.org, OECD/IEA, Paris, 2013.

Ouldboukhitine, S.-E., Belarbi, R., Jaffal, I., Trabelsi, A. (2011). Assessment of green roof thermal behavior: A coupled heat and mass transfer model. *Building and Environment*, 46, 2624-2631.

Parizotto, S., Lamberts, R. (2011). Investigation of green roof thermal performance in temperate climate: A case study of an experimental building in Florianópolis city, Southern Brazil. *Energy and Buildings*, 43, 1712-1722.

Peri, G., Traverso, M., Finkbeiner, M., Rizzo, G. (2012). The cost of green roofs disposal in a life cycle perspective: covering the gap. Energy, 48, 406–414.

Permpituck, S., Namprakai, P. (2012). The energy consumption performance of roof lawn gardens in Thailand. *Renewable Energy*, 40, 98-103.

Quezada-García, S., Espinosa-Paredes, G., Escobedo-Izquierdo, M.A., Vásquez-Rodríguez, A., Vásquez-Rodríguez, R., Ambriz-García, J.J. (2017). Heterogeneous model for heat transfer in Green Roof Systems. *Energy and Buildings*, 139, 205–213.

Refahi, A. H., & Talkhabi, H. (2015). Investigating the effective factors on the reduction of energy consumption in residential buildings with green roofs. Renewable Energy, 80, 595–603. https://doi.org/10.1016/j.renene.2015.02.030

Richman, R., Simpson, R. (2016). Towards quantifying energy saving strategies in big-box retail stores: A case study in Ontario (Canada), Sustainable Cities and Society, 20, 61-70.

Sailor, D. J. (2008). A green roof model for building energy simulation programs. *Energy and Buildings*, 40, 1466-1478.

Sailor, D. J., Hagos, M. (2011). An updated and expanded set of thermal property data for green roof growing media. *Energy and Buildings*, 43, 2298-2303.

Sailor, D. J., Elley, T. B., Gibson, M. (2012). Exploring the building energy impacts of green roof design decisions – a modeling study of buildings in four distinct climates. *Journal of Building Physics*, 35, 372-391.

Santamouris, M. (2014). Cooling the cities – A review of reflective and green roof mitigation technologies to fight heat island and improve comfort in urban environments. *Solar Energy*, 103, 682-703.

Santamouris, M., Pavlou, C., Doukas, P., Mihalakakou, G., Synnefa, A., Hatzibiros, A., Patargias, P. (2007). Investigating and analysing the energy and environmental

performance of an experimental green roof system installed in a nursery school building in Athens, Greece. *Energy*, 32, 1781-1788.

Schaap, M. G., & van Genuchten, M. T. (2006). A Modified Mualem–van Genuchten Formulation for Improved Description of the Hydraulic Conductivity Near Saturation. Vadose Zone Journal, 5(1), 27. https://doi.org/10.2136/vzj2005.0005

Sellers, P. J., Mintz, Y., Sud, Y. C., Dalcher, A., Sellers, P. J., Mintz, Y., … Dalcher, A. (1986). A Simple Biosphere Model (SIB) for Use within General Circulation Models. Journal of the Atmospheric Sciences, 43(6), 505–531. https://doi.org/10.1175/1520-0469(1986)043<0505:ASBMFU>2.0.CO;2

Shimmy. (2012). A brief history of roof gardens. http://www.heathershimmin.com/a-brief-history-of-roof-gardens

Silva, C. M., Gomes, M. G., & Silva, M. (2016). Green roofs energy performance in Mediterranean climate. Energy and Buildings, 116, 318–325. https://doi.org/10.1016/j.enbuild.2016.01.012

Speak, A. F., Rothwell, J. J., Lindley, S. J., & Smith, C. L. (2013). Rainwater runoff retention on an aged intensive green roof. Science of The Total Environment, 461, 28–38. https://doi.org/10.1016/j.scitotenv.2013.04.085

Squier, M., Davidson, C. (2016). Heat flux and seasonal thermal performance of an extensive Green roof. Building and Environment, 107, 235-244.

Sun T, Bou-Zeid E, Wang ZH, Zerba E, Ni GH. (2013). Hydrometeorological determinants of green roof performance via a vertically-resolved model for heat and water transport. *Building Environmental*, 60, 211–24.

Starry, O., Lea-Cox, J.D., Kim, J., Van Iersel, M.W. (2014). Photosynthesis and water use by two Sedum species in green roof substrate. *Environmental and Experimental Botany*, 107, 105–112.

Tabares-Velasco, P. C. (2009). Predictive heat and mass transfer model for plant-based roofing materils for assessment of energy savings. Ph.D. Thesis, Pennsylvania State University.

Tabares-Velasco, P. C., Srebric, J. (2011). A heat transfer model for assessment of plant based roofing systems in summer conditions. *Building and Environment*, 49, 310-323.

Tabares-Velasco, P. C., Zhao, M., Peterson, N., Srebric, J., Berghage, R. (2012). Validation of predictive heat and mass transfer green roof model with extensive green roof field data. *Ecological Engineering*, 47, 165-173.
Takebayashi, H., Moriyama, M. (2007). Surface heat budget on green roof and high reflection roof for mitigation of urban heat island. *Building and Environment*, 42, 2971-2979.

Teemusk, A., & Mander, Ü. (2009). Greenroof potential to reduce temperature fluctuations of a roof membrane: A case study from Estonia. Building and Environment, 44(3), 643–650. https://doi.org/10.1016/j.buildenv.2008.05.011

Theodosiou, T. G. (2003). Summer period analysis of the performance of a planted roof as a passive cooling technique. *Energy and Buildings*, 35, 909-917.

Tiana, H., Fanomezana, T., Morau, D. 2015. Dynamic Simulation of the Green Roofs Impact on Building Energy Performance, Case Study of Antananarivo, Madagascar. *Buildings*, 5(2), 497-520
Townshend, D. (2007). Study on Green Roof Application in Hong Kong. Architectural Services Department, 1–157.

U.S Department of Energy. (2016). EnergyPlus Input Output Reference. [online] Available at: https://energyplus.net/sites/all/modules/custom/nrel_custom/pdfs/pdfs_v8.5.0/InputOutputReference.pdf [Accessed 12 Jun. 2017].

UNEP. (2009). Buildings and Climate Change: Summary for Decision-Makers. Paris: United Nations Environment Programme, *Sustainable Buildings & Climate Change*.

Valipour, M. (2014). Future of agricultural water management in Africa. *Archives of Agronomy and Soil Science,* 61(7), 907-927.

Valipour, M. (2015). Land use policy and agricultural water management of the previous half of century in Africa. *Applied Water Science,* 5, 367–395.

Van Renterghem, T., Hornikx, M., Forssen, J., Botteldooren, D. (2013). The potential of building envelope greening to achieve quietness. *Building Environmental*, 61, 34–44.
Van Renterghem, T, Botteldooren, D. 2014. Influence of rainfall on the noise shielding by a green roof. Building and Environment, 82, 1-8.

VanWoert, N. D., Rowe, D. B., Andresen, J. A., Rugh, C. L., Fernandez, R. T., & Xiao, L. (2005). Green roof stormwater retention: effects of roof surface, slope, and media depth. Journal of Environmental Quality, 34(3), 1036–44. https://doi.org/10.2134/jeq2004.0364

Vera, S., Pinto, C., Victorero, F., Bustamante, W., Bonilla, C., Gironás, J., & Rojas, V. (2015). Influence of plant and substrate characteristics of vegetated roofs on a supermarket energy performance located in a semiarid climate. In Energy Procedia (Vol. 78, pp. 1171–1176). Elsevier. https://doi.org/10.1016/j.egypro.2015.11.089

Vera, S., Pinto, C., Tabares-Velasco, P. C., Bustamante, W., Victorero, F., Gironás, J., Bonilla, C. (2017). Influence of vegetation, substrate, and thermal insulation of an extensive vegetated roof on the thermal performance of retail stores in semiarid and marine climates. *Energy and Buildings*. 146, 312–321

Vijayaraghavan, K. (2016). Green roofs: A critical review on the role of components, benefits, limitations and trends. Renewable and Sustainable Energy Reviews, 57, 740–752. https://doi.org/10.1016/j.rser.2015.12.119

Vijayaraghavan, K., & Joshi, U. M. (2014). Can green roof act as a sink for contaminants? A methodological study to evaluate runoff quality from green roofs. Environmental Pollution, 194, 121–129. https://doi.org/10.1016/j.envpol.2014.07.021
Vijayaraghavan, K., Joshi, U. M., & Balasubramanian, R. (2012). A field study to evaluate runoff quality from green roofs. Water Research, 46(4), 1337–1345. https://doi.org/10.1016/j.watres.2011.12.050

Villarreal, E. L., & Bengtsson, L. (2005). Response of a Sedum green-roof to individual rain events. Ecological Engineering, 25(1), 1–7. https://doi.org/10.1016/j.ecoleng.2004.11.008

Wang, Z.-H., Bou-Zeid, E., Smith, J. (2012). A coupled energy transport and hydrological model for urban canopies evaluated using a wireless sensor network. *Quarterly Journal of the Royal Meteorological Society*, 139, 1643-1657.

Weng, Q., Lu, D., Schubring, J. (2004). Estimation of land surface temperature–vegetation abundance relationship for urban heat island studies. *Remote Sensing of Environment*, 89, 467-483.

Williams, N.S.G., Lundholm, J., Scott MacIvor, J. (2014). FORUM: Do green roofs help urban biodiversity conservation?, Journal of Applied Ecology, 51 (6), 1643-1649.

Williams, N.S.G., Rayner, J.P., Raynor, K.J. (2010). Green roofs for a wide brown land: opportunities and barriers for rooftop greening in Australia. Urban Forest Urban Green, 9, 245–251

Wolf, J. (1960). Der Diurnale Säurerhythmus. In: Ruhland, W. (Ed.). Encyclopedia of Plant Physiology. Springer Verlag, Berlin, 809–889.

Wolf D, Lundholm JT. (2008). Water uptake in green roof microcosms: effects of plant species and water availability. *Ecological Engineering*, 33, 179–86.

Wong NH, Cheong DKW, Yan H, Soh J, Ong CL, Sia A. (2003). The effects of rooftop garden on energy consumption of a commercial building in Singapore. *Energy Building*, 35, 353–64.

Yaghoobian, N., & Srebric, J. (2015). Influence of plant coverage on the total green roof energy balance and building energy consumption. Energy and Buildings, 103, 1–13. https://doi.org/10.1016/j.enbuild.2015.05.052

Yang HS, Kang J, Choi MS. (2012). Acoustic effects of green roof systems on a lowprofiled structure at street level. *Building Environmental*, 50, 44–55.

Zhao, M., Tabares-Velasco, P. C., Srebric, J., Komarneni, S., & Berghage, R. (2014). Effects of plant and substrate selection on thermal performance of green roofs during the summer. Building and Environment, 78, 199–211. https://doi.org/10.1016/j.buildenv.2014.02.011

Zhang, J.Q., Fang, X.P., Zhang, H.X., Yang, W., Zhu, C.C. (1997). A heat balance model for partially vegetated surfaces. *Infrared Physics & Technology*, 38 (5), 287-294

Zhang, X., Shen, L., Tam, V.W.Y., Lee, W.W.Y. (2012). Barriers to implement extensive green roof systems: a Hong Kong study. Renewable and Sustainable Energy Reviews, 16(1), 314–319.